

AN ABSTRACT OF THE THESIS OF

Gisela A. González-Montiel for the degree of Master of Science in Chemistry presented on July 11, 2019.

Title: Bioprospecting the Chemical Diversity of Plant-associated Fungi

Abstract approved:

Sandra Loesgen

Fungi have long been used for discovery of new chemical scaffolds. In the clinical setting, the fungal natural products penicillin, statins, and cyclosporine have revolutionized medicine to treat diseases and infections. In the environment, fungal natural products have been used as herbicides, fungicides, and insecticides to protect crops, livestock, and commercial forests. As part of a broad survey of secondary metabolites produced by plant-associated fungi, the research presented includes three fungi from terrestrial and marine sources that were assessed for their chemical diversity. Chemical analysis led to the isolation of a new metabolite from *Zasmidium pseudotsugae*, an epiphytic fungus closely associated with Douglas-fir trees. From *Penicillium crustosum*, an algal-derived fungal endophyte, known metabolites were isolated and subjected to antimicrobial screening. Lastly, eight isolates of the wheat pathogen *Fusarium graminearum* exhibiting different *in planta* pathogenicity were subjected to comparative, metabolomic analysis. In each instance presented, fungi produced different molecules that can be used as tools to understand the chemical ecology of fungi.

©Copyright by Gisela A. González-Montiel
July 11, 2019
All Rights Reserved

Bioprospecting the Chemical Diversity of Plant-associated Fungi

by
Gisela A. González-Montiel

A THESIS

submitted to

Oregon State University

in partial fulfillment of
the requirements for the
degree of

Master of Science

Presented July 11, 2019
Commencement June 2020

Master of Science thesis of Gisela A. González-Montiel presented on July 11, 2019.

APPROVED:

Major Professor, representing Chemistry

Head of the Department of Chemistry

Dean of the Graduate School

I understand that my thesis will become part of the permanent collection of Oregon State University libraries. My signature below authorizes release of my thesis to any reader upon request.

Gisela A. González-Montiel, Author

ACKNOWLEDGEMENTS

First and foremost, I would like to thank Dr. Sandra Loesgen for her support throughout these past years in graduate school. She has been a great mentor and I am forever grateful for the opportunity to be part of her research team. I would like to thank my research lab members for all their support, guidance, and feedback through my research experiences, including the difficult and uplifting moments. Finally, I would like to thank my amazing and loving family. Thank you for always believing in me, for pushing me forward, and for lifting me up along the way. I would not be here today without the support they have given me through this journey.

CONTRIBUTION OF AUTHORS

Dr. Sandra Loesgen was the major advisor on all projects and assisted with the design and writing of all chapters contained herein. Prof. Jeffrey Stone (OSU) supplied the fungus *Zasmidium pseudotsugae* and has provided the genome data in Chapter two. Dr. Tom O'Hare and Orlando Antelope (Huntsman Cancer Institute, Salt Lake City) tested samples against an AML cancer cell line panel in Chapter two. Prof. Dr. Axel Zeeck and Hans-Peter Kroll (Biovitica) provided the marine algal endophyte *Penicillium crustosum*, subjected of Chapter three. Dr. Lev Zakharov (OSU/UO) performed X-ray crystallography analysis in Chapter three. Dr. Ludovic Bonhomme and Tarek Alouane (INRA) supplied the eight *Fusarium graminearum* isolates, the information about the level of aggressiveness of the strains and performed genomic sequencing and transcriptomics in Chapter four. Elizabeth Kaweesa (OSU) performed cytotoxic testing of all compounds in Chapters two, three, and four.

TABLE OF CONTENTS

	<u>Page</u>
1 General Introduction	1
1.1 Thesis overview.....	1
1.2 Natural products	2
1.3 Fungi and fungal natural products	6
1.4 Metabolomics approaches in natural products discovery	11
2 Douglas-fir tree associated fungus <i>Zasmidium pseudotsugae</i>	12
2.1 Abstract	12
2.2 Introduction	12
2.3 Results & Discussion	14
2.3.1 Physiochemical properties of 8,8'-bijuglone.....	17
2.3.2 Solubility and stability of 8,8'-bijuglone	18
2.3.3 Antimicrobial activity	19
2.3.4 Cytotoxicity activity	20
2.3.5 AntiSMASH results of <i>Z. pseudotsugae</i>	23
2.4 Conclusion	25
2.5 Materials & Methods	26
2.5.1 Foliage sampling	26
2.5.2 Culture media & fermentation	27
2.5.3 Preparation of organic extracts	27
2.5.4 General spectroscopic and chromatographic procedures	27
2.5.5 HPLC isolation & purification of 8,8'-bijuglone	28

TABLE OF CONTENTS (Continued)

	<u>Page</u>
2.5.6 Antimicrobial assays	28
2.5.7 Cytotoxicity assay	29
2.6 Acknowledgements	30
3 Algal-derived fungal endophyte <i>Penicillium crustosum</i>	31
3.1 Abstract	31
3.2 Introduction	31
3.3 Results & Discussion	33
3.3.1 Physiochemical properties of the secondary metabolites	34
3.3.2 Antimicrobial activity	35
3.3.3 Cytotoxicity activity	36
3.4 Conclusion	37
3.5 Acknowledgements	38
3.6 Materials & Methods	38
3.6.1 Biological material	38
3.6.2 Culture media & fermentation	38
3.6.3 Identification of the fungus	39
3.6.4 Phylogeny analysis	40
3.6.5 Preparation of organic extracts	41
3.6.6 General spectroscopic and chromatographic procedures	41
3.6.7 HPLC isolation and purification of secondary metabolites	42
3.6.8 X-ray crystallographic analysis	42

TABLE OF CONTENTS (Continued)

	<u>Page</u>
3.6.9 Antimicrobial assays	43
3.6.10 Cytotoxicity assay	44
4 <i>Fusarium graminearum</i> pathogenesis & metabolomics	45
4.1 Abstract	45
4.2 Introduction	46
4.3 Results & Discussion	49
4.4 Conclusion	54
4.5 Materials & Methods	55
4.5.1 Strains and culture conditions	55
4.5.2 General spectroscopic and chromatographic procedures	55
4.5.3 Metabolomics analysis	56
4.6 Acknowledgements	57
5 General Conclusion	57
6 References	59
7 Supplementary Information	70
7.1 Material for Section 2	70
7.2 Material for Section 3	80

LIST OF FIGURES

<u>Figure</u>	<u>Page</u>
1. Timeline of antibiotics introduced and antibiotic resistance	4
2. Examples of fungal natural products	7
3. Secondary metabolite, 8,8'-bijuglone (1), from <i>Zasmidium pseudotsugae</i> isolated from Douglas-fir tree (<i>Pseudotsuga menziesii</i> var. <i>menziesii</i>)	15
4. LC/MS analysis of 8,8'-bijuglone (1)	16
5. LC/MS analysis of extracts of <i>Z. pseudotsugae</i> fungal cells vs. supernatant	17
6. Acid/Base effect of 8,8'-bijuglone.	18
7. Analogs of 8,8'-bijuglone	20
8. IC ₅₀ curve of 8,8'-bijuglone against human colon carcinoma (HCT-116)	21
9. Mean graph display of NCI-60 cell line screening data for 8,8'-bijuglone	22
10. Biosynthetic gene clusters in <i>Z. pseudotsugae</i> generated identified by antiSMASH	24
11. LC/MS traces of <i>Z. pseudotsugae</i> extract (extract) and VLCC fractions F1-F8	25
12. Secondary metabolites isolated from marine algal-associated endophytic fungi	32
13. Secondary metabolites from <i>Penicillium crustosum</i> (2-3)	33
14. LC/MS analysis of compounds 2 and 3 from liquid glycerin-based medium (G20) cultures of <i>P. crustosum</i> (absorptions at 280 nm)	34
15. (A) The X-ray crystal structure of 3. (B) Part of the crystal lattice packing diagram to illustrate the hydrogen-bonded complementarity found in the X-ray crystal structure	35
16. Colony morphology of the eight <i>Fg</i> strains	48
17. Phylogeny of the eight <i>Fg</i> strains	48

LIST OF FIGURES (Continued)

<u>Figure</u>	<u>Page</u>
18. In planta symptoms from the eight <i>Fg</i> inoculations on wheat measured at 72hpi	49
19. A principal component analysis (PCA) plot for PC1 and PC2 of the LC/MS-based metabolomics data of the eight <i>Fg</i> trains	51
20. Volcano plot visualizing the chemical differences between <i>Fg</i> U1 to <i>Fg</i> 1 isolates	52
21. Heat map comparing relative LC/MS ion abundances of identified secondary metabolites	54

LIST OF TABLES

<u>Table</u>		<u>Page</u>
1.	Biological activities of 8,8'-bijuglone (1)	20
2.	Antimicrobial and cytotoxic activities of <i>P. crustosum</i> extract and compounds (2-3)	37

LIST OF APPENDIX FIGURES

<u>Figure</u>	<u>Page</u>
A1. Synthesis of 8,8'-bijuglone by Laatsch	71
A2. ¹ H-NMR spectrum of 8,8'-bijuglone (1) in CDCl ₃ (500MHz)	73
A3. COSY spectrum of 8,8'-bijuglone (1) in CDCl ₃ (500MHz)	74
A4. ¹³ C-NMR spectrum of 8,8'-bijuglone (1) in CDCl ₃ (500MHz)	75
A5. HSQC spectrum of 8,8'-bijuglone (1) in CDCl ₃ (500MHz)	76
A6. HMBC spectrum of 8,8'-bijuglone (1) in CDCl ₃ (500MHz)	77
A7. IR spectrum of 8,8'-bijuglone (1)	78
A8. LC/MS traces of 8,8'-bijuglone in acidic and basic conditions	79
A9. Phylogenetic analysis of <i>Penicillium</i> sp. (G17N) strain by maximum likelihood method of ITS region	80
A10. Phylogenetic analysis of <i>Penicillium</i> sp. (G17N) strain by maximum likelihood method of beta-tubulin region	80
A11. Consensus sequence of <i>Penicillium</i> genus from the ITS region using primers ITS1 and ITS4	81
A12. Consensus sequence of <i>P. crustosum</i> species from the β-tubulin region using primers Bt2a and Bt2b	81
A13. Thin layer chromatography of <i>P. crustosum</i> (G17N) organic extracts.....	82
A14. IR spectrum of clavatul (2)	83
A15. ¹ H-NMR spectrum of clavatul (2) in CDCl ₃ (700MHz)	85
A16. COSY spectrum of clavatul (2) in CDCl ₃ (700MHz)	86
A17. ¹³ C-NMR spectrum of clavatul (2) in CDCl ₃ (700MHz)	87
A18. HSQC spectrum of clavatul (2) in CDCl ₃ (700MHz)	88

LIST OF APPENDIX FIGURES (Continued)

<u>Figure</u>	<u>Page</u>
A19. HMBC spectrum of clavatol (2) in CDCl ₃ (700MHz)	89

LIST OF APPENDIX TABLES

<u>Table</u>	<u>Page</u>
A1. ^1H and ^{13}C NMR data of 8,8'-bijuglone (1) at 500MHz in CDCl_3	70
A2. Reported bioactivities of similar compounds to (1)	72
A3. ^1H -NMR and ^{13}C -NMR data of clavatol (2) at 700MHz in CDCl_3	84

1 General Introduction

1.1 Thesis overview

Chapter 1 gives a summary of natural products, specifically fungal natural products, and the importance for discovery of new chemical scaffolds to combat microbial resistance, disease contaminant in crops, livestock, and forestry industry, as well as to understand the chemical language associated with their plant-host interactions. In addition, a brief introduction of metabolomics is presented as a useful tool for screening natural product extracts.

Chapter 2 details the chemical analysis and isolation of a novel secondary metabolite from an epiphytic fungus, associated with Douglas-fir needles, *Zasmidium pseudotsugae* which was isolated by Prof. Jeff Stone (OSU). This fungus has not been chemically studied previously. Its close relationship with Oregonian Douglas-fir tree might be based on chemical interactions. LC/MS analysis illustrated one dominant metabolite which was isolated and structurally elucidated by one- and two-dimensional NMR. The metabolite, 8,8'-bijuglone, showed weak cytotoxic *in vitro* and was subjected to cytotoxicity screening at the NCI. These results are currently prepared for publication.

Chapter 3 presents the chemical analysis of *Penicillium crustosum*, an algal-derived fungal endophyte. The fungus was cultured in nutrient rich medium and the resulting extracts were profiled by LC/MS analyses. The structures of two known compounds were elucidated by X-ray crystallography and/or by one- and two-

dimensional NMR. All metabolites were subjected to antimicrobial and cytotoxicity screening.

Chapter 4 details the metabolomics guided identification of known secondary metabolites from eight *Fusarium graminearum* strains with different levels of pathogenicity *in planta* against wheat. LC/MS-based, log ratio analysis guided the potential identification of known natural products from *F. graminearum*. This is a collaborative project with Dr. Ludovic Bonhomme and graduate student Tarek Alounet at INRA Joint Unit of Genetics, Diversity and Ecophysiology of Cereals and Cereal Diseases Team (France). A publication on the connection between *in planta* pathogenicity with *in vitro* secondary metabolite profiles is in preparation.

Chapter 5 presents a conclusion of the work presented.

1.2 Natural products

Natural products are one of the most important sources for new bioactive, chemical scaffolds. These natural products are compounds isolated from natural sources such as plants, fungi, algae, bacteria, and animals in the form of primary or secondary metabolites. Secondary metabolites are non-essential for survival, but aid in signaling processes, development, and on the establishment of interactions or as defense mechanisms against other organisms.¹ It is remarkable how nature can generate an inexhaustible chemical diversity of natural products out of simple building blocks from the primary metabolism by highly evolved enzymes. In a biochemical sense, natural products with their highly complex and diverse structures have been driven by

the continual evolution of biosynthetic genes clusters due to mutations, intragenic rearrangements & duplications, horizontal gene transfer, and natural selection of genes and the modular enzyme classes including polyketide synthases (PKSs), non-ribosomal peptide-synthetase (NRPS), terpenes synthases, and dimethylallyl tryptophan synthases (DMATSs) resulting in the production of a vast chemical diversity.²⁻³ In fact, there are many areas of investigation in natural products enzymology to identify new chemical reactions and harvest the chemical machinery that makes up complex molecules in nature.⁴

Historically, microbial natural products as well as plant remedies have been a source of valuable medicinal compounds.⁵ Along with semisynthetic derivatives and synthetic mimics, natural products represent more than 50% of all FDA approved drugs since 1981 to 2014.⁶⁻⁷ Modern medicine depends on nature's small molecule bounty to treat a variety of health problems ranging from bacterial and fungal infections to cancer, they enable organ transplantations by providing potent immune suppressants, and surgeries with various analgesics. Especially for antibiotics, microbial derived natural products were a lead source for discovery. When antibiotics were first introduced in the 1920s, they saved hundredths of millions of lives.⁸ However, their continual widespread use has led to complications including: (a) drug-drug interactions that range from minor to severe consequences,⁹ (b) high dose concentrations that lead to toxicity and negative side effects,¹⁰ and most importantly (c) induced pathogen resistance to current drugs (Figure 1).¹¹⁻¹³ In the last 70 years, a couple of the listed drugs showed resistance in 40 years, others in 15 years, but for most of the listed drugs, it only took

about 5 years or less for there to be a resistance. The drugs we rely on to combat infectious diseases are quickly becoming ineffective. There is an ever-growing need for new medicinal agents with fewer drug adverse events to address specific toxicity and resistance in microbial infections.

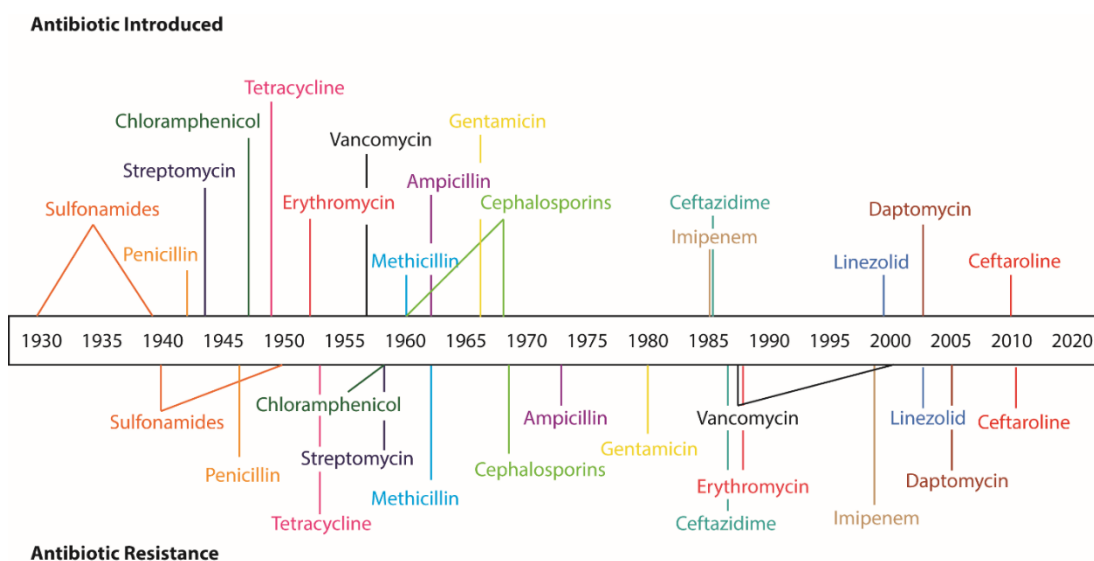


Figure 1. Timeline of antibiotics introduced and antibiotic resistance (reproduced from ¹²⁻¹³).

Apart from the long history of the medicinal and pharmaceutical applications, natural products are also of interest for novel agrochemicals to treat diseases and contaminants in crops, livestock, and commercial forest industry.¹⁴ Some of the existing herbicides, fungicides, and insecticides have originated from microbial natural products and a variety of other natural sources.¹⁵ One important group of fungicides are the strobilurins, wherein azoxystrobin has been the market lead with an end user sale at \$1,758 million USD in 2016 (Figure 2).¹⁶ Strobilurins inhibit the electron transfer in mitochondrial respiration and are produced by several basidiomycetes fungi,

such as *Strobilurus tenacellus*, *Xeryla* sp., and *Cyphellopsis anomala*.¹⁷⁻¹⁸ Interestingly, there is little to no fungal natural products acting as insecticides and herbicides.¹⁵ As in the medical field, antimicrobial resistance continues to be a problem, also challenging our food security.¹¹ For agrochemical application, natural products should not be toxic to the environment or unstable, challenges which need to be resolved before they can become commercial products in agricultural settings. However, with success stories like the application of the fungal natural product strobilurin, more microbial sources, including fungi, are yet to be explored that could potentially lead to novel agrochemicals.

Due to the worrying trend of evolving microbial resistance in agricultural and medicinal relevant pathogens, the search for new natural products with novel modes of action continues to be a high priority. In the medical field, we need new natural products to combat infectious diseases and cancer, including selectively binding protein targets,¹⁹ inhibition of cell wall and membrane synthesis,²⁰ target signaling pathways,²¹ and interference in genetic integrity.²² Of most importance, there is a need for new bioactive compounds that affect the five major therapeutic families which are: class A G-protein-coupled receptors (GPCRs), protein kinases, ion channels, nuclear receptors, and proteases.²³ In agriculture, novel natural products are still needed to control insects, fungal pathogens, and weeds on crops.¹⁶ In general, most natural products have a function or activity for the organisms, and the fact that modes of action of many of these natural products have yet to be determined indicates the importance

for the discovery of next generation molecules for human health and agriculture applications.

1.3 Fungi and fungal natural products

Among the various sources of natural products, fungi have been shown to be an incredible source with a wide range of valuable chemical leads in the fight against human diseases and infections. This began with the discovery of penicillin in 1929 from a *Penicillium* sp., saving millions of lives, affecting the course of World War II, and revolutionizing medicine, which set off a race for the discovery of potential natural product antibiotics from microorganisms.^{8, 24-25} Further surveying of the fungal world for new chemical scaffolds that can be used for new medicines can result in the discovery of extraordinary bioactive metabolites. Classic fungal natural products in use today include the immunosuppressant drugs cyclosporin A (*Tolypocladium inflatum*) and mizoribine (*Penicillium brefeldianum*), the cholesterol suppressant lovastatin (*Aspergillus terreus*), the lipid-lowering medication simvastatin (*Aspergillus terreus*), the antifungal agents strobilurins (*Strobilurus tenacellus*), griseofulvin (*Penicillium*) and caspofungin (*Glarea lozoyensis*), and the cytotoxin irofulven (*Clitocybe illudens*) (Figure 2).^{15, 26-30} Other examples of fungal secondary metabolites constructed from the core biosynthetic enzymes include polyketides (aflatoxin, T-toxin, and perylenequinone toxins), non-ribosomal peptides (HC-toxin and ferricrocin), and terpenes (ergotamine, paxilline, and lolitreme). Despite the thorough efforts into the discovery of fungal natural products, fungal genomes sequencing indicates that there

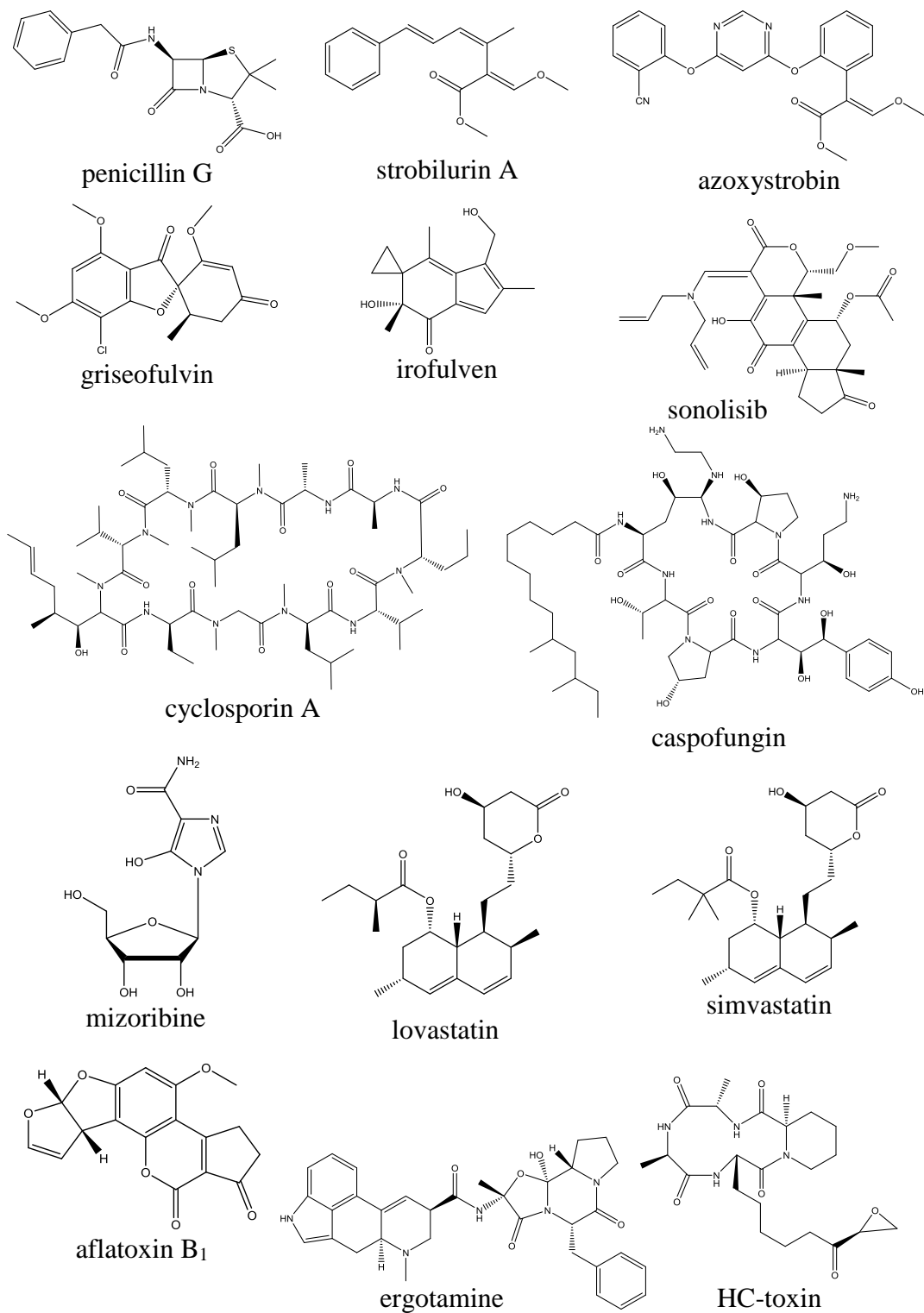


Figure 2. Examples of fungal natural products.

are far more gene clusters encoding for secondary metabolites than the number of compounds identified likely due to transcription suppression.³¹ In fact, some gene clusters are cryptic and no known secondary metabolite can be bioinformatically related to that identified gene. Many of these cryptic genes are not expressed under laboratory conditions and can sometimes be activated *in planta* conditions for example for fungal endophytes, or upon contact/challenge with other organisms.³¹ On top of this, even though more than 100,000 fungal species have been chemically investigated, there is evidence indicating that over one million fungal species have yet to be discovered and explored.³² Therefore, the combination of species, biodiversity, and cryptic secondary metabolites present make fungi a promising source for continued natural product discovery efforts.

In natural habitats, fungi face not only different environmental constraints, but also competitors and natural enemies. Probably for this reason, fungi are using biological active molecules to gain an advantage over other microbes and organisms.³³ Due to the high plasticity of fungal genomes and ability to rapidly reproduce, fungi harbor an evolutionary adaptation advantage with the capacity to produce structurally different molecules.¹¹

Plant-associated fungal microbiota, for example the root-associated mycorrhiza, play an important role in both partners' ability to co-exist. There are three major symbiotic interactions, namely mutualism, commensalism, and parasitism.³⁴ Mutualism fungi increase a plant's survival such as drought tolerance,³⁵ growth promotion,³⁶ microbial resistance and stimulation of defense mechanisms,³⁷ and

enhanced nutrient uptake.³⁸ Commensalism fungi have no influence on their host plant.³⁹ Parasitism fungi cause infections and disease on plants by production of toxic secondary metabolites disrupting cellular physiology resulting in the destruction of plant growth.⁴⁰⁻⁴¹ Apart from the different nature of plant-fungal symbiotic relations, plant-fungal communities are also further complex based on plant species, location, and parts. The microbes associated with root surface and soil layers are known as the mycorrhizal fungi, which can be divided into ecto- or endomycorrhizae, depending in their ability to colonize the roots.⁴² The microbes on the outer surfaces of leaves and needles of aerial plant parts are known as the phyllosphere, also known as epiphytic fungi.⁴³ The microbes residing within plant tissues are termed endospheres or endophytic fungi,⁴⁴ defined by Anton de Bary in the mid-19th century, and later defined as cryptic microorganisms residing within plant tissues without causing any apparent effects of infection for part of their life cycle.⁴⁵ Most terrestrial fungi belong to the phyla of Ascomycota, Basidiomycota and Glomeromycota,⁴⁴ and although these phytobiome communities have been well studied for decades, recent advances in genome sequencing and chemical detection enables now natural product chemists to understand the chemical language associated with plant-host interactions.

Endophytic fungi can live as either free-living microbes, saprobic ones, or as pathogens in their lifecycle. Of the more than 300,000 plant species on earth, including those in aquatic regions, each one is expected to have at least one or many cultivable and uncultivable endophytic fungi living within.⁴⁶⁻⁴⁸ In order to survive, adapt, and co-evolve in a plant environment, endophytes tend to produce various phytochemicals for

different purposes such as increasing alkaloid production, production of precursors, quorum sensing molecules, epigenetic modulators, pathogen resistance, and direct physical organismal interactions.^{47, 49-50} One example of a plant-associated endophytic fungus is *Neotyphodium coenophialum* which inhabits the tall fescue *Festuca arundinacea*. This fungus produces toxic alkaloids, defending the grass from herbivorous mammals and causing “fescue toxicosis” in livestock.⁵¹ Epiphytic fungi, i.e., phylloplane fungi, grow on the surface of leaves and needles of plants supplemented by external moisture and nutrient sources. Although there has been many studies on endophytic fungi,⁵²⁻⁵³ there have been very few reports on epiphytic fungal communities in relation to secondary metabolites. One study reports the production of the ergot alkaloids from the epiphytic fungus *Claviceps purpurea*.⁵⁴ Two other recent studies isolated novel polyketide-like metabolites from epiphytic fungi associated with marine algae, exhibiting activity against phytoplankton species.⁵⁵⁻⁵⁶ With only a few natural products being known from epiphytic fungi, there is an enormous potential to discover novel natural products.

Given that endophytes and epiphytes are highly diverse, it is important to explore these fungal species and the secondary metabolites they produce to better understand plant-microbe interactions that can affect ecological dynamics. We can also take advantage of these metabolites for potential biological applications in the medical and agricultural fields. Of interest in this study are metabolites with potential to be useful as novel anticancer agents, antibiotics, novel immunosuppressive compounds, antioxidants, fungicides, herbicides, and insecticides.

1.4 Metabolomics approaches in natural products discovery

Metabolomics is a comprehensive analysis tool used to profile all the molecules in a chemical sample in order to compare identifiable molecules relative to molecules in other chemical samples without bias.⁵⁷⁻⁵⁹ In the case of untargeted metabolomics, it begins with analysis of the metabolites of a sample by using mass spectrometry (MS) technologies such as liquid chromatography coupled with MS (LC/MS) as well as nuclear magnetic resonance (NMR).⁵⁸ After data acquisition, the data are analyzed by a nonlinear retention time alignment, peak picking, and smoothing. Relative changes in metabolite abundances amongst all the tested samples are compared for identification of metabolite features, which are detected ions measured by a mass-to-charge ratio (m/z) value with a corresponding retention time.⁵⁷ The use of metabolomics can aid in the discovery of microbial natural products that may or may not be identifiable under normal laboratory conditions. Multivariate analyses of mass spectrometric data can greatly accelerate the detection and dereplication of secondary metabolites.^{58, 60} Statistical approaches in metabolomics applications can be used to observe changes in metabolic profiles across different treatment conditions, such as nutrient conditions, co-culture, or chemical elicitation conditions.⁶¹⁻⁶² Metabolomics can also be used as a starting analysis for prioritizing samples that illustrate metabolites in higher or lower abundances relative to other tested samples for metabolic isolation and purification efforts from mixed organic extracts. LC/MS-based metabolomics is a simple but powerful method of comparative, chemical analysis.^{61, 63-64}

2 Douglas-fir tree associated fungus *Zasmidium pseudotsugae*

2.1 Abstract

All trees on planet earth live in close association with fungi. As part of a broad survey of secondary metabolites produced by tree-associated phylloplane fungi, an epiphytic fungus *Zasmidium pseudotsugae* was isolated from Oregonian Douglas-fir needles by Prof. Jeff Stone (OSU). An agar plate extract of *Z. pseudotsugae* produced only one dominant secondary metabolite identified as 8,8'-bijuglone (**1**). This is the first time **1** is identified from a natural source. The quinone was characterized using LC/MS and NMR spectroscopy methods. Compound **1** has weak cytotoxic activity against human colon carcinoma (HCT-116) cell line with an IC₅₀ of 130 μM. Analysis of the fungal genome sequence and its metabolic potential was implemented using the bioinformatic tool antiSMASH, which suggested the biosynthetic potential to produce (-)-mellein, elsinochrome A, and aureobasidin A₁. Compounds closely related to these aforementioned metabolites, including *O*-methylnellein, elsinochrome A, and bassianolide, were detected in organic extracts of the fungus by EIC-LC/MS as predicted from the biosynthetic gene clusters. In summary, fungi collected in Oregon's forests have the potential to produce new, bioactive compounds.

2.2 Introduction

Douglas-fir evergreen tree (*Pseudotsuga menziesii* var. *menziesii*) is an important commercial conifer species in forest plantations for timber and also most

commonly used as a Christmas tree in western North America, Europe, and New Zealand.⁶⁵⁻⁶⁶ In fact, Douglas-fir is the state tree of Oregon, showing how important it is to Oregon's economy and ecology. However, populations of western North America Douglas-fir, which is native, are susceptible to the fungal disease Swiss needle cast (SNC), which is caused by the pathogenic endophytic fungus *Nothophaeocryptopus gaeumannii*.⁶⁶⁻⁷⁰ The disease causes trees to shed needles prematurely. In 2016, a report showed that Douglas-fir volume growth across the northwest Oregon Coast Range was reduced 23-50% from 1996 to 2015 by SNC.⁷¹ *Apiosporina collinsii*, *Stomiopeltis* sp. and *Zasmidium pseudotsugae* are other Douglas-fir associated fungi that often occur together with *N. gaeumannii*.⁶⁸ The foliar microbiome of Douglas-fir is an elaborate communal ecosystem with a complex, underexplored chemical ecology. A thorough study of Douglas-fir associated fungi, focusing on their secondary metabolism, can shed light on these complex interactions with the chance to gain a deeper understanding of fungal tree communities with the goal to prevent SNC.

Identifying secondary metabolites from understudied epiphytes associated with conifer needles is inherently difficult because the strains are often sterile in laboratory settings, as in the fungus does not produce spores, and some biosynthetic gene clusters are only active *in planta*.⁷² Here, we sought out to assess the fungal secondary metabolites from *Z. pseudotsugae*, previously known as *Rasutoria pseudotsugae*.⁷³ This fungus is within the *Dothideomycetes* class, part of the order *Capnodiales*, and included in the family of *Mycosphaerellaceae*.⁷³ A recent isolate was grown on malt-

media and the compound 8,8'-bijuglone (**1**) was isolated. **1** was characterized with a combination of LC/MS and one- and two-dimensional NMR techniques. **1** was also tested for antimicrobial and cytotoxicity activity. To our knowledge, this is the first bioactive metabolite isolated from *Z. pseudotsugae*. In future studies we will explore the chemical, ecological function of 8,8'-bijuglone. Since *Z. pseudotsugae* closely interacts with *N. gaeumannii*, the cause of SCN, their secreted secondary metabolites might be playing a role in virulence and plant pathogenicity.

2.3 Results & Discussion

Zasmidium pseudotsugae isolated from the needles of *Pseudotsuga menziesii* var. *menziesii* by Prof. Jeff Stone's Laboratory at OSU, was grown on 1% malt-based agar. Plates were extracted with organic solvents and the major component of the extract was identified as 8,8'-bijuglone (**1**) (Figure 3). This quinone has been reported by Laatsch in 1985 who made it synthetically (Figure A1),⁷⁴ but this is the first report of the compound from a natural source. Biosynthetically, this biaryl natural product could potentially be constructed from an oxidative coupling of monomers catalyzed by a laccase, peroxidase, or cytochrome P450 enzyme (CYP) within *Z. pseudotsugae*.⁷⁵

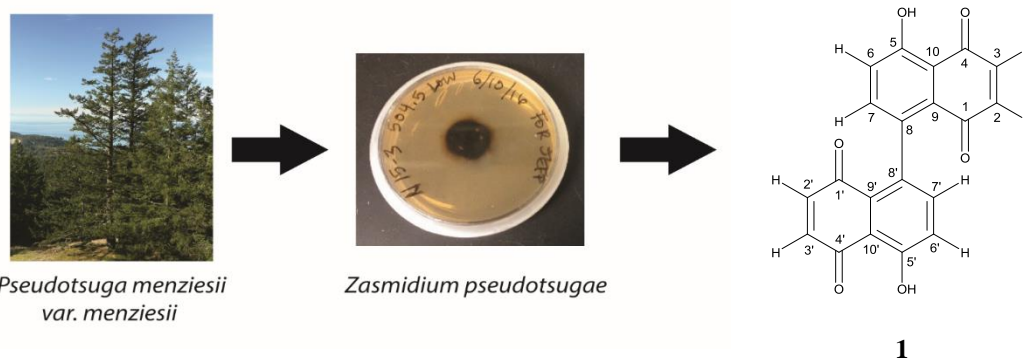


Figure 3. Secondary metabolite, 8,8'-bijuglone (**1**), from *Zasmidium pseudotsugae* isolated from Douglas-fir tree (*Pseudotsuga menziesii* var. *menziesii*).

Analysis of an agar culture extract by LC/MS exhibited only one dominant metabolite at retention time 21 minutes (Figure 4). Negative ionization showed 345.0 m/z for $[M-H]^-$ and 712.9 m/z for $[2M-2H+Na]^-$, while positive ionization detected 347.1 m/z for $[M+H]^+$. The compound was purified by semipreparative HPLC using an isocratic elution of 50:50 ACN/H₂O + 0.05% formic acid. The structure of the compound was established by 1D and 2D NMR (Table A1 and Figures A1-A5), referenced to Laatsch's NMR data,⁷⁴ where the proton and carbon environments are chemically equivalent, resulting in double the amount of signals for the formation of the dimer structure of **1**. Other 1,4-naphthoquinone dimers are known that demonstrate chemical equivalent environments across the aryl sigma bond, including marinone and mamegakinone, but these are all plant metabolites from *Diospyros maritima*.⁷⁶⁻⁷⁷ To determine if the fungus produced and retained **1** in its cells or if it was secreted, extracts derived from cells and supernatant of a liquid culture were analyzed by LC/MS (Figure 5). The $[M-H]^-$ ion (extract-ion chromatogram at 345 m/z) was only observed in the cell extract and not in the supernatant, suggesting that **1** is kept intracellularly

and not secreted into the medium. Bioactivity tests show that this natural product has potential cytotoxicity activity against colon carcinoma cells HCT-116 (Table 1) and leukemia cells (Figure 9) (more in Antimicrobial Activity and Cytotoxicity Activity sections).

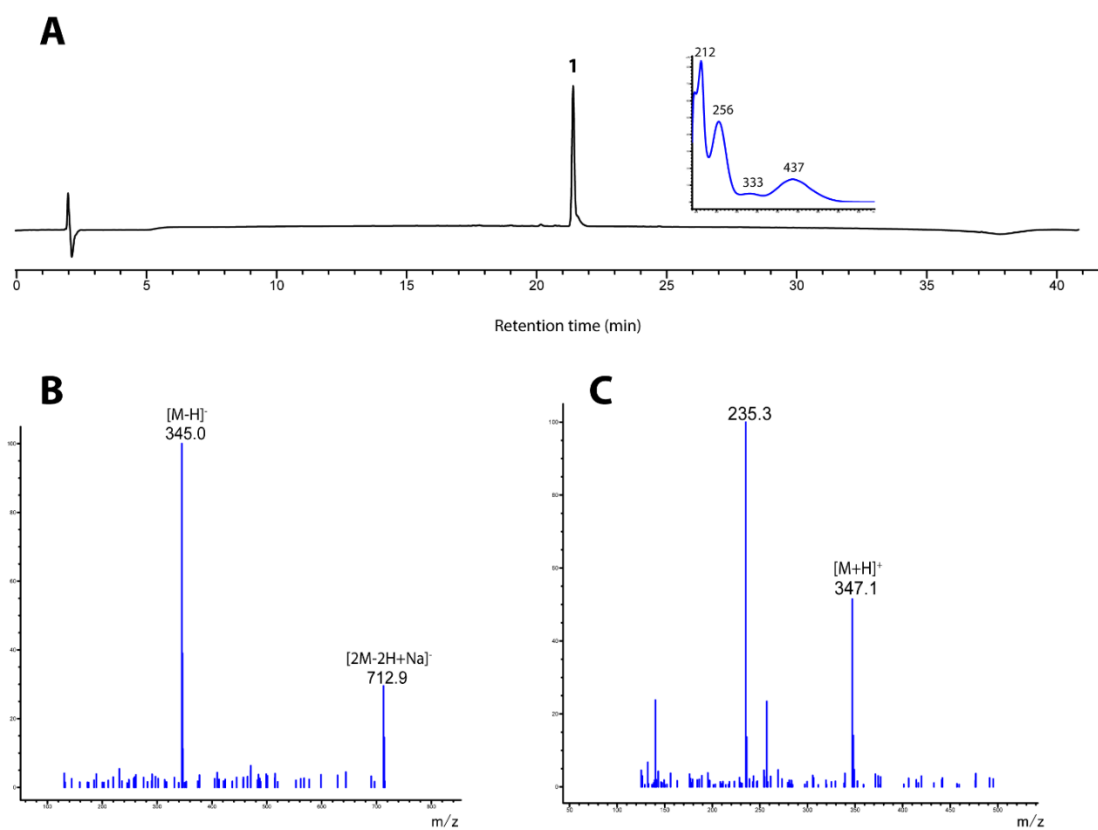


Figure 4. LC/MS analysis of 8,8'-bijuglone (1). (A) Absorption at 210 nm in black with UV chromophore insert in blue, (B) MS spectrum in negative ionization, (C) MS spectrum in positive ionization.

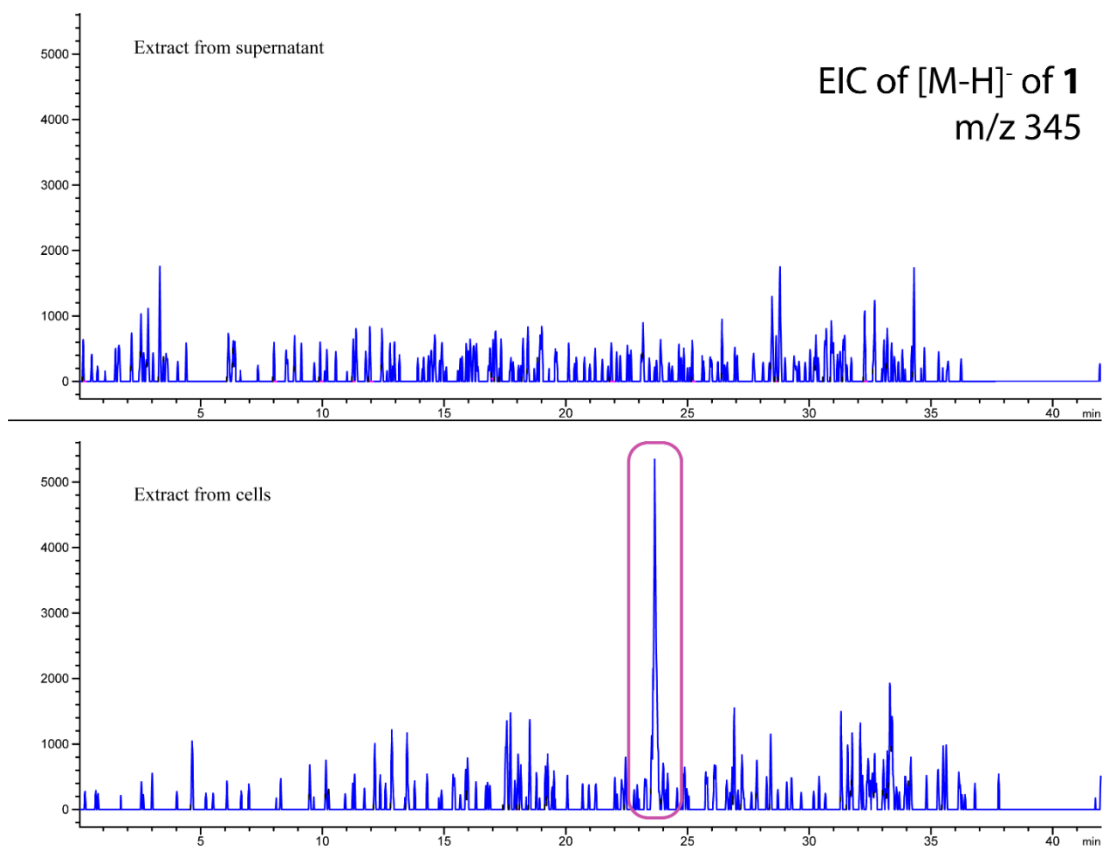


Figure 5. LC/MS analysis of extracts of *Z. pseudotsugae* fungal cells vs. supernatant. EICs refer to $[M-H]^-$ ion for (1) are illustrated for extract from the supernatant (top chromatogram) vs. extract from the cells (bottom chromatogram).

2.3.1 Physiochemical properties of 8,8'-bijuglone

8,8'-bijuglone (**1**): orange, needle-like crystal; $[\alpha]_D^{20} = 0$; The molecular formula was determined as $C_{20}H_{10}O_6$ based on the QTOF-HRMS with m/z 346.0477 $[M]^-$ calcd. for $C_{20}H_{10}O_6^-$, 346.04829; IR (ATIR) 2924, 2854, 1640 cm^{-1} ; 1H -NMR (500 MHz, $CDCl_3$) δ 12.49 (s, 1H, 5-OH, 5'-OH), 7.31 (d, 1H, $J=8.7$ Hz, 6-CH, 6'-CH), 7.24 (d, 1H, $J=8.7$ Hz, 7-CH, 7'-CH), 6.92 (d, 1H, $J=10.2$ Hz, 2-CH, 2'-CH), 6.71 (d, $J=10.2$ Hz, 1H, 3-CH, 3'-CH); ^{13}C -NMR (500 MHz, $CDCl_3$) δ 190.8 (4-C, 4'-C), 184.9 (1-C, 1'-C), 161.9 (5-C, 5'-C), 140.6 (3-CH, 3'-CH), 138.7 (7-CH, 7'-CH), 138.0 (2-CH, 2'-CH),

135.2 (8-C, 8'-C), 128.3 (9-C, 9-'C), 124.8 (6-C, 6-'C), 115.5 (10-C, 10-'C). 2D NMR spectroscopic data in the [Supplementary Information](#).

2.3.2 Solubility and stability of 8,8'-bijuglone

1 was soluble in ethyl acetate, ethanol, methanol, acetone, dimethyl sulfoxide (DMSO) and acetonitrile. While soluble, **1** was unstable in DMSO. Overtime, **1** formed a dark-amber-orange precipitate in DMSO, which was insoluble in ethyl acetate, ethanol, methanol, acetone, and acetonitrile. This unknown compound was either a degradation product or a larger structure made of the naphthoquinone. It is possible that an oxidation-reduction (redox) reaction occurred where DMSO was reduced to dimethyl sulfide, and **1** was oxidizes into a larger, unidentified compound.⁷⁸⁻⁸¹

Another possible reaction was that **1** could undergo an acid-base reaction. To test this idea, the compound was dissolved in acetonitrile at 10 mg/mL and then a drop of either 1M hydrochloric acid (HCl) or 1M sodium hydroxide (NaOH) was added. In the acidic condition, there was no change in physical appearance. In the basic condition, the solution



Figure 6. Acid/Base effect of 8,8'-bijuglone. In acetonitrile plus one drop of 1M HCl (left vial) or in acetonitrile plus one drop of 1M NaOH (right vial).

turned purple and there was a precipitate (Figure 6). This characteristic color change could potentially be explained by an electron donation from the hydroquinone portion, after the base removed the chelating proton, into the benzoquinone portion of **1**, as illustrated by the purple quinhydrone via a charge-transfer complex.⁸² Addition of

methanol (MeOH) dropwise shifted the precipitate back into solution. Both the acid and base solutions of **1** were analyzed by LC/MS on standard gradient of 10%-100% acetonitrile + 0.05% formic acid over 35 minutes (**Figure A8**). The acidic sample still showed **1** at the expected retention time with same UV spectrum. However, the basic sample did not show **1**, suggesting that the deprotonated form of **1** was not readily detectable in our LC/MS system. From these results, **1** was most stable in acidic conditions and unstable in basic conditions.

2.3.3 Antimicrobial activity

1 was evaluated for antimicrobial activity against three Gram-positive bacteria, methicillin-resistant *Staphylococcus aureus* (MRSA) BAA-41, *Bacillus subtilis* (ATCC 49343), and *Mycobacterium smegmatis* (ATCC 14468), two Gram-negative bacteria, *Escherichia coli* (ATCC 8739) and *Pseudomonas aeruginosa* (ATCC 15442), and a fungal strain *Candida albicans* (ATCC 90027). **1** showed moderate activity against MRSA and *B. subtilis* (Table 1). Against MRSA, **1** induced 29.3% bacterial cell survival and against *B. subtilis* bacterial cell survival was 32.6% when tested at 125 $\mu\text{g}/\text{mL}$ in ethanol (Table 1). Other similar compounds like **1** have been reported to have antibacterial activity, including 8,8'-biplumbaign (also called maritinone),^{76, 83} chitranone⁷⁶ and diospyrin,⁸⁴ (Figure 7 and Table A2).



Figure 7. Analogs of 8,8'-bijuglone.

Table 1. Biological activities of 8,8'-bijuglone (1).

SAMPLE	Antibacterial					Antifungal
	MRSA	<i>Bacillus subtilis</i>	<i>Mycobacterium smegmatis</i>	<i>Escherichia coli</i>	<i>Pseudomonas aeruginosa</i>	<i>Candida albicans</i>
8,8'-bijuglone	29.3%	32.6%	91.5%	97.1%	86.0%	99.5%
positive control	0.0%	15.1%	1.5%	11.6%	0.2%	23.6%
	vancomycin	chloramphenicol	rifampicin	ampicillin	kanamycin	amphotericin B
negative control	> 100%	68.4%	100%	89.0%	92.4%	100%
	ethanol	ethanol	DMSO	ethanol	ethanol	ethanol

Samples & positive controls were tested to a final concentration of 125 µg/mL
 Negative controls were tested at 1.25% ethanol, expect *M. smegmatis* in DMSO.

Methicillin-resistant *Staphylococcus aureus* (BAA-44) = MRSA
Bacillus subtilis (ATCC 49343)
Mycobacterium smegmatis (ATCC 14468)
Escherichia coli (ATCC 8739)
Pseudomonas aeruginosa (ATCC 15442)
Candida albicans (ATCC 90027)

2.3.4 Cytotoxicity activity

To assess the cytotoxicity of **1**, the highly enriched extract was tested against the human colon carcinoma cell line HCT-116 (ATCC® CCL-247™). The compound was active on the first single dose MTT assay with 15.6% average cell survival when tested at 10 µg/mL (29 µM) (Table 2). The IC₅₀ value of **1** against HCT-116 was determined to be 130 µM (0.13 mM), exhibiting weak cytotoxicity (Figure 8). Due to

this activity, **1** was submitted to the National Cancer Institute (NCI) for evaluation against their NCI-60 cancer cell line panel. The compound showed lethal activity against all six leukemia cancer cell lines (Figure 9). In order to obtain an IC_{50} value against a panel of leukemia cancer cell lines, Dr. Tom O'Hare and his team at Huntsman Cancer Institute, Utah tested the compound against eight acute myeloid leukemia (AML) cell lines different from the ones used by the NCI. However, **1** had no effect against their cell lines, most likely due to the high percentage of ethanol when the dilution samples were prepared for the assay or degradation of **1**.

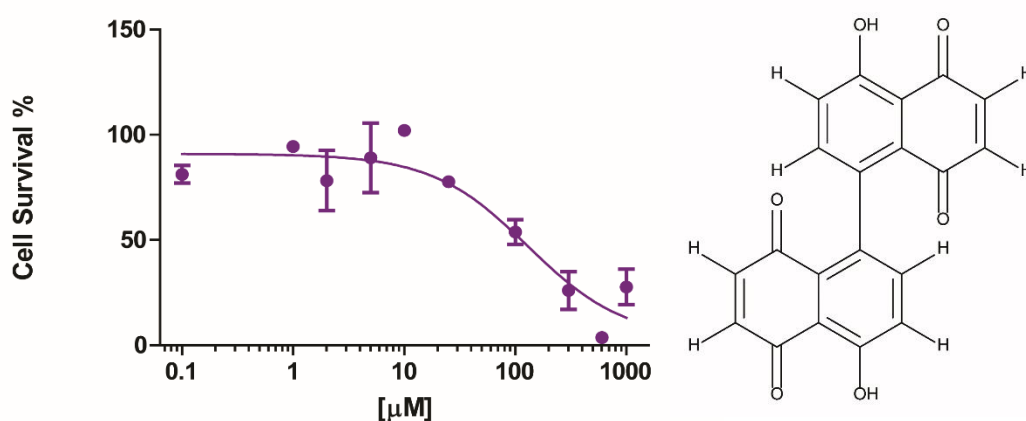


Figure 8. IC_{50} curve of 8,8'-bijuglone against human colon carcinoma (HCT-116). The IC_{50} value was determined to be 130 μM (0.13mM).

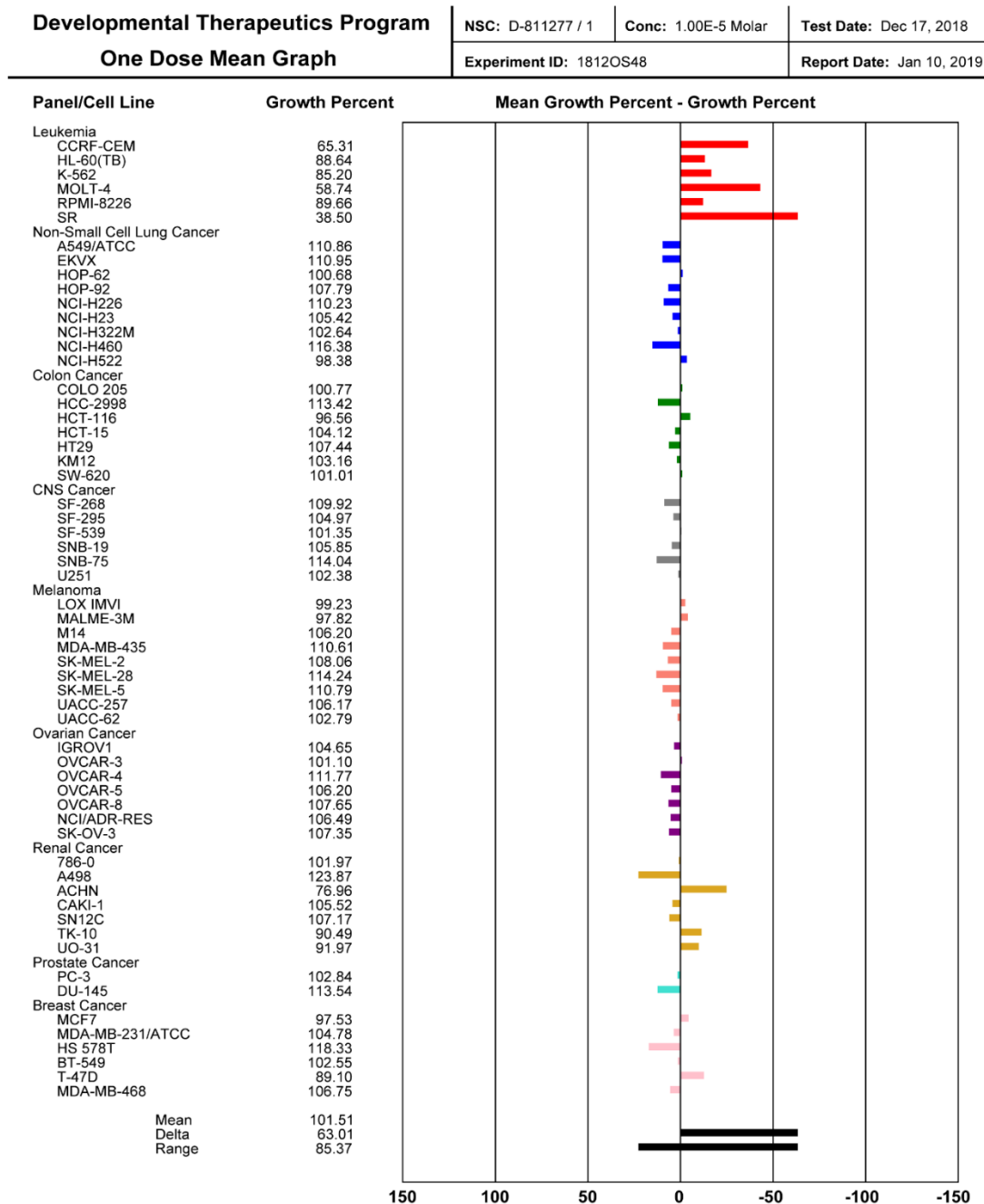


Figure 9. Mean graph display of NCI-60 cell line screening data for 8,8'-bijuglone. Sample concentration at 10 μ M. Bars to the right indicate high lethality, bars to the left indicate growth inhibition. Experiments were performed at the NCI-DTP. ⁸⁵

2.3.5 AntiSMASH results of *Z. pseudotsugae*

Genome mining is now widely used for identification and connection of biosynthetic gene clusters (BGCs) to their respective secondary metabolites in microorganism and plants. Bioinformatic tools have become an important complementary asset for compound-driven natural product discovery. A draft genome for *Z. pseudotsugae* was made available to Dr. Jeff Stone and we applied the genome mining software antiSMASH to generate and identify BGCs in *Z. pseudotsugae* (Figure 10).⁸⁶ A total of 36 BGCs were predicted by the software, including 14 NRPS-like, 17 Type 1 PKS (T1PKS), two terpenes and one fungal ribosomally synthesized and post-translationally modified peptides (fungal-RiPP). Of these, a few BGCs showed a match for a small molecule class searched against a comprehensive gene cluster database known as Minimum Information about a Biosynthetic Gene cluster (MIBiG) of characterized gene clusters,⁸⁷ some of which exhibited 100% similarity to known compounds, including (-)-mellein (T1PKS), cercosporin (NRPS), aureobasidin A1 (NRPS), phomopsins (fungal-RiPP), and elsinochrome A (T1PKS). Interestingly, the compounds cercosporin and elsinochrome have a core structure that resembles **1** (highlighted in blue in Figure 10), suggesting that **1** could possibly be a precursor to form these type of compounds in *Z. pseudotsugae* or that clusters may generate compounds identical to already known compounds.

Since the antiSMASH results detected compounds with 100% similarity, an extract of *Z. pseudotsugae* was analyzed by extracted-ion chromatogram (EIC) for the presence of the above mentioned molecules (**Figure 11**). The extract was further

fractionated by vacuum liquid column chromatography (VLCC) with a gradient of dichloromethane (DCM) to methanol (MeOH) to give eight fractions. By EIC, there is a possibility that there is *O*-methylmellein and other mellein analogous in VLCC F4 at ~10 min retention time, elsinochrome A in VLCC F3 at ~18 min, and bassianolide in VLCC F4 at ~26 min. To further prove the presence of these compounds, they would need to be purified by high performance liquid chromatography (HPLC) and analyzed by NMR to verify their structures.

Identified secondary metabolite regions			
Region	Type	Most similar known cluster	Similarity
Region 7.1	NRPS-like ☞		
Region 17.1	T1PKS ☞	Aflatoxin/sterigmatocystin ☞ t1pks	23%
Region 57.1	NRPS-like ☞		
Region 83.1	T1PKS ☞		
Region 109.1	T1PKS ☞		
Region 136.1	NRPS-like ☞		
Region 136.2	NRPS ☞		
Region 149.1	NRPS ☞ , T1PKS ☞		
Region 149.2	T1PKS ☞		
Region 228.1	T1PKS ☞	(-)-Mellein ☞ t1pks	100%
Region 248.1	NRPS-like ☞		
Region 286.1	T1PKS ☞	Cercosporin ☞ t1pks	100%
Region 296.1	NRPS ☞	Aureobasidin A1 ☞ NRPS	100%
Region 340.1	T1PKS ☞ , terpene ☞		
Region 431.1	T1PKS ☞	F9775 ☞ t1pks	30%
Region 469.1	T1PKS ☞	Terreic acid ☞ t1pks	22%
Region 577.1	NRPS-like ☞		
Region 618.1	terpene ☞		
Region 658.1	NRPS-like ☞		
Region 658.2	T1PKS ☞	Emericellin ☞ t1pks	28%
Region 692.1	NRPS-like ☞		
Region 779.1	NRPS ☞		
Region 795.1	NRPS ☞		
Region 801.1	T1PKS ☞	F9775 ☞ t1pks	20%
Region 807.1	T1PKS ☞	Azaphilone ☞ t1pks	8%
Region 824.1	NRPS ☞		
Region 876.1	fungal-RiPP ☞	Phomopsins ☞ other	100%
Region 901.1	T1PKS ☞		
Region 927.1	terpene ☞		
Region 938.1	NRPS ☞ , NRPS-like ☞		
Region 945.1	T1PKS ☞		
Region 948.1	T1PKS ☞	Neurosporin A ☞ t1pks	20%
Region 951.1	T1PKS ☞		
Region 957.1	T1PKS ☞	Trans-resorcyliide ☞ t1pks	33%
Region 977.1	NRPS-like ☞		
Region 1012.1	T1PKS ☞	Elsinochrome A ☞ t1pks	100%

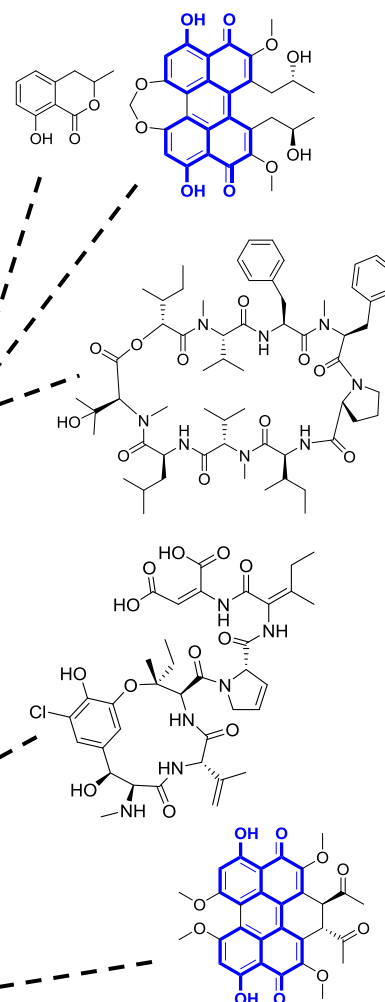


Figure 10. Biosynthetic gene clusters in *Z. pseudotsugae* generated identified by antiSMASH. Clusters with 100% similarity to a compound are shown on the right. The structure of 8,8'-bijuglone is highlighted in blue in the core structures of cercosporin and elsinochrome.

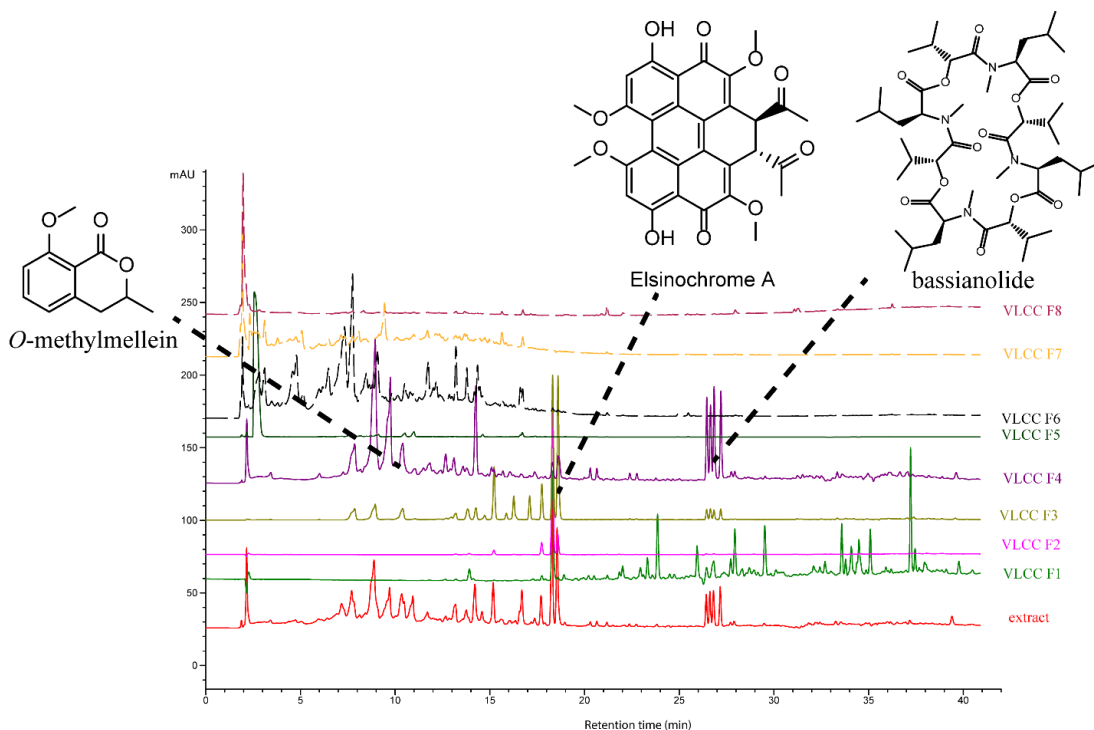


Figure 11. LC/MS traces of *Z. pseudotsugae* extract (extract) and VLCC fractions F1-F8. Absorbance at 280 nm. Possible core structures identified in these fractions by extract-ion chromatogram based on expected masses (EIC).

2.4 Conclusion

In the 1990s, large-scale defoliation was seen on Douglas-fir in the Pacific Northwest, leading to decreased growth and yield. The associated fungus *Nothophaeocryptopus gaumannii* was found to be the causal agent linked to Swiss needle cast (SCN). Other Douglas-fir associated fungi, such as the epiphytic fungus *Zasmidium pseudotsugae*, are also found in the fir microbiome with *N. gaumannii*, but this fungus has not been shown to cause any harm to the trees. Here, we present preliminary results of the chemical exploration of *Z. pseudotsugae*. We report 8,8'-bijuglone (**1**) to be isolated from a natural source for the first time. **1** shows weak

cytotoxicity activity against colon carcinoma (HCT-116) with an IC_{50} value of $130\ \mu\text{M}$ ($0.13\ \text{mM}$). There is also potential for **1** to be selective cytotoxic against leukemia cells according to NCI results. Additionally, we tested **1** for antimicrobial and antifungal activity, but without effect. We continue in our search for more compounds produced from *Z. pseudotsugae* along with its plant pathogenic counterpart *N. gaeumannii* for novel and bioactive secondary metabolites in order to shed light on fungal-fungal and fungal-plant chemical interactions.

2.5 Materials & Methods

2.5.1 Foliage sampling

At each site, foliage was collected from second- and third-year internodes on secondary branches in the upper crowns of five randomly selected 10- to 30-year-old Douglas-fir trees. From one of the five trees sampled at each of the SNC sites, foliage samples were also collected from the lower, mid, and upper crowns to assess within-tree diversity. The foliage was stored on ice and promptly returned to the campus of Oregon State University for storage in a cold room for no longer than 5 days prior to processing. Needles with pseudothecia fungi were attached to the lids of Petri dishes with double-sided adhesive tape, placed over water agar, and incubated for 48–72 hours. Individual ascospores were removed from the agar with sterilized forceps and transferred onto 2% malt agar (MA) (Difco Laboratories, Detroit, MI). Cultures were incubated at $18^\circ\ \text{C}$ for a minimum of 2–6 months.

2.5.2 Culture media & fermentation

2% Malt: malt extract (2% g/L) (CriterionTM Malt Extract, Hardy Diagnostic) and no pH adjustment prior to sterilization. For agar plates 15 g/L nutrient agar was added to the culture media before sterilization. *Zasmidium pseudotsugae* was inoculated onto 2% malt agar plates (MA) (40 × 25 mL) with a 1 cm² piece of agar from a single culture and allowed to grow at ambient light and temperature for 5 months. Broth cultures (50 mL) were inoculated with a 1 cm² piece of agar from the 5-month-old agar culture and allowed to grow at 28 °C on an orbital shaker at 110 rpm for 1 month. Large scale broth cultures (1L) were inoculated with 20 mL culture material from a 50 mL broth culture and allowed to grow at 28 °C on an orbital shaker at 110 rpm for 2-3 months.

2.5.3 Preparation of organic extracts

The agar cultures were blended with an equivalent portion of ethyl acetate, while the broth cultures were extracted using equal parts ethyl acetate for 24 h with stirring. The organic layer from either the agar cultures or broth culture was separated and then concentrated under reduced vacuum. The extracts were solubilized in acetonitrile and were subjected to LC/MS analysis.

2.5.4 General spectroscopic and chromatographic procedures

Optical rotation was measured on a JACS P-1010 polarimeter. Infrared (IR) spectra were recorded on a Thermo Scientific Nicolet IR100 FTIR spectrometer. Low-resolution ESI-MS mass spectra were recorded on Agilent 1100 series LC with MSD 1946 (LC/MS). High-resolution ESI-MS spectra were recorded on an Agilent 6545

LC/Q-TOF MS. The mobile phase consisted of ultra-pure water (A) and acetonitrile (ACN) (B) with 0.05% formic acid. A gradient method from 10% B to 100% B in 35 min at a flow rate of 0.8 ml/min was used. The column (Phenomenex Kinetex C18, 5 μm x 150 mm x 4.6 mm) was re-equilibrated before each injection, and the column compartment was maintained at 30 °C throughout each run. Agilent 1100 Infinity HPLC system was used for semipreparative separations equipped with photodiode array detectors. NMR spectra were acquired on a Bruker Avance III 500 MHz spectrometer, equipped with a 5 mm TXI probe. Solvent peaks of CDCl_3 (δ_{H} 7.26; δ_{C} 77.06) was used as internal standard.⁸⁸ Solvents, media ingredients, and general reagents were from Sigma-Aldrich Corp., Fisher Scientific, and VWR International.

2.5.5 HPLC isolation & purification of 8,8'-bijuglone

The ethyl acetate extract from the agar plate was subjected to semipreparative HPLC using an isocratic elution of (ACN/ H_2O (50:50) + 0.05% formic acid) for purification to yield 1.2 g of compound **1**.

2.5.6 Antimicrobial assays

Extracts, fractions, and pure compounds were tested for activity in cell-based microbroth single dose assays following established protocols.⁸⁹ The antimicrobial activity was evaluated against these microorganisms: Methicillin-resistant *Staphylococcus aureus* (BAA-44), *Bacillus subtilis* (ATCC 49343), *Mycobacterium smegmatis* (ATCC 14468), *Escherichia coli* (ATCC 8739), *Pseudomonas aeruginosa* (ATCC 15442) and *Candida albicans* (ATCC 90027). Antibiotic positive controls

(vancomycin, chloramphenicol, rifampicin, ampicillin, kanamycin, and amphotericin, respectively) were used at 125 $\mu\text{g}/\text{mL}$, while DMSO was used as the negative control at 1.25% v/v. Compound (1) was prepared at 10 mg/mL in DMSO, added to wells in duplicate at a final concentration of 125 $\mu\text{g}/\text{mL}$.

2.5.7 Cytotoxicity assay

Extracts, fractions, and pure compounds were tested for cytotoxicity activity in cell-based assays following established protocols.⁹⁰ Effects on mammalian cell viability were determined by measuring the reduction of the tetrazolium salt MTT (3-(4,5-dimethylthiazolyl-2)-2,5-diohenyltetrazolium bromide) by metabolically active cells. Human colon cancer (HCT-116) cell line was obtained from the American Type Culture Collection (ATCC). HCT-116 cells were maintained in MEM supplemented with 10% (v/v) fetal bovine serum, penicillin (100 U/mL), and streptomycin (100 $\mu\text{g}/\text{mL}$). The cell lines were incubated at 37 °C in 5% CO₂. Cells were plated into 96-well plates at 7000 cells/well cell density, incubated overnight, and treated with the addition of 10 $\mu\text{g}/\text{mL}$ compound and controls to each well. After 48 h, MTT (5 mg/mL in phosphate-buffered saline) was added to each well at a final concentration of 0.5 mg/mL. The plates were incubated for 2 h at 37 °C. The medium was removed, and the purple formazan product solubilized by the addition of 50 μL of DMSO. Absorbance was measured at 550 nm using the Biotek Synergy 96-well plate reader. Metabolic activity of vehicle-treated cells (0.1% v/v DMSO) was defined as 100% cell growth. Etoposide (250 μM) was used as a positive control. IC₅₀ value for pure compound was determined using a 10-point dilution dissolved in PBS + 5% ethanol. Effect on acute

myeloid leukemia (AML) cells were determined at University of Utah, where they focus on molecular mechanism of resistance related to chronic myeloid leukemia (CML).⁹¹ The cytotoxicity activity was evaluated against eight AML cells: OCI-AML2, CMK, HL-60, MOLM-13, MOLM-14, KG1a, OCI-AML3, SKM. Compound was dosed from a 10 mM stock dissolved in ethanol.

2.6 Acknowledgements

We thank Dr. Jeffrey Stone (Oregon State University), his lab team, and his collaborators for supplying the fungal strains and the genome data. We also thank Dr. Tom O'Hare and Orlando Antelope (University of Utah) for testing samples against their AML cancer cell line panel.

3 Algal-derived fungal endophyte *Penicillium crustosum*

3.1 Abstract

Two known compounds, clavatol (**2**) and hydroxyclavatol methyl ether (**3**) were isolated from an algal-derived fungal endophyte, identified as *Penicillium crustosum*. The structures of **2** and **3** were deduced based on IR, NMR, HRMS, and X-ray crystallography spectral analyses. The fungal extract was evaluated for its antimicrobial activity against bacterial and fungal human pathogens (*Bacillus subtilis*, methicillin-resistant *Staphylococcus aureus* (MRSA), *Mycobacterium smegmatis*, *Pseudomonas aeruginosa*, *Candida albicans*) and evaluated for cytotoxicity activity against human colon carcinoma (HCT-116).

3.2 Introduction

In recent years, natural products discovery programs have continued to shift to less explored biospheres. For example, marine natural products have shown striking structural features compared to terrestrial microorganisms.⁹²⁻⁹⁴ Fungi associated with marine algae have been good sources for new structurally diverse chemical compounds with biological activity.^{89, 95} These are known as “marine algicolous fungi” (MAF), fungi that can inhabit or associate with marine algae, not including fungi associated with seagrass, freshwater algae, and other marine plant materials.⁹⁶⁻⁹⁷ MAF can either live in the inner tissues of algal cells as endophytes or live superficially as epiphytes. In either case, these fungi may form parasitic, saprobic, symbiotic, or pathogenic

associations with their algal hosts.⁹⁷ Evidently, natural products may play a key role in maintaining associated relationships between algal and fungal cells, and the production of these secondary metabolites can have a wide range of bioactivities. For examples, from the culture of the endophytic fungus *Trichoderma harzianum* isolated from the brown alga *Laminaria japonica*, two unique diterpenes, 3*R*-hydroxy-9*R*,10*R*-dihydroharzianone and 11*R*-methoxy-5,9,13-proharzitrine-3-ol, were isolated with antialgal and antibacterial activities.⁹⁸ From another algal-associated endophytic fungus *Talaromyces islandicus*, isolated from a red alga *Laurencia okamurai*, various new hydroanthraquinones were isolated and identified: 8-hydroxyconiothyronone B, 4*S*,8-dihydro-10-*O*-methyldendryol E, among other polyhydroxylated hydroanthraquinones with antimicrobial, antioxidant, and cytotoxic activities.⁹⁹

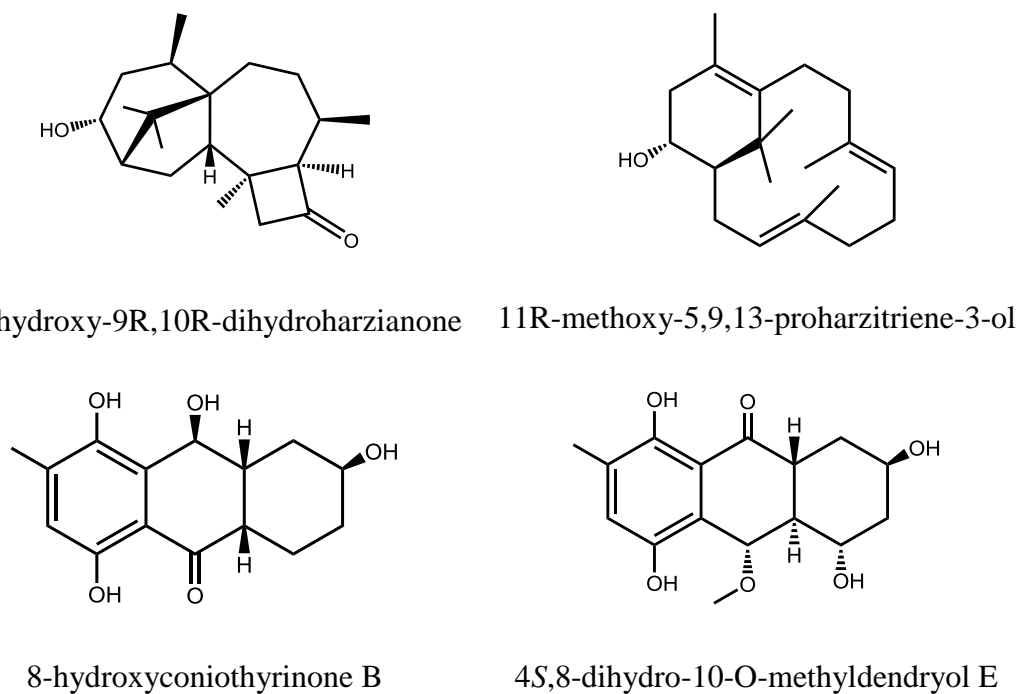


Figure 12. Secondary metabolites isolated from marine algal-associated endophytic fungi.⁹⁸⁻⁹⁹

In the on-going search for potentially bioactive or novel secondary metabolites from algae-derived fungi, a fungal endophyte was collected off the coast of the Gozo Island in the Mediterranean Sea. Chemical investigation of the organic extract led to the isolation of known compounds (**2-3**) (Figure 13). The fungal extract and the purified hydroxyclovatol methyl ether **3** were evaluated in selected bioassays. ITS based sequencing identified the endophyte as *Penicillium crustosum*. Herein, the details of the isolation, structure elucidation, and bioactivities of the compounds is reported.

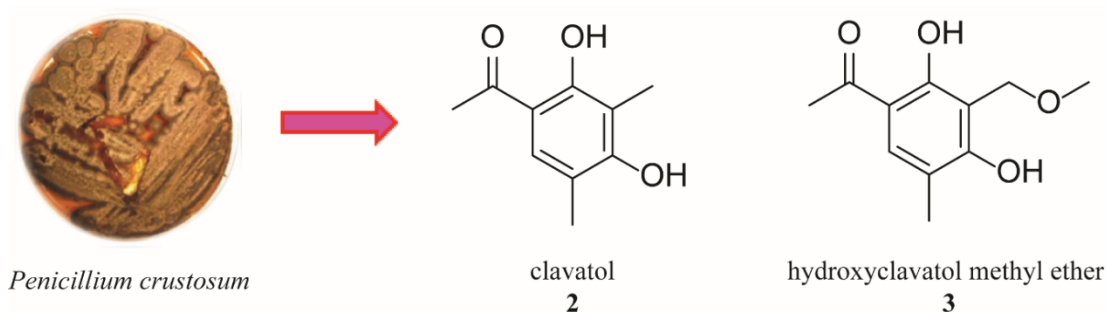


Figure 13. Secondary metabolites from *Penicillium crustosum* (**2-3**).

3.3 Results & Discussion

The strain of *Penicillium crustosum* was isolated from a marine alga by BioViotica Naturstoffe GmbH (Germany) and provided to us for chemical analysis. The species was identified by Sanger sequencing of PCR fragments amplified from the ITS and β -tubulin loci and sequencing results were matched with MEGA7 to known fungal species.¹⁰⁰ DNA sequences showed 100% sequence identity to *Penicillium crustosum* (Figures A7-A8).

Secondary metabolites of *P. crustosum* grown in a glycerin-based medium were extracted and analyzed by LC/MS (Figure 14). Glycerin was the best nutrient media based on more observation of compounds present in the extract by thin-layer chromatography (TLC) (Figure A13). One dominant metabolite was detected in a 14 day-old 1L shaking culture, which was identified as hydroxyclavatul methyl ether (**3**) after HPLC isolation and X-ray based solid state analysis (Figure 15). From an 11-day-old 5L shaking culture, another metabolite was identified as clavatul (**2**) after HPLC isolation and structure elucidated by NMR (Figures A3-A7).¹⁰¹⁻¹⁰⁴

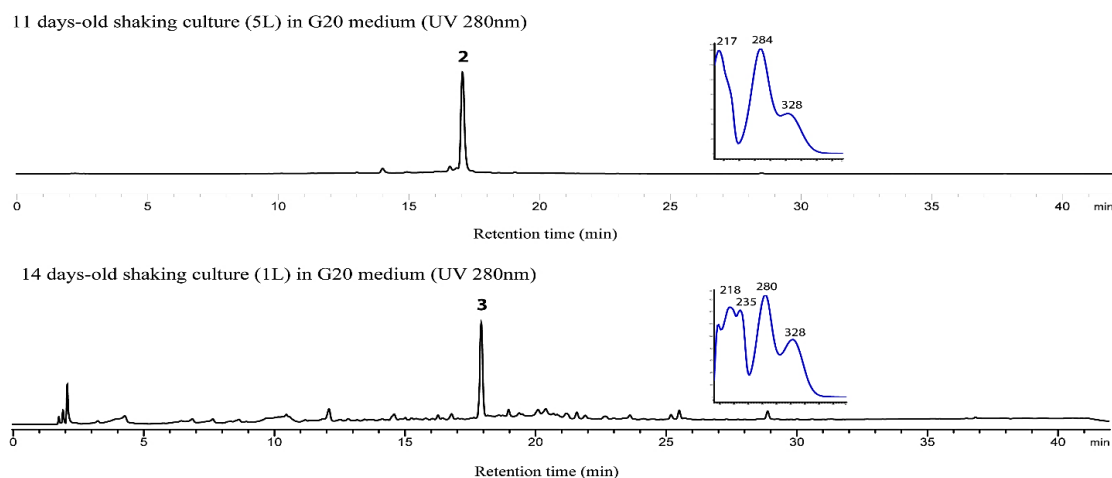


Figure 14. LC/MS analysis of compounds **2** and **3** from liquid glycerin-based medium (G20) cultures of *P. crustosum* (absorptions at 280 nm). UV spectra are shown in blue insert.

3.3.1 Physicochemical properties of the secondary metabolites

Clavatul (**2**): colorless solid; The molecular formula was determined as $C_{10}H_{12}O_3$ based on the QTOF-HRMS peaked at m/z 179.0714 $[M - H]^-$ calcd. for $C_{10}H_{11}O_3^-$, 179.07137; IR (ATIR) 3396, 2981, 2926, 1628 cm^{-1} ; 1H -NMR (700 MHz, $CDCl_3$) δ 12.86 (s, 1H, 2'-OH), 7.35 (s, 1H, 6'-CH), 5.22 (s, 1H, 4'-OH), 2.54 (s, 3H, 1- CH_3), 2.19 (d, $J=0.73$ Hz, 3H, 7'- CH_3), 2.12 (s, 3H, 8'- CH_3); ^{13}C -NMR (700 MHz, $CDCl_3$) δ 202.9 (2-C),

161.5 (4'-C), 158.9 (2'-C), 130.1 (6'-C), 114.7 (5'-C), 113.6 (3'-C), 110.4 (1'-C), 26.5 (1-CH₃), 15.8 (7'-CH₃), 7.6 (8'-CH₃). 2D NMR spectroscopic data in the [Supplementary Information](#).

Hydroxyclavatul methyl ether (**3**): colorless needles; The molecular structure was determined by X-ray single crystal diffraction (Figure 15) and determined as hydroxyclavatul methyl ether, also known as 2,4-dihydroxy-3-methoxymethyl-5-methylacetophenone.

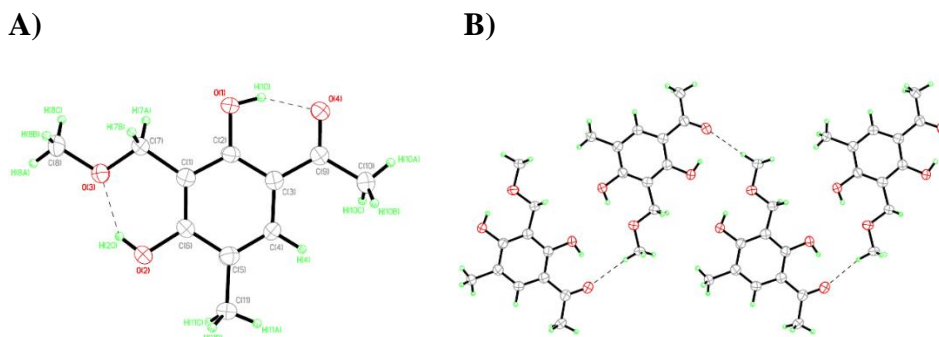


Figure 15. (A) The X-ray crystal structure of **3**. (B) Part of the crystal lattice packing diagram to illustrate the hydrogen-bonded complementarity found in the X-ray crystal structure.

3.3.2 Antimicrobial activity

The fungal extract of *Penicillium crustosum* was evaluated for antimicrobial activity against three Gram-positive bacteria, methicillin-resistant *Staphylococcus aureus* (MRSA) (BAA-41), *Bacillus subtilis* (ATCC 49343), and *Mycobacterium smegmatis* (ATCC 14468), one Gram-negative bacterium, *Pseudomonas aeruginosa* (ATCC 15442), and a fungal pathogen, *Candida albicans* (ATCC 90027). The extract exhibited activity against MRSA with 20.4% bacterial cell survival, *B. subtilis* with 4.6% bacterial cell survival, and *M. smegmatis* with 5.7% bacterial cell survival all

tested at 125 $\mu\text{g}/\text{mL}$ (Table 2). Purified compound **3** was evaluated in selected antimicrobial assays but showed no activity (Table 2). Compound **2** was not tested again because it was isolated from a previously inactive fraction. Unfortunately, the activity found in the extract against MRSA could not be identified. However, there have been a few reports of extracts or compounds isolated from *P. crustosum* with activity against *S. aureus*. De Souza et al. reported *P. crustosum* to inhibit *S. aureus* with a moderate minimum inhibition concentration (MIC) of 256 $\mu\text{g}/\text{mL}$,¹⁰⁵ although no compound was mentioned. Zhang et al. reported a few quinolinones from a shark gill-derived *P. crustosum* AP2T1 with weak inhibition against *S. aureus* in an agar disk diffusion assay.¹⁰⁶ Even though *Penicillium crustosum* has been studied previously and some compounds have been isolated, it seems that new secondary metabolites could potentially be found with bioactivity.

3.3.3 Cytotoxicity activity

To assess cytotoxic potential, the fungal extract was tested against the human colon carcinoma cell line HCT-116 (ATCC[®] CCL-247TM). The organic extract was not active at a final concentration of 10 $\mu\text{g}/\text{mL}$, compound **3** was tested at a final concentration of 1 $\mu\text{g}/\text{mL}$ and not active either (Table 2).

Table 2. Antimicrobial and cytotoxic activities of *P. crustosum* extract and compounds 2-3.

SAMPLE	ANTIBACTERIAL				ANTIFUNGAL	Cytotoxicity
	MRSA	<i>Bacillus subtilis</i>	<i>Mycobacterium smegmatis</i>	<i>Pseudomonas aeruginosa</i>	<i>Candida albicans</i>	HCT-116
organic extract	24.1%	4.6%	5.7%	85.7%	>100%	83.2%
2	N/A	N/A	N/A	N/A	N/A	N/A
3	>100%	>100%	N/A	93.2%	N/A	N/A
positive control	0.0%	15.1%	1.5%	0.2%	7.9%	31.1%
	vancomycin	chloramphenicol	rifampicin	kanamycin	amphotericin B	etoposide
negative control 1	100%	47.2%	100%	100%	100%	100%
	DMSO	DMSO	DMSO	DMSO	DMSO	DMSO
negative control 2	>100%	68.4%	N/A	92.4%	N/A	N/A
	ethanol	ethanol	N/A	ethanol	N/A	N/A

Samples and positive controls for antibacterial and antifungal were tested to a final concentration of 125 µg/mL. Samples for cytotoxicity were tested to a final concentration of 10 µg/mL for extracts or 1 µg/mL for pure samples. Positive control for cytotoxicity assay tested at 250 µM. Negative control for antimicrobial assays at 1.25% v/v DMSO. Negative control for cytotoxicity assay at 0.1% v/v DMSO or ethanol. N/A: not applicable because it was not tested.

Methicillin-resistant *Staphylococcus aureus* (BAA-44) = MRSA
Bacillus subtilis (ATCC 49343)
Mycobacterium smegmatis (ATCC 14468)
Escherichia coli (ATCC 8739)
Pseudomonas aeruginosa (ATCC 15442)
Candida albicans (ATCC 90027)

3.4 Conclusion

Known clavatols (**2-3**) were isolated from the Mediterranean alga derived fungus *Penicillium crustosum*. These compounds have been isolated from other *Penicillium* species.^{102, 107-108} In fact, through gene deletion, feeding experiments, and biochemical investigations, it was recently discovered that a nonreducing PKS (NR-PKS) ClaF is responsible for the formation of clavatul, then ClaD oxidizes clavatul to hydroxylavatul by a nonheme Fe^{II}/2-oxoglutarate-dependent oxygenase, and hydroxylavatul methyl ether is subsequently formed from non-enzymatic conversions from hydroxylavatul.¹⁰² Herein, we also assessed the bioactivity potential of the fungal

extract and the isolated compounds. The fungal broth was analyzed in several assays to provide information on its antimicrobial and cytotoxic activities. Notably, the fungal extract was active in the MRSA assay with 20.4% inhibition of growth at 125 µg/mL. For future work, it would be interesting to study the full metabolomic potential of *Penicillium crustosum* using a bioassay-guided approach with MRSA activity to identify the secondary metabolite that is responsible for the activity observed in the fungal extract.

3.5 Acknowledgements

We thank BioViotica (Prof. Dr. Axel Zeeck and Hans-Peter Kroll) for providing the marine algal endophyte. We also thank Dr. Lev Zakharov who performed X-ray crystallography analysis.

3.6 Materials & Methods

3.6.1 Biological material

The fungal strain used in this study was isolated from an alga off the coast of the Gozo Island in the Mediterranean Sea by BioViotica Naturstoffe GmbH (Germany).

3.6.2 Culture media & fermentation

For broth culture grows of *P. crustosum*, the medium G20 was used containing glycerin (20 g/L), malt extract (10 g/L), and yeast (4 g/L) with no pH adjustment prior to sterilization. For agar cultures, the medium 2% malt was used containing malt extract (2% g/L) and nutrient agar (15 g/L) with no pH adjustment prior to sterilization.

Broth fungal cultures in G20 medium (50 mL, n=2 replicates) were inoculated with a 1 cm² piece of fungus grown on 2% malt agar plates (1-2 weeks old) and cultivated at 28 °C on an orbital shaker at 110 rpm for 7-9 days. The 50 mL starter culture was then propagated into subsequent larger growths of G20 media (1 L) and grown at 28 °C on an orbital shaker at 110 rpm for 11-14 days.

3.6.3 Identification of the fungus

The fungal strain was grown in 50 mL of G20 media for 3-4 days and 0.5 mL of mycelia cells were collected by centrifugation. The cell pellet was frozen dry in a mixture of acetone and dry ice then 0.5 mL of zirconium silicate beads were added and the mixture vortexed for 10 minutes. DNA extraction was extracted and purified using *E.Z.N.A.[®] SP Fungal DNA Mini Kit* (Norcross, GA, USA) following the manufacturer's instructions. For taxonomic analysis, the internal transcribed spacer regions (ITS) and the β -tubulin (Bt) region were amplified and sequenced using electrophoretic sequencing on an ABI Prism 3730 genetic analyzer (Applied Biosystems) using a Big Dye Terminator v 3.1 cycle sequencing kit. Primers used: ITS1/ITS4¹⁰⁹ and Bt2a/Bt2b.¹¹⁰⁻¹¹¹ The resultant 475 base-pair consensus for the ITS region matched 100% identity with accession number MK817632 and the resultant 385 base-pair consensus for the beta-tubulin region matched 100% identity with accession number MK519552. Both accession numbers identified to *Penicillium crustosum*.

3.6.4 Phylogeny analysis

Phylogeny analysis of ITS region: The evolutionary history was inferred by using the Maximum Likelihood method based on the Tamura-Nei model.¹¹² The tree with the highest log likelihood (-1527.50) is shown. Initial tree(s) for the heuristic search were obtained automatically by applying Neighbor-Join and BioNJ algorithms to a matrix of pairwise distances estimated using the Maximum Composite Likelihood (MCL) approach, and then selecting the topology with superior log likelihood value. The tree is drawn to scale, with branch lengths measured in the number of substitutions per site. The analysis involved 9 nucleotide sequences. All positions containing gaps and missing data were eliminated. There was a total of 411 positions in the final dataset. Evolutionary analyses were conducted in MEGA7.¹⁰⁰

Phylogeny analysis for beta-tubulin region: The evolutionary history was inferred by using the Maximum Likelihood method based on the Tamura-Nei model.¹¹² The tree with the highest log likelihood (-1035.49) is shown. Initial tree(s) for the heuristic search were obtained automatically by applying Neighbor-Join and BioNJ algorithms to a matrix of pairwise distances estimated using the Maximum Composite Likelihood (MCL) approach, and then selecting the topology with superior log likelihood value. The tree is drawn to scale, with branch lengths measured in the number of substitutions per site. The analysis involved 8 nucleotide sequences. All positions containing gaps and missing data were eliminated. There was a total of 271 positions in the final dataset. Evolutionary analyses were conducted in MEGA7.¹⁰⁰

3.6.5 Preparation of organic extracts

The pH of the fungal culture media after inoculation was around pH of 5-6. Prior to extraction, the fungal culture was pH adjusted to around a pH of 4-5, and then filtered through cheesecloth to separate the supernatant from the mycelia. The culture broth (supernatant) was extracted using equal parts ethyl acetate (EtOAc) to media for 24 h with stirring, while the mycelia was extracted using 500 mL acetone by sonication for 1 h. The organic layers (ethyl acetate from the supernatant and acetone from the fungal cells) were collected separately and then concentrated under reduced vacuum. The extracts were solubilized in 1:1 acetonitrile to water and were subjected to LC/MS analysis. For the extracts that showed similar LC/MS chromatograms were combined for higher yield and handling of compounds.

3.6.6 General spectroscopic and chromatographic procedures

Infrared (IR) spectra were recorded on a Thermo Scientific Nicolet IR100 FTIR spectrometer. Low-resolution ESI-MS mass spectra were recorded on Agilent 1100 series LC with MSD 1946 (LC/MS). High-resolution ESI-MS spectra were recorded on an Agilent 6545 LC/Q-TOF MS. The column (Phenomenex Kinetex C18, 5 μ m x 150 mm x 4.6 mm) was re-equilibrated before each injection, and the column compartment was maintained at 30 °C throughout each run. The mobile phase consisted of ultra-pure water (A) and acetonitrile (ACN) (B) with 0.05% formic acid in each solvent. A gradient method from 10% B to 100% B in 35 min at a flow rate of 0.8 ml/min was used. Agilent 1260 Infinity HPLC system was used for preparative separations equipped with photodiode array detectors. NMR spectra were acquired on

a Bruker Avance III 700 MHz spectrometer, equipped with a ^{13}C cryoprobe. Solvent peaks of CDCl_3 (δ_{H} 7.26; δ_{C} 77.06) was used as internal standard.⁸⁸ Solvents, media ingredients, and general reagents were from Sigma-Aldrich Corp., Fisher Scientific, and VWR International.

3.6.7 HPLC isolation and purification of secondary metabolites

Clavatul (**2**): The ethyl acetate extract from the culture broth (supernatant) was subjected to preparative HPLC using a gradient elution of 5-100% ACN to H_2O to yield five fractions (F1-F5). Fraction 3 was further purified by preparative HPLC using an isocratic elution of 40% ACN and 60% H_2O to yield compound **2**.

Hydroxyclavatul methyl ether (**3**): The ethyl acetate extract from the culture broth (supernatant) was subjected to preparative HPLC using an isocratic elution of 40% ACN + 0.05% formic acid and 60% H_2O + 0.05% formic acid to yield nine fractions (F1-F9). Compound **3** was isolated and concentrated under reduced vacuum (0.75 mg, colorless crystal). From the evaporation, compound **3** crystalized and was subjected to X-ray crystallography.

3.6.8 X-ray crystallographic analysis

Diffraction intensities for compound **3** were collected at 173 K on a Bruker Apex2 DUO CCD diffractometer using $\text{Cu K}\alpha$ radiation, $\lambda = 1.54178 \text{ \AA}$. Absorption correction was applied by SADABS.¹¹³ Space group was determined based on intensity statistics. Structure was solved by direct methods and Fourier techniques and refined on F^2 using full matrix least-squares procedures. All non-H atoms were refined with

anisotropic thermal parameters. H atoms in the aromatic rings were found on the residual density map and refined with isotropic thermal parameters. Methyl H atoms were refined in calculated positions without restrictions on rotation around the C—C bonds, HFIX 138 in SHELXL.¹¹⁴ All calculations were performed by the Bruker SHELXL-2014/7 package.¹¹⁴ *Crystallographic Data for 3*: C₁₂H₁₂O₃, M = 204.22, 0.10 x 0.05 x 0.04 mm, T = 173(2) K, Triclinic, space group *P*-1, *a* = 6.9631(3) Å, *b* = 10.9375(4) Å, *c* = 13.2925(5) Å, α = 89.743(2)°, β = 81.014(2)°, γ = 80.834(2)°, *V* = 986.93(7) Å³, *Z* = 4, *Z'* = 2, *D*_c = 1.374 Mg/m³, μ (Cu) = 0.810 mm⁻¹, *F*(000) = 432, $2\theta_{\max}$ = 133.15°, 12378 reflections, 3466 independent reflections [*R*_{int} = 0.0532], *R*1 = 0.0447, *wR*2 = 0.1167 and GOF = 1.024 for 3466 reflections (307 parameters) with *I* > 2σ(*I*), *R*1 = 0.0573, *wR*2 = 0.1267 and GOF = 1.024 for all reflections, max/min residual electron density +0.265/-0.267 eÅ⁻³.

3.6.9 Antimicrobial assays

Extracts, fractions, and pure compounds were tested for antibiotic activity in cell-based microbroth single dose assays following established protocols.⁸⁹ The antimicrobial activity was evaluated against these microorganisms: *Bacillus subtilis* (ATCC 49343), Methicillin-resistant *Staphylococcus aureus* (MRSA) BAA-41, *Mycobacterium smegmatis* (ATCC 14468), *Pseudomonas aeruginosa* (ATCC 15442), and *Candida albicans* (ATCC 90027). Antibiotic positive controls (chloramphenicol, vancomycin, rifampicin, kanamycin, and amphotericin, respectively) were used at 125 μg/mL, while DMSO was used as the negative control at 1.25% v/v. Samples to be tested were prepared at 10 mg/mL in DMSO for extract samples or 1 mg/mL in DMSO for pure

compounds. For MRSA and *M. smegmatis*, the final sample concentration was 125 10 $\mu\text{g}/\text{mL}$, while for *B. subtilis* and *C. albicans*, the final dosage was 125 μg .

3.6.10 Cytotoxicity assay

Extracts, fractions, and pure compounds were tested for cytotoxicity activity in cell-based assays following established protocols.⁹⁰ Effects on mammalian cell viability were determined by measuring the reduction of the tetrazolium salt MTT (3-(4,5-dimethylthiazolyl-2)-2,5-diohenyltetrazolium bromide) by metabolically active cells. Human colon cancer (HCT-116) cell line was obtained from the American Type Culture Collection (ATCC). HCT-116 cells were maintained in MEM supplemented with 10% (v/v) fetal bovine serum, penicillin (100 U/mL), and streptomycin (100 $\mu\text{g}/\text{mL}$). The cell lines were incubated at 37 °C in 5% CO₂. Cells were plated into 96-well plates at 7000 cells/well cell density, incubated overnight, and treated with the addition of 10 $\mu\text{g}/\text{mL}$ extract or 1 $\mu\text{g}/\text{mL}$ for pure compounds and 10 $\mu\text{g}/\text{mL}$ for controls to each well. After 48 h, MTT (5 mg/mL in phosphate-buffered saline) was added to each well at a final concentration of 0.5 mg/mL. The plates were incubated for 2 h at 37 °C. The medium was removed, and the purple formazan product solubilized by the addition of 50 μL DMSO. Absorbance was measured at 550 nm using the Biotek Synergy 96-well plate reader. Metabolic activity of vehicle-treated cells (0.1 % ethanol or DMSO) was defined as 100% cell growth. Etoposide (250 μM) was used as a positive control.

4 *Fusarium graminearum* pathogenesis & metabolomics

4.1 Abstract

Fusarium head blight (FHB) is a worldwide destructive disease of cereal crops, particularly wheat, caused by the filamentous fungus *Fusarium graminearum* (*Fg*). Specific pathogenicity mechanisms to invade their hosts may include mycotoxins and secreted effector proteins. In collaboration with Dr. Ludovic Bonhomme and his team, eight strains of *Fg*, varying in location of sampling and pathogenicity, were chemically analyzed for their secondary metabolites. In previous studies, fungal biomass development *in planta* was measured by monitoring wheat spike symptoms at 72 hours post infection (hpi) after inoculation of *Fg* spores to monitor levels of plant aggressiveness. Herein, an LC/MS-based metabolomics analysis was carried out with the same eight strains to shed light on secondary metabolite identity and abundance. First, we employed principal component analysis (PCA) and to our surprise, the *least* pathogenic isolate *Fg*U1 and the *most* pathogenic isolate *Fg*1 clustered together in this comparative analysis, suggesting a similar set of secondary metabolites present. In addition, the fusarin class of compounds was found to be most abundant in isolates *Fg*593 and *Fg*202. While secondary metabolite expression varied drastically among these *Fg* isolates, no direct correlation was found between the *in vitro* secondary metabolite profile and the *in planta* pathogenicity. This initial study indicates that secondary metabolites alone are most likely not responsible for the different levels of

aggressiveness observed in FHB and that effector proteins may have a stronger influence in the pathogenicity.

4.2 Introduction

The ascomycete *Fusarium* has the ability to infect agricultural plants rendering them unsuitable for consumption due to the mycotoxins produced. Among the most destructive of these species is *Fusarium graminearum* (*Fg*), one of the causal agents of Fusarium Head Blight (FHB) affecting wheat, barley, oats, and corn.¹¹⁵⁻¹¹⁷ This has a tremendous impact in agriculture economy since infected plants become unsuitable for consumption. In fact, in the US alone, the annual economic loss of postharvest wheat is more than 300 million dollars.¹¹⁸ When *Fg* invades plant hosts, it depends on virulence factors to cause disease and promote fungal colonization. Virulence factors includes mycotoxins (secondary metabolism) and secreted effector proteins (primary metabolism) that redirect host metabolism, immunity, and development.¹¹⁹ Many mycotoxins are known from *Fg* including trichothecenes (e.g. deoxynivalenols, nivalenol), zearalenones, fumonisins, and culmorins.^{116, 120-122} In some instances, these mycotoxins may be important for virulence towards specific host plant invasion. For instance, trichothecene mycotoxins can promote virulence toward wheat and maize but not barley.¹¹⁹ On the other hand, secreted effector proteins can target a plant's proteins, RNA or DNA framework, altering host-cell structure and function resulting in FHB.¹²³ In fact, the diversity and function of these secreted effectors remain largely unknown in *Fg*.

In the last few years, significant progress has been made towards a better understanding of the pathogenesis processes in cereal-infecting *Fg* often through the use of functional and comparative genomic analyses. Comparative genomic analysis with next generation sequencing (NGS) has provided new opportunities to identify genes and their respective gene products that have roles in virulence and host infection. From the functional factors, Fabre et al. performed a proteomics analysis approach to investigate the molecular interchange involved in the early stage of FHB in wheat, including *Fg* spores, germinating spores, and life cycle *in planta*.¹²³ They report that putative fungal effector proteins accumulated during the early stages of infection, including in the spore stage development, playing an important role in fungal pathogenicity. Considering these results, Dr. Ludovic Bonhomme at INRA Joint Unit of Genetics, Diversity and Ecophysiology of Cereals and Cereal Diseases Team (France) and his team in collaboration with the Loesgen lab are interested in genome-wide characterization of potential effectors and small molecule virulence factors of different *Fg* isolates with contrasting levels of pathogenicity on wheat (*publication in progress*).

From Dr. Bonhomme, eight *Fg* strains were obtained for secondary metabolism analysis. These strains include four French strains (*Fg13*, *FgU1*, *Fg5*, and *Fg1*), three from Italy (*Fg851*, *Fg593*, and *Fg202*), and one strain from Germany (*Fg8*) (Figure 17). Dr. Bonhomme's team described the intragenomic variations between the eight strains of *Fg* and characterized their aggressiveness in wheat (T. Alouane's PhD project) (Figure 18). They also identified and characterized putative effector proteins

related to *Fg* virulence by sequencing and comparative genomics. Our part and objective in this collaborative research was to analyze these eight isolates by using liquid chromatography coupled to mass spectrometry (LC/MS)-based metabolomics for their chemodiversity. In the eight genomes, a total of 359 secondary metabolite biosynthetic gene clusters (BGC) were found using antiSMASH version 5.0,⁸⁶ including PKS and NRPS clusters.

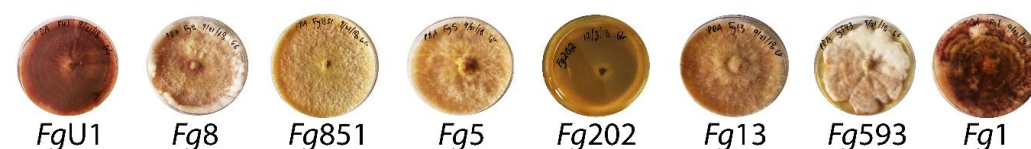


Figure 16. Colony morphology of the eight *Fg* strains. Strains were grown on PDA plates.

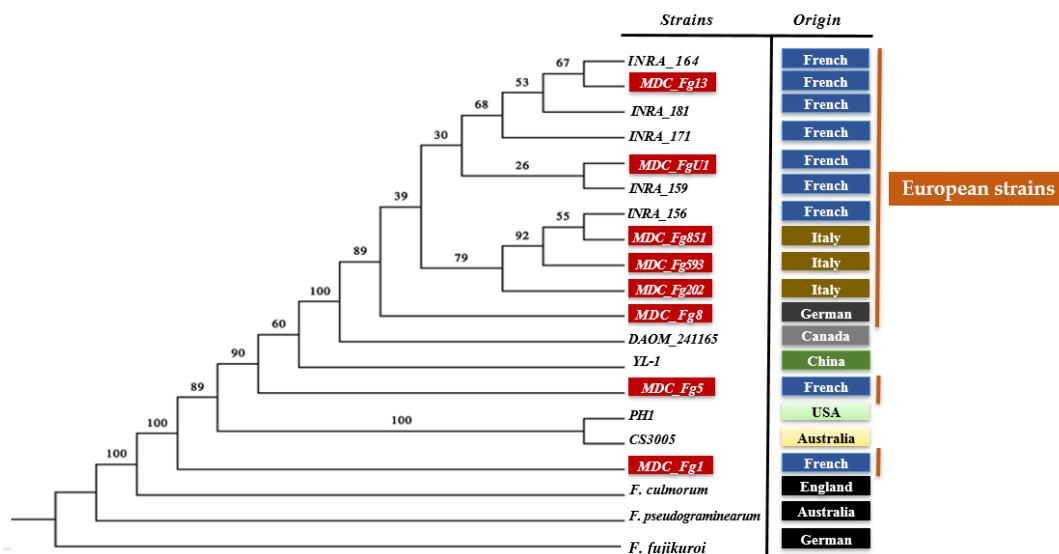


Figure 17. Phylogeny of the eight *Fg* strains. Analysis was based on 7740 orthologous single-copy amino acid sequences. Strains of interest are highlighted in red.

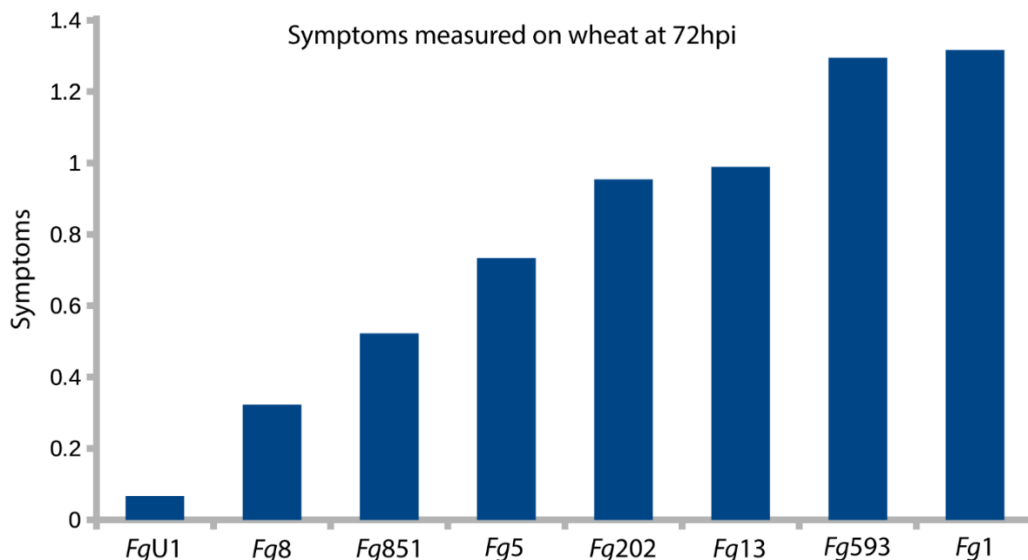


Figure 18. *In planta* symptoms from the eight *Fg* inoculations on wheat measured at 72hpi.

4.3 Results & Discussion

Metabolomics profiling of natural products is a tool to identify and potentially elucidate the sets of characteristic metabolites.⁶⁰ Using liquid chromatography coupled with mass spectrometry (LC/MS), a chemical profile can be generated for each extract that can be used to identify different metabolites.⁵⁸ Eight *Fg* isolates (Figure 16) were inoculated onto potato dextrose solid agar-based media (PDA). After eight days, the agar plates were subjected to an organic solvent extraction and were chemically profiled using LC/MS. Next, multivariate analysis was employed following published procedure using MZmine 2.32 and MetaboAnalyst 4.0, for automated peak picking and smoothing, and statistical computation.^{24, 124-125} The metabolic profiles of the eight cultures were compared, each strain was grown in biological replicates (n=4) and injected twice into the LC/MS. The final data matrix used for analyses was obtained

after removing all ions from media and solvent samples, allowing to focus solely on the fungal metabolites.

A principal component analysis (PCA) of the LC/MS data was generated with MZmine 2.32 and MetaboAnalyst 4.0. Briefly and in this case, the PCA plot illustrated metabolome similarities or differences between the different *Fg* isolates (Figure 19). Certain isolates that were separated from the other isolates in the PCA projection were interpreted as chemically unique or differently abundant. From the PCA plot, the overall total variability of all the metabolites projected from the eight *Fg* isolates was 48.4%. The isolates *Fg*593 (pink) and *Fg*202 (purple blue) clustered together, which was interesting as they are both derived from the same area in Italy. Additionally, isolates *Fg*851 (grey) and *Fg*5 (turquoise) clustered together, which show similarity low levels of pathogenicity, (Figure 18). Somewhat unexpectedly, the *least* pathogenic isolate *Fg*U1 and the *most* pathogenic isolate *Fg*1 clustered in the same group, suggesting a similar set and abundance of secondary metabolites present.

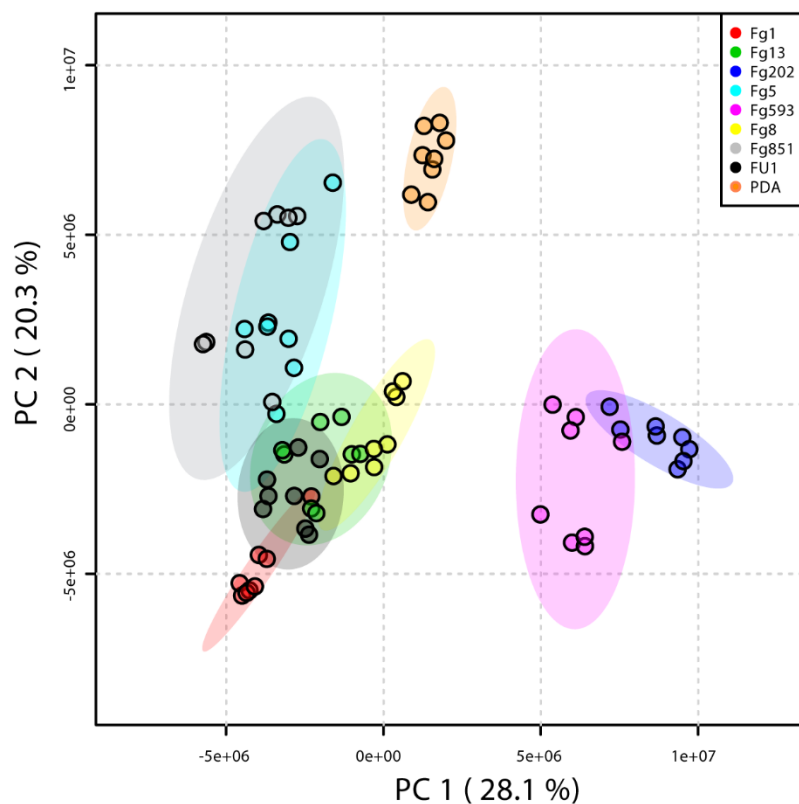


Figure 19. A principal component analysis (PCA) plot for PC1 and PC2 of the LC/MS-based metabolomics data of the eight *Fg* trains.

A multivariate statistical comparison of differentially expressed metabolites between the least (*FgU1*) and most (*Fg1*) aggressive isolates was visualized using a volcano plot (Figure 20). Briefly, a volcano plot is a scatterplot of replicated data points between two conditions to quickly identify the most meaningful changes by plotting the statistical significance in the y-axis versus fold-change in the x-axis. In the center region of the volcano plot in grey data points are common metabolites shared between the two isolates. Both in the left and right outmost direction of the volcano plot are the most statistically significant metabolites detected consistently in all the replicates.

Among the metabolites detected in *FgU1*, the entry with 237.3 *m/z* at RT 13.2 min correlated with either culmorone or apotrichothecenes, and the entry of 211.3 *m/z* at RT 9.9 min correlated with either prolipyrone A or B, both in positive ionization mode. Among the metabolites detected in *Fg1*, the entry with 659.5 *m/z* at RT 27.9 min and 681.4 *m/z* at RT 28.0 min best correlated with fusaristatin A for $[M+H]^+$ and $[M+Na]^+$ respectively. This suggested that compounds like fusaristatin A could be a contributing factor as to why *Fg1* was more pathogenic compared to compounds like culmorone and apotrichothecenes found in less pathogenic strains.

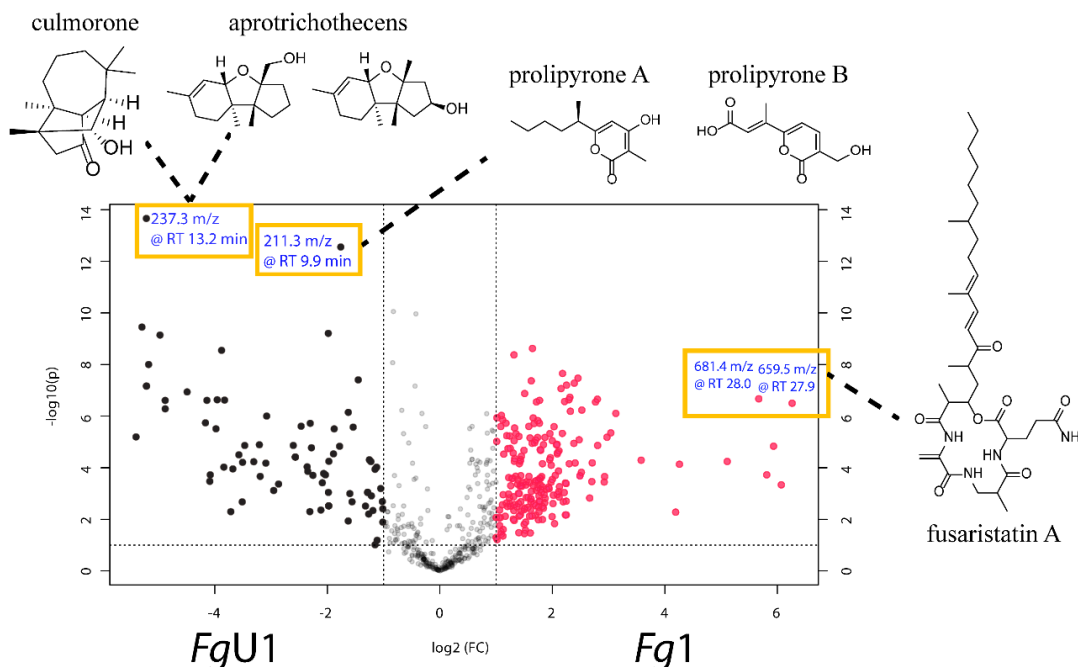


Figure 20. Volcano plot visualizing the chemical differences between *FgU1* to *Fg1* isolates. The x-axis is \log_2 ratio of metabolite expression levels between the two strains. The y-axis is the adjusted p value based on $-\log_{10}$. The colored dots in black (*FgU1*) and red (*Fg1*) represent the differentially expressed metabolites based on $p < 0.1$ and 2-fold change threshold expression difference (represented by the black dotted vertical lines).

The extracts from the eight *F. graminearum* strains were further chemically investigated by relative LC/MS peak areas of identified secondary metabolites presented in a heat map (Figure 21). Briefly, the LC/MS-based relative expression analysis in combination with evaluation of individual LC/MS traces can identify the most abundant and unique metabolites in each isolate. The data was sorted according to level of pathogenicity in the x-axis, with left being the least pathogenic *FgU1* isolate and on the right *Fg1*, the most pathogenic, and in the y-axis represent chemical entities with their designated m/z value in positive ionization and retention time. Tentative assignments were based on low-resolution mass, retention times, UV spectra, and fragmentation ions. Interestingly, the two strains, *Fg593* and *Fg202*, that clustered in the PCA plot showed high abundance for fusarins (Fusarin C/D & Fusarin A/Z) and 13-hydroxy-tricho-2(12), 9(10)-diene-3-one. The occurrence of rubrofusarin mainly in *FgU1* and *Fg1* correlated with the physical red appearance of the strains on PDA (Figure 16). Unexpectedly, there was no single, high abundant metabolite detected in *Fg1* compared to the other strains that could directly explain why *Fg1* is most pathogenic. This initial study suggests that secondary metabolites most likely do not play a central role in the observed level of FHB aggressiveness, and instead proteins or other effectors may be in charge for the pathogenicity observed in the colonization of various *F. graminearum* isolates in wheat.

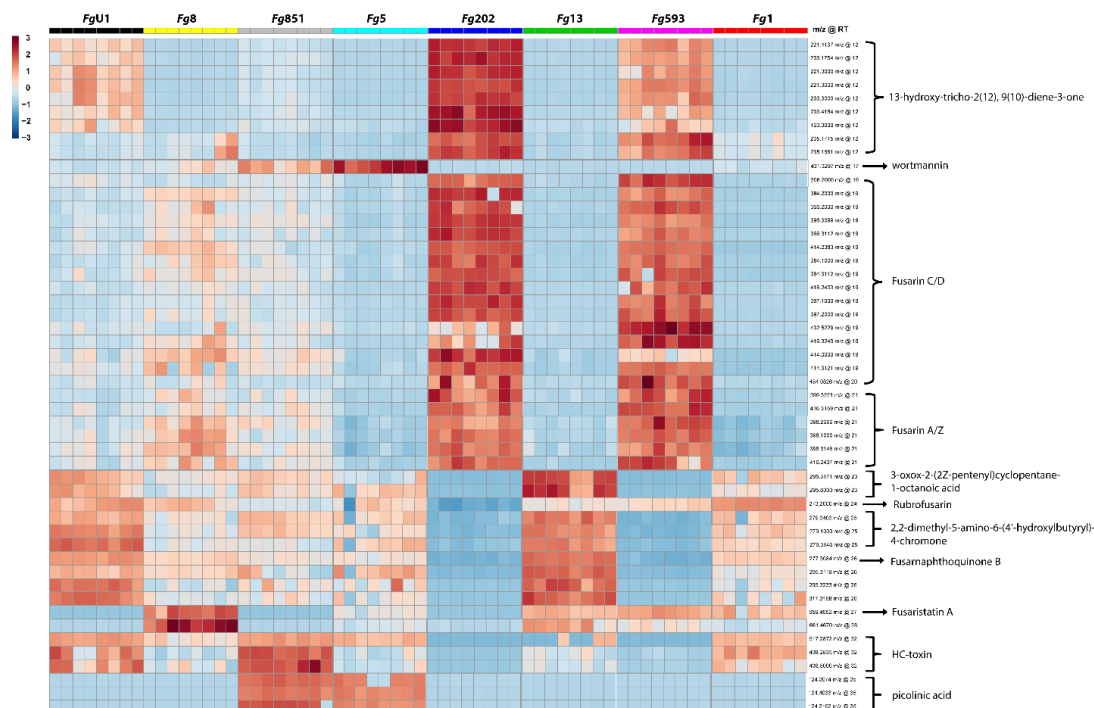


Figure 21. Heat map comparing relative LC/MS ion abundances of identified secondary metabolites. The strains (columns) are sorted in increasing levels of pathogenicity (similar to Figure 13). The compounds (rows) are sorted by retention time with designated m/z value in positive ionization. Relative intensity ranging from red color for high AUC (area under the curve) to blue for low abundance. Tentative assignment of the compounds based on low-resolution mass, retention times, UV spectra, and mass fragmentation.

4.4 Conclusion

Fusarium graminearum (*Fg*) virulence factors play an important role in the fitness and success of the fungus in plant colonization. Secondary metabolism and secreted effector proteins are specific pathogenicity mechanisms during *Fg*-plant interactions, greatly influencing the resultant FHB disease in agriculture cereals. In order to better understand the potential and ability of *Fg* to cause FHB infectious disease in wheat, eight *Fg* strains, isolated from different regions across Europe, were analyzed by genomic sequencing, gene expression analysis, and protein/small molecule presence in a collaborative effort. Herein, LC/MS-based metabolomics results

illustrated that the most and least pathogenic *Fg* isolates exhibited similar chemical profiles in a PCA plot based on multivariate analysis of LC/MS based data. Furthermore, although a heat map analysis helped in identification of potential secondary metabolites found in each strain, there was no direct correlation between known bioactive metabolites present and the pathogenicity. LC/MS-based metabolomics tool was successfully employed as an integrated strategy for the detection and identification of fungal secondary metabolites in an important cereal pathogen.

4.5 Materials & Methods

4.5.1 Strains and culture conditions

Strains were grown on PDA (Potato Dextrose Agar Difco, 1.5% agar) plates for eight days incubated at 25 °C to collect fungal cell culture. For metabolomics analysis, four cultures of each strain were grown.

4.5.2 General spectroscopic and chromatographic procedures

Low-resolution ESI-MS mass spectra were recorded on Agilent 1100 series LC with MSD 1946. The mobile phase consisted of ultra-pure water (A) and acetonitrile (ACN) (B) with 0.05% formic acid in each solvent. A gradient method from 10% B to 100% B in 35 min at a flow rate of 0.8 ml/min was used. The column (Phenomenex Kinetex C18, 5 µm x 150 mm x 4.6 mm) was re-equilibrated before each injection, and the column compartment was maintained at 30 °C throughout each run. Solvents, media

ingredients, and general reagents were from Sigma-Aldrich Corp., Fisher Scientific, and VWR International.

4.5.3 Metabolomics analysis

Four cultures of each strain in PDA medium were extracted with 50 mL ethyl acetate (EtOAc), shaking at 200 rpm and ambient temperature for 48 h. The ethyl acetate extracts were dried *in vacuo*. Each extract was prepared to 40 mg/mL in 1:1 ACN:methanol (MeOH) for LC/MS analysis. Each sample was analyzed in duplicate on an Agilent 1100 series LC/MS platform. Positive mode ionization was used to detect metabolites. Data sets were exported from Agilent's Chemstation software as .netCDF files and imported into MZmine 2.3.¹²⁴ Peak picking was performed with established protocols.⁶² Mass detection was centroid with 1.7E4 minimum height. Chromatogram building was limited to peaks greater than 0.1 min with 0.1 m/z tolerance and 1.8E4 minimum height. Chromatogram deconvolution utilized local minimum search with 92%-99% threshold, 40 min search range, 1% relative height, 1.9E4 minimum abs. height, 1 minimum ratio of top/edge, and peak duration from 0.10-10.00 minutes. All treatments were then aligned with a tolerance of 0.05 m/z and retention time tolerance of 3.0 relative (%). Peak finder gap filling was performed with 25% intensity tolerance and 0.1 m/z tolerance. Duplicated peaks were combined with a tolerance of 0.5 m/z and 0.3 min. The normalized data were processed using MetaboAnalyst software 4.0.¹²⁵ Data were log-transformed and scaled to unit variance for a multivariate modeling approach (PCA) to check for variability based on overall metabolite profiles. Two strains were selected for volcano plot analyses thereby considering fold change

threshold of two and statistical p-value less than 0.1. Signal ion abundance intensities were averaged over technical replicates, log-transformed to improve normality, and compared between strains using a two-sample, two-tailed t-test as a heat map.

4.6 Acknowledgements

We thank Dr. Ludovic Bonhomme, Dr. Thierry Langin and Tarek Alouane at INRA Joint Unit Genetics, Diversity and Ecophysiology of Cereals and Cereal Diseases in France for supplying the strains and the information on the strain's pathogenic levels. We thank Jörg Bormann and Michael Freitag for fruiting discussion on *Fusarium graminearum* metabolism and biology.

5 General Conclusion

The fungal kingdom is present in every niche of this planet, often associated with other organisms both in terrestrial and marine habitats. The rich and unique chemical diversity of fungal natural products are important for discovery of new classes of drugs including antibiotic, antifungal, and anticancer drugs. In addition, new drugs are needed to combat the growing threat of antimicrobial resistance found in the clinical setting and in the environment. Fungi associated with plants can be classified in a fluidic range from symbionts to pathogens and most often engage in interspecies chemical cross talk. In chapter two, the exploration of the tree-fungus symbiosis between Douglas-fir tree and *Zasmidium pseudotsugae* illustrates the success of traditional microbial cultivation approach with the discovery of 8,8'-bijuglone, a compound newly discovered from a natural source. The compound, although not

potent, did show weak cytotoxicity against human colon carcinoma (HCT-116) cell line and exhibited lethal activity against the leukemia cell lines in the NCI-60 cell line panel at the National Cancer Institute (NCI). In addition, this is the first report of secondary metabolites from *Z. pseudotsugae*, which gives insight into the chemical interactions that govern complex microbiomes. In chapter three, an algal derived *Penicillium crustosum* was screened for new chemical and biological active metabolites. The extract of *P. crustosum* exhibited high MRSA activity and two known, inactive compounds, clavatul and hydroxyclavatul methyl ether, were isolated from the fungus. The active principle is yet to be discovered. In chapter four, eight geographically distinct isolates of cereal pathogen *Fusarium graminearum* were analyzed for secondary metabolites present using comparative metabolomics. Various metabolites were tentatively identified, and chemical differences can be observed between the eight isolates. The secondary metabolites identified *in vitro* did not directly correlate with observed *in planta* pathogenicity. Future studies will tie protein expression of known effector proteins to secondary metabolism. Overall, the efforts presented here will continue to enlarge the chemical diversity from fungi in the future. Discovery of novel structural motifs from fungi will serve to inform our understanding of the environmental purposes these secondary metabolites, as well as provide new tools to understand the chemical ecology of fungi. For humankind, fungal chemical exploration may help to combat antimicrobial resistance and agricultural pests.

6 References

1. Dewick, P. M., *Medicinal natural products: a biosynthetic approach*. John Wiley & Sons: **2002**.
2. Walsh, C. T.; Tang, Y., *Natural Product Biosynthesis*. Royal Society of Chemistry: **2017**.
3. Fischbach, M. A.; Walsh, C. T.; Clardy, J., The evolution of gene collectives: How natural selection drives chemical innovation. *Proceedings of the National Academy of Sciences* **2008**, *105* (12), 4601-4608.
4. Holdgate, G. A.; Meek, T. D.; Grimley, R. L., Mechanistic enzymology in drug discovery: a fresh perspective. *Nature Reviews Drug Discovery* **2017**, *17* (2), 115.
5. Katz, L.; Baltz, R. H., Natural product discovery: past, present, and future. *Journal of Industrial Microbiology & Biotechnology* **2016**, *43* (2), 155-176.
6. Newman, D. J.; Cragg, G. M., Natural products as sources of new drugs from 1981 to 2014. *Journal of natural products* **2016**, *79* (3), 629-661.
7. Newman, D. J.; Cragg, G. M., Natural products as sources of new drugs over the 30 years from 1981 to 2010. *Journal of natural products* **2012**, *75* (3), 311-335.
8. Kardos, N.; Demain, A. L., Penicillin: the medicine with the greatest impact on therapeutic outcomes. *Applied microbiology and biotechnology* **2011**, *92* (4), 677.
9. Niu, J.; Straubinger, R. M.; Mager, D. E., Pharmacodynamic Drug-Drug Interactions. *Clinical Pharmacology & Therapeutics* **2019**, *105* (6), 1395-1406.
10. Lestner, J. M.; Roberts, S. A.; Moore, C. B.; Howard, S. J.; Denning, D. W.; Hope, W. W., Toxicodynamics of itraconazole: implications for therapeutic drug monitoring. *Clinical infectious diseases* **2009**, *49* (6), 928-930.
11. Fisher, M. C.; Hawkins, N. J.; Sanglard, D.; Gurr, S. J., Worldwide emergence of resistance to antifungal drugs challenges human health and food security. *Science* **2018**, *360* (6390), 739-742.
12. Clatworthy, A. E.; Pierson, E.; Hung, D. T., Targeting virulence: a new paradigm for antimicrobial therapy. *Nature chemical biology* **2007**, *3* (9), 541.
13. Ventola, C. L., The antibiotic resistance crisis: part 1: causes and threats. *Pharmacy and therapeutics* **2015**, *40* (4), 277.
14. Dayan, F. E.; Cantrell, C. L.; Duke, S. O., Natural products in crop protection. *Bioorganic & medicinal chemistry* **2009**, *17* (12), 4022-4034.

15. Sparks, T. C.; Hahn, D. R.; Garizi, N. V., Natural products, their derivatives, mimics and synthetic equivalents: role in agrochemical discovery. *Pest management science* **2017**, *73* (4), 700-715.
16. Sparks, T. C.; Hunter, J. E.; Lorsbach, B. A.; Hanger, G.; Gast, R. E.; Kemmitt, G.; Bryant, R. J., Crop Protection Discovery: Is Being the First Best? *Journal of agricultural and food chemistry* **2018**, *66* (40), 10337-10346.
17. Cantrell, C. L.; Dayan, F. E.; Duke, S. O., Natural Products As Sources for New Pesticides. *Journal of Natural Products* **2012**, *75* (6), 1231-1242.
18. Von Jagow, G.; Gribble, G. W.; Trumpower, B. L., Mucidin and strobilurin A are identical and inhibit electron transfer in the cytochrome bc₁ complex of the mitochondrial respiratory chain at the same site as myxothiazol. *Biochemistry* **1986**, *25* (4), 775-780.
19. Lomenick, B.; Olsen, R. W.; Huang, J., Identification of direct protein targets of small molecules. *ACS chemical biology* **2011**, *6* (1), 34-46.
20. Mc Dermott, P. F.; Walker, R. D.; White, D. G., Antimicrobials: Modes of Action and Mechanisms of Resistance. *International Journal of Toxicology* **2003**, *22* (2), 135-143.
21. Guzmán, E. A., Regulated Cell Death Signaling Pathways and Marine Natural Products That Target Them. *Marine Drugs* **2019**, *17* (2), 76.
22. Dixon, N.; Wong, L. S.; Geerlings, T. H.; Micklefield, J., Cellular targets of natural products. *Natural Product Reports* **2007**, *24* (6), 1288-1310.
23. Jasial, S.; Hu, Y.; Bajorath, J. r., Assessing the growth of bioactive compounds and scaffolds over time: implications for lead discovery and scaffold hopping. *Journal of chemical information and modeling* **2016**, *56* (2), 300-307.
24. Thomford, N.; Senthebane, D.; Rowe, A.; Munro, D.; Seele, P.; Maroyi, A.; Dzobo, K., Natural products for drug discovery in the 21st century: Innovations for novel drug discovery. *International journal of molecular sciences* **2018**, *19* (6), 1578.
25. Alharbi, S. A.; Wainwright, M.; Alahmadi, T. A.; Salleeh, H. B.; Faden, A. A.; Chinnathambi, A., What if Fleming had not discovered penicillin? *Saudi journal of biological sciences* **2014**, *21* (4), 289-293.
26. Endo, A., A historical perspective on the discovery of statins. *Proceedings of the Japan Academy, Series B* **2010**, *86* (5), 484-493.
27. Allison, A. C., Immunosuppressive drugs: the first 50 years and a glance forward. *Immunopharmacology* **2000**, *47* (2-3), 63-83.

28. Roemer, T.; Krysan, D., Antifungal drug development: challenges, unmet clinical needs, and new approaches. *Cold Spring Harb perspectives in medicine* **2014**, *4* (5), a019703.
29. Saravolatz, L. D.; Deresinski, S. C.; Stevens, D. A., Caspofungin. *Clinical Infectious Diseases* **2003**, *36* (11), 1445-1457.
30. Kinghorn, A. D.; De Blanco, E. J. C.; Lucas, D. M.; Rakotondraibe, H. L.; Orjala, J.; Soejarto, D. D.; Oberlies, N. H.; Pearce, C. J.; Wani, M. C.; Stockwell, B. R., Discovery of anticancer agents of diverse natural origin. *Anticancer research* **2016**, *36* (11), 5623-5637.
31. Sieber, C. M.; Lee, W.; Wong, P.; Münsterkötter, M.; Mewes, H.-W.; Schmeitzl, C.; Varga, E.; Berthiller, F.; Adam, G.; Güldener, U., The *Fusarium graminearum* genome reveals more secondary metabolite gene clusters and hints of horizontal gene transfer. *PLoS One* **2014**, *9* (10), e110311.
32. Schueffler, A.; Anke, T., Fungal natural products in research and development. *Natural Product Reports* **2014**, *31* (10), 1425-48.
33. Firn, R. D.; Jones, C. G., Natural products—a simple model to explain chemical diversity. *Natural Product Reports* **2003**, *20* (4), 382-391.
34. Rodriguez, R. J.; Henson, J.; Van Volkenburgh, E.; Hoy, M.; Wright, L.; Beckwith, F.; Kim, Y.-O.; Redman, R. S., Stress tolerance in plants via habitat-adapted symbiosis. *The Isme Journal* **2008**, *2* (4), 404.
35. Wu, Q.-S.; Zou, Y.-N., Arbuscular mycorrhizal fungi and tolerance of drought stress in plants. In *Arbuscular Mycorrhizas and Stress Tolerance of Plants*, Springer: **2017**; pp 25-41.
36. Hossain, M. M.; Sultana, F.; Islam, S., Plant growth-promoting fungi (PGPF): phytostimulation and induced systemic resistance. In *Plant-microbe interactions in agro-ecological perspectives*, Springer, Singapore: **2017**; pp 135-191.
37. García-Garrido, J. M.; Ocampo, J. A., Regulation of the plant defence response in arbuscular mycorrhizal symbiosis. *Journal of Experimental Botany* **2002**, *53* (373), 1377-1386.
38. Read, D., Mycorrhiza—the state of the art. In *Mycorrhiza*, Springer: **1999**; pp 3-34.
39. Redman, R. S.; Dunigan, D. D.; Rodriguez, R. J., Fungal symbiosis from mutualism to parasitism: who controls the outcome, host or invader? *New Phytologist* **2001**, *151* (3), 705-716.

40. Stringlis, I. A.; Zhang, H.; Pieterse, C. M. J.; Bolton, M. D.; de Jonge, R., Microbial small molecules - weapons of plant subversion. *Natural Product Reports* **2018**, *35* (5), 410-433.
41. Dean, R.; Van Kan, J. A.; Pretorius, Z. A.; Hammond-Kosack, K. E.; Di Pietro, A.; Spanu, P. D.; Rudd, J. J.; Dickman, M.; Kahmann, R.; Ellis, J.; Foster, G. D., The Top 10 fungal pathogens in molecular plant pathology. *Molecular Plant Pathology* **2012**, *13* (4), 414-430.
42. Balestrini, R.; Lumini, E., Focus on mycorrhizal symbioses. *Applied Soil Ecology* **2018**, *123*, 299-304.
43. Yao, H.; Sun, X.; He, C.; Maitra, P.; Li, X.-C.; Guo, L.-D., Phyllosphere epiphytic and endophytic fungal community and network structures differ in a tropical mangrove ecosystem. *Microbiome* **2019**, *7* (1), 57.
44. Terhonen, E.; Blumenstein, K.; Kovalchuk, A.; Asiegbu, F. O., Forest Tree Microbiomes and Associated Fungal Endophytes: Functional Roles and Impact on Forest Health. *Forests* **2019**, *10* (1), 42.
45. Domka, A. M.; Rozpałdek, P.; Turnau, K., Are Fungal Endophytes Merely Mycorrhizal Copycats? The Role of Fungal Endophytes in the Adaptation of Plants to Metal Toxicity. *Frontiers in Microbiology* **2019**, *10* (371).
46. Strobel, G.; Daisy, B., Bioprospecting for Microbial Endophytes and Their Natural Products. *Microbiology and Molecular Biology Reviews* **2003**, *67* (4), 491-502.
47. Gao, H.; Li, G.; Lou, H.-X., Structural Diversity and Biological Activities of Novel Secondary Metabolites from Endophytes. *Molecules* **2018**, *23* (3), 646.
48. Strobel, G., The Emergence of Endophytic Microbes and Their Biological Promise. *Journal of Fungi* **2018**, *4* (2), 57.
49. Furtado, B. U.; Gołębiowski, M.; Skorupa, M.; Hulisz, P.; Hryniewicz, K., Exploring bacterial and fungal endophytic microbiomes of *Salicornia europaea*. *Applied and Environmental Microbiology* **2019**, *85* (13), e00305-19.
50. Wolfe, E. R.; Younginger, B. S.; LeRoy, C. J., Fungal endophyte-infected leaf litter alters in-stream microbial communities and negatively influences aquatic fungal sporulation. *Oikos* **2019**, *128* (3), 405-415.
51. Lyons, P.; Plattner, R.; Bacon, C., Occurrence of peptide and clavine ergot alkaloids in tall fescue grass. *Science* **1986**, *232* (4749), 487-489.
52. Meena, H.; Hnamte, S.; Siddhardha, B., Secondary Metabolites from Endophytic Fungi: Chemical Diversity and Application. In *Advances in Endophytic Fungal Research*, Springer: **2019**; pp 145-169.

53. Tejesvi, M. V.; Pirttilä, A. M., Potential of Tree Endophytes as Sources for New Drug Compounds. In *Endophytes of Forest Trees*, Springer: **2018**; pp 441-462.
54. Newman, D. J.; Cragg, G. M., Endophytic and epiphytic microbes as “sources” of bioactive agents. *Frontiers in Chemistry* **2015**, *3* (34).
55. Shi, Z.-Z.; Miao, F.-P.; Fang, S.-T.; Yin, X.-L.; Ji, N.-Y., Trichorenins A–C, Algicidal Tetracyclic Metabolites from the Marine-Alga-Epiphytic Fungus *Trichoderma virens* Y13-3. *Journal of Natural Products* **2018**, *81* (4), 1121-1124.
56. Shi, Z.-Z.; Miao, F.-P.; Fang, S.-T.; Liu, X.-H.; Yin, X.-L.; Ji, N.-Y., Sesteralterin and Tricycloalterfurenes A–D: Terpenes with Rarely Occurring Frameworks from the Marine-Alga-Epiphytic Fungus *Alternaria alternata* k21-1. *Journal of Natural Products* **2017**, *80* (9), 2524-2529.
57. Patti, G. J.; Yanes, O.; Siuzdak, G., Innovation: Metabolomics: the apogee of the omics trilogy. *Nature reviews Molecular cell biology* **2012**, *13* (4), 263-269.
58. Kuhlisch, C.; Pohnert, G., Metabolomics in chemical ecology. *Natural product reports* **2015**, *32* (7), 937-955.
59. Fiehn, O., Metabolomics—the link between genotypes and phenotypes. In *Functional genomics*, Springer: **2002**; pp 155-171.
60. Hautbergue, T.; Jamin, E.; Debrauwer, L.; Puel, O.; Oswald, I., From genomics to metabolomics, moving toward an integrated strategy for the discovery of fungal secondary metabolites. *Natural product reports* **2018**, *35* (2), 147-173.
61. Adpressa, D. A.; Stalheim, K. J.; Proteau, P. J.; Loesgen, S., Unexpected biotransformation of the HDAC inhibitor vorinostat yields aniline-containing fungal metabolites. *ACS chemical biology* **2017**, *12* (7), 1842-1847.
62. Adpressa, D. A.; Loesgen, S., Bioprospecting chemical diversity and bioactivity in a marine derived *Aspergillus terreus*. *Chemistry & biodiversity* **2016**, *13* (2), 253-259.
63. Hou, Y.; Braun, D. R.; Michel, C. R.; Klassen, J. L.; Adnani, N.; Wyche, T. P.; Bugni, T. S., Microbial Strain Prioritization Using Metabolomics Tools for the Discovery of Natural Products. *Analytical Chemistry* **2012**, *84* (10), 4277-4283.
64. Uppal, K.; Walker, D. I.; Liu, K.; Li, S.; Go, Y.-M.; Jones, D. P., Computational Metabolomics: A Framework for the Million Metabolome. *Chemical Research in Toxicology* **2016**, *29* (12), 1956-1975.

65. Hansen, E.; Stone, J.; Capitano, B.; Rosso, P.; Sutton, W.; Winton, L.; Kanaskie, A.; McWilliams, M., Incidence and impact of Swiss needle cast in forest plantations of Douglas-fir in coastal Oregon. *Plant Disease* **2000**, *84* (7), 773-778.
66. Kimberley, M.; Hood, I.; Knowles, R., Impact of Swiss needle-cast on growth of Douglas-fir. *Phytopathology* **2011**, *101* (5), 583-593.
67. Stone, J. K.; Capitano, B. R.; Kerrigan, J. L., The histopathology of *Phaeocryptopus gaeumannii* on Douglas-fir needles. *Mycologia* **2008**, *100* (3), 431-444.
68. Winton, L. M.; Stone, J. K.; Hansen, E. M.; Shoemaker, R., The systematic position of *Phaeocryptopus gaeumannii*. *Mycologia* **2007**, *99* (2), 240-252.
69. Winton, L.; Manter, D.; Stone, J.; Hansen, E., Comparison of biochemical, molecular, and visual methods to quantify *Phaeocryptopus gaeumannii* in Douglas-Fir foliage. *Phytopathology* **2003**, *93* (1), 121-126.
70. Bennett, P.; Stone, J., Assessments of population structure, diversity, and phylogeography of the Swiss needle cast fungus (*Phaeocryptopus gaeumannii*) in the US Pacific Northwest. *Forests* **2016**, *7* (1), 14.
71. Ritóková, G.; Shaw, D.; Filip, G.; Kanaskie, A.; Browning, J.; Norlander, D., Swiss needle cast in western Oregon Douglas-fir plantations: 20-year monitoring results. *Forests* **2016**, *7* (8), 155.
72. Chooi, Y.-H.; Krill, C.; Barrow, R. A.; Chen, S.; Trengove, R.; Oliver, R. P.; Solomon, P. S., An in planta-expressed polyketide synthase produces (R)-mellein in the wheat pathogen *Parastagonospora nodorum*. *Applied and Environmental Microbiology* **2015**, *81* (1), 177-186.
73. Videira, S.; Groenewald, J.; Nakashima, C.; Braun, U.; Barreto, R. W.; de Wit, P. J.; Crous, P., Mycosphaerellaceae—chaos or clarity? *Studies in mycology* **2017**, *87*, 257-421.
74. Laatsch, H., Dimere Naphthochinone, XVI. Synthese von Maritinon und anderen 8, 8'-Bijuglonen. *Liebigs Annalen der Chemie* **1985**, *1985* (12), 2420-2442.
75. Aldemir, H.; Richarz, R.; Gulder, T. A., The biocatalytic repertoire of natural biaryl formation. *Angewandte Chemie International Edition* **2014**, *53* (32), 8286-8293.
76. Gu, J.-Q.; Graf, T. N.; Lee, D.; Chai, H.-B.; Mi, Q.; Kardono, L. B. S.; Setyowati, F. M.; Ismail, R.; Riswan, S.; Farnsworth, N. R.; Cordell, G. A.; Pezzuto, J. M.; Swanson, S. M.; Kroll, D. J.; Joseph O. Falkinham, I.; Wall, M. E.; Wani, M. C.; Kinghorn, A. D.; Oberlies, N. H., Cytotoxic and Antimicrobial Constituents of the Bark of *Diospyros maritima* Collected in

- Two Geographical Locations in Indonesia. *Journal of natural products* **2004**, *67* (7), 1156-1161.
77. Higa, M.; Takashima, Y.; Yokaryo, H.; Harie, Y.; Suzuka, T.; Ogihara, K., Naphthoquinone Derivatives from *Diospyros maritima*. *Chemical and Pharmaceutical Bulletin* **2017**, *65* (8), 739-745.
78. Görner, H., Photoreactions of p-Quinones with Dimethyl Sulfide and Dimethyl Sulfoxide in Aqueous Acetonitrile. *Photochemistry and photobiology* **2006**, *82* (1), 71-77.
79. Zhu, X.-Q.; Wang, C.-H., Accurate estimation of the one-electron reduction potentials of various substituted quinones in DMSO and CH₃CN. *The Journal of organic chemistry* **2010**, *75* (15), 5037-5047.
80. Widhalm, J. R.; Rhodes, D., Biosynthesis and molecular actions of specialized 1,4-naphthoquinone natural products produced by horticultural plants. *Horticulture Research* **2016**, *3*, 16046.
81. Elhabiri, M.; Sidorov, P.; Cesar-Rodo, E.; Marcou, G.; Lanfranchi, D. A.; Davioud-Charvet, E.; Horvath, D.; Varnek, A., Electrochemical properties of substituted 2-methyl-1,4-naphthoquinones: redox behavior predictions. *Chemistry-A European Journal* **2015**, *21* (8), 3415-3424.
82. Regeimbal, J.; Gleiter, S.; Trumpower, B. L.; Yu, C.-A.; Diwakar, M.; Ballou, D. P.; Bardwell, J. C. A., Disulfide bond formation involves a quinhydrone-type charge-transfer complex. *PNAS* **2003**, *100* (24), 13779-13784.
83. Salae, A.-W.; Karalai, C.; Ponglimanont, C.; Kanjana-Opas, A.; Yuenyongsawad, S., Naphthalene derivatives from *Diospyros wallichii*. *Canadian Journal of Chemistry* **2010**, *88* (9), 922-927.
84. McGaw, L. J.; Lall, N.; Hlokwe, T. M.; Michel, A. L.; Meyer, J. J. M.; Eloff, J. N., Purified compounds and extracts from *Euclea* species with antimycobacterial activity against *Mycobacterium bovis* and fast-growing mycobacteria. *Biological and Pharmaceutical Bulletin* **2008**, *31* (7), 1429-1433.
85. Shoemaker, R. H., The NCI60 human tumour cell line anticancer drug screen. *Nature Reviews Cancer* **2006**, *6* (10), 813.
86. Blin, K.; Shaw, S.; Steinke, K.; Villebro, R.; Ziemert, N.; Lee, S. Y.; Medema, M. H.; Weber, T., antiSMASH 5.0: updates to the secondary metabolite genome mining pipeline. *Nucleic Acids Research* **2019**, *47* (W1), W81-W87.
87. Medema, M. H.; Kottmann, R.; Yilmaz, P.; Cummings, M.; Biggins, J. B.; Blin, K.; De Bruijn, I.; Chooi, Y. H.; Claesen, J.; Coates, R. C., Minimum information about a biosynthetic gene cluster. *Nature chemical biology* **2015**, *11* (9), 625.

88. Babij, N. R.; McCusker, E. O.; Whiteker, G. T.; Canturk, B.; Choy, N.; Creemer, L. C.; Amicis, C. V. D.; Hewlett, N. M.; Johnson, P. L.; Knobelsdorf, J. A., NMR chemical shifts of trace impurities: industrially preferred solvents used in process and green chemistry. *Organic Process Research & Development* **2016**, *20* (3), 661-667.
89. Mandelare, P. E.; Adpressa, D. A.; Kaweesa, E. N.; Zakharov, L. N.; Loesgen, S., Coculture of Two Developmental Stages of a Marine-Derived *Aspergillus alliaceus* Results in the Production of the Cytotoxic Bianthrone Allianthrone A. *Journal of natural products* **2018**, *81* (4), 1014-1022.
90. Plitzko, B.; Kaweesa, E. N.; Loesgen, S., The natural product mensacarcin induces mitochondrial toxicity and apoptosis in melanoma cells. *Journal of Biological Chemistry* **2017**, *292* (51), 21102-21116.
91. Eide, C. A.; O'Hare, T., Chronic myeloid leukemia: advances in understanding disease biology and mechanisms of resistance to tyrosine kinase inhibitors. *Curr Hematol Malig Rep* **2015**, *10* (2), 158-166.
92. Jiménez, C., Marine Natural Products in Medicinal Chemistry. *ACS Medicinal Chemistry Letters* **2018**, *9*, 959-961.
93. Romano, G.; Costantini, M.; Sansone, C.; Lauritano, C.; Ruocco, N.; Ianora, A., Marine microorganisms as a promising and sustainable source of bioactive molecules. *Marine Environmental Research* **2017**, *128*, 58-69.
94. Shang, J.; Hu, B.; Wang, J.; Zhu, F.; Kang, Y.; Li, D.; Sun, H.; Kong, D.-X.; Hou, T., Cheminformatic insight into the differences between terrestrial and marine originated natural products. *Journal of chemical information and modeling* **2018**, *58* (6), 1182-1193.
95. de Vera, C.; Díaz Crespín, G.; Hernández Daranas, A.; Montalvão Looga, S.; Lillsunde, K.-E.; Tammela, P.; Perälä, M.; Hongisto, V.; Virtanen, J.; Rischer, H., Marine Microalgae: Promising Source for New Bioactive Compounds. *Marine drugs* **2018**, *16* (9), 317.
96. Ji, N.-Y.; Wang, B.-G., Mycochemistry of marine algicolous fungi. *Fungal diversity* **2016**, *80* (1), 301-342.
97. Ogaki, M. B.; de Paula, M. T.; Ruas, D.; Pellizzari, F. M.; García-Laviña, C. X.; Rosa, L. H., Marine Fungi Associated with Antarctic Macroalgae. In *The Ecological Role of Micro-organisms in the Antarctic Environment*, Springer: **2019**; pp 239-255.
98. Song, Y.-P.; Fang, S.-T.; Miao, F.-P.; Yin, X.-L.; Ji, N.-Y., Diterpenes and sesquiterpenes from the marine algicolous fungus *Trichoderma harzianum* X-5. *Journal of natural products* **2018**, *81* (11), 2553-2559.
99. Li, H.-L.; Li, X.-M.; Li, X.; Wang, C.-Y.; Liu, H.; Kassack, M. U.; Meng, L.-H.; Wang, B.-G., Antioxidant hydroanthraquinones from the marine algal-

- derived endophytic fungus *Talaromyces islandicus* EN-501. *Journal of natural products* **2016**, *80* (1), 162-168.
100. Kumar, S.; Stecher, G.; Tamura, K., MEGA7: molecular evolutionary genetics analysis version 7.0 for bigger datasets. *Molecular biology and evolution* **2016**, *33* (7), 1870-1874.
 101. Zhang, C.-L.; Zheng, B.-Q.; Lao, J.-P.; Mao, L.-J.; Chen, S.-Y.; Kubicek, C. P.; Lin, F.-C., Clavatul and patulin formation as the antagonistic principle of *Aspergillus clavatonanicus*, an endophytic fungus of *Taxus mairei*. *Applied microbiology and biotechnology* **2008**, *78* (5), 833-840.
 102. Fan, J.; Liao, G.; Kindinger, F.; Ludwig-Radtke, L.; Yin, W.-B.; Li, S.-M., Peniphenone and penilactone formation in *Penicillium crustosum* via 1, 4-Michael additions of ortho-quinone methide from hydroxyclovatul to γ -butyrolactones from crustosic acid. *Journal of the American Chemical Society* **2019**, *141* (10), 4225-4229.
 103. da Silva, B. F.; Rodrigues-Fo, E., Production of a benzylated flavonoid from 5, 7, 3', 4', 5'-pentamethoxyflavanone by *Penicillium griseoroseum*. *Journal of Molecular Catalysis B: Enzymatic* **2010**, *67* (3-4), 184-188.
 104. Astudillo, L.; Schmeda-Hirschmann, G.; Soto, R.; Sandoval, C.; Afonso, C.; Gonzalez, M.; Kijjoo, A., Acetophenone derivatives from Chilean isolate of *Trichoderma pseudokoningii* Rifai. *World Journal of Microbiology and Biotechnology* **2000**, *16* (6), 585.
 105. de Souza, G. G.; Pfenning, L. H.; de Moura, F.; Salgado, M.; Takahashi, J. A., Isolation, identification and antimicrobial activity of propolis-associated fungi. *Natural Product Reports* **2013**, *27* (18), 1705-1707.
 106. Zhang, Y.; Mu, J.; Essmann, F.; Feng, Y.; Kramer, M.; Bao, H.-y.; Grond, S., A new quinolinone and its natural/artificial derivatives from a shark gill-derived fungus *Penicillium polonicum* AP2T1. *Natural product research* **2017**, *31* (9), 985-989.
 107. Wu, G.; Ma, H.; Zhu, T.; Li, J.; Gu, Q.; Li, D., Penilactones A and B, two novel polyketides from Antarctic deep-sea derived fungus *Penicillium crustosum* PRB-2. *Tetrahedron* **2012**, *68* (47), 9745-9749.
 108. Wang, J.; Liu, P.; Wang, Y.; Wang, H.; Li, J.; Zhuang, Y.; Zhu, W., Antimicrobial aromatic polyketides from gorgonian-associated fungus, *Penicillium commune* 518. *Chinese Journal of chemistry* **2012**, *30* (6), 1236-1242.
 109. White, T., Amplification and direct sequencing of ribosomal RNA genes and the internal transcribed spacer in fungi. *PCR-protocols and applications-a laboratory manual* **1990**, 315-322.

110. Glass, N. L.; Donaldson, G. C., Development of primer sets designed for use with the PCR to amplify conserved genes from filamentous ascomycetes. *Applied and Environmental Microbiology* **1995**, *61* (4), 1323-1330.
111. Visagie, C.; Houbraken, J.; Frisvad, J. C.; Hong, S.-B.; Klaassen, C.; Perrone, G.; Seifert, K.; Varga, J.; Yaguchi, T.; Samson, R., Identification and nomenclature of the genus *Penicillium*. *Studies in mycology* **2014**, *78*, 343-371.
112. Tamura, K.; Nei, M., Estimation of the number of nucleotide substitutions in the control region of mitochondrial DNA in humans and chimpanzees. *Molecular biology and evolution* **1993**, *10* (3), 512-526.
113. Sheldrick, G. M., *Bruker/Siemens Area Detector Absorption Correction Program*. Bruker AXS, Madison, WI: **1998**.
114. Sheldrick, G. M., *Acta Crystallogr., Sect. C: Struct. Chem.* **2015**, *71* (1), 3-8.
115. Xu, X.; Nicholson, P., Community ecology of fungal pathogens causing wheat head blight. *Annual review of phytopathology* **2009**, *47*, 83-103.
116. Chen, Y.; Kistler, H. C.; Ma, Z., Fusarium graminearum Trichothecene Mycotoxins: Biosynthesis, Regulation, and Management. *Annual Review of Phytopathology* **2019**, *57* (1).
117. Ferrigo, D.; Raiola, A.; Causin, R., Fusarium toxins in cereals: occurrence, legislation, factors promoting the appearance and their management. *Molecules* **2016**, *21* (5), 627.
118. Zhang, Y.; Pei, F.; Fang, Y.; Li, P.; Xia, J.; Sun, L.; Zou, Y.; Shen, F.; Hu, Q., Interaction between fungal community, Fusarium mycotoxins and components of harvested wheat under simulated storage conditions. *Journal of Agricultural and Food Chemistry* **2019**.
119. Ma, L.-J.; Geiser, D. M.; Proctor, R. H.; Rooney, A. P.; O'Donnell, K.; Trail, F.; Gardiner, D. M.; Manners, J. M.; Kazan, K., Fusarium pathogenomics. *Annual review of microbiology* **2013**, *67*, 399-416.
120. Alexander, N. J.; Proctor, R. H.; McCormick, S. P., Genes, gene clusters, and biosynthesis of trichothecenes and fumonisins in Fusarium. *Toxin reviews* **2009**, *28* (2-3), 198-215.
121. Weber, J.; Vaclavikova, M.; Wiesenberger, G.; Haider, M.; Hametner, C.; Fröhlich, J.; Berthiller, F.; Adam, G.; Mikula, H.; Fruhmann, P., Chemical synthesis of culmorin metabolites and their biologic role in culmorin and acetyl-culmorin treated wheat cells. *Organic & Biomolecular Chemistry* **2018**, *16* (12), 2043-2048.
122. Desjardins, A. E., *Fusarium mycotoxins: chemistry, genetics, and biology*. American Phytopathological Society (APS Press): **2006**.

123. Fabre, F.; Vignassa, M.; Urbach, S.; Langin, T.; Bonhomme, L., Time-resolved dissection of the molecular crosstalk driving Fusarium head blight in wheat provides new insights into host susceptibility determinism. *Plant, cell & environment* **2019**, *42* (7), 2291-2308.
124. Pluskal, T.; Castillo, S.; Villar-Briones, A.; Orešič, M., MZmine 2: modular framework for processing, visualizing, and analyzing mass spectrometry-based molecular profile data. *BMC bioinformatics* **2010**, *11* (1), 395.
125. Chong, J.; Soufan, O.; Li, C.; Caraus, I.; Li, S.; Bourque, G.; Wishart, D. S.; Xia, J., MetaboAnalyst 4.0: towards more transparent and integrative metabolomics analysis. *Nucleic acids research* **2018**, *46* (W1), W486-W494.

7 Supplementary Information

7.1 Material for Section 2

Table A1. ^1H and ^{13}C NMR data of 8,8'-bijuglone (**1**) at 500MHz in CDCl_3

Compound				
	position	δ_{C} , type	δ_{H} , mult (J in Hz)	δ_{H} , mult (J in Hz) ^a
	1, 1'	184.89, C	-	
	2, 2'	138.02, CH	6.9, d (10.2 Hz)	6.94 (10 Hz)
	3, 3'	140.57, CH	6.7, d (10.2 Hz)	6.73 (10 Hz)
	4, 4'	190.82, C	-	
	5, 5'	161.91, C	-	
	6, 6'	124.75, CH	7.3, d (8.7 Hz)	7.34 (8 Hz)
	7, 7'	138.72, CH	7.2, d (8.7 Hz)	7.27 (8 Hz)
	8, 8'	135.16, C	-	
	9, 9'	128.30, C	-	
	10, 10'	115.52, C	-	
	5-OH, 5'-OH	-	12.5, s	12.52, s

^aNMR: Varian FT-80 and XL 100

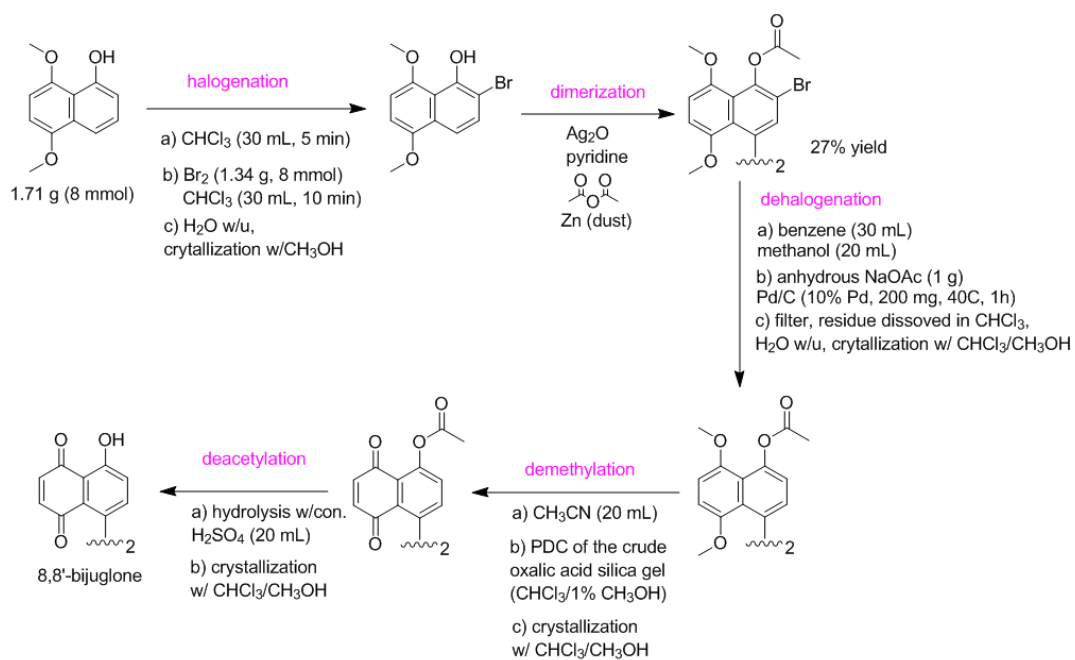


Figure A1. Synthesis of 8,8'-bijuglone by Laatsch in 1985.⁷⁴

Table A2. Reported bioactivities of similar compounds to **1**.^{76, 83-84}

COMPOUND	Antibacterial (MIC, $\mu\text{g/mL}$)			Antifungal (MIC, $\mu\text{g/mL}$)			
	<i>Bacillus subtilis</i>	<i>Enterococcus faecalis</i>	<i>Mycobacterium smegmatis</i>	<i>Candida albicans</i>	<i>Candida neoformas</i>	<i>Saccharomyces cerevisiae</i>	<i>Aspergillus niger</i>
8,8'- biplumbain = maritinone	150	150	20	40	20	9	40
chitranone	N/A	N/A	6	10	3	3	6
diospyrin	N/A	N/A	2.44	N/A	N/A	N/A	N/A

N/A = not reported

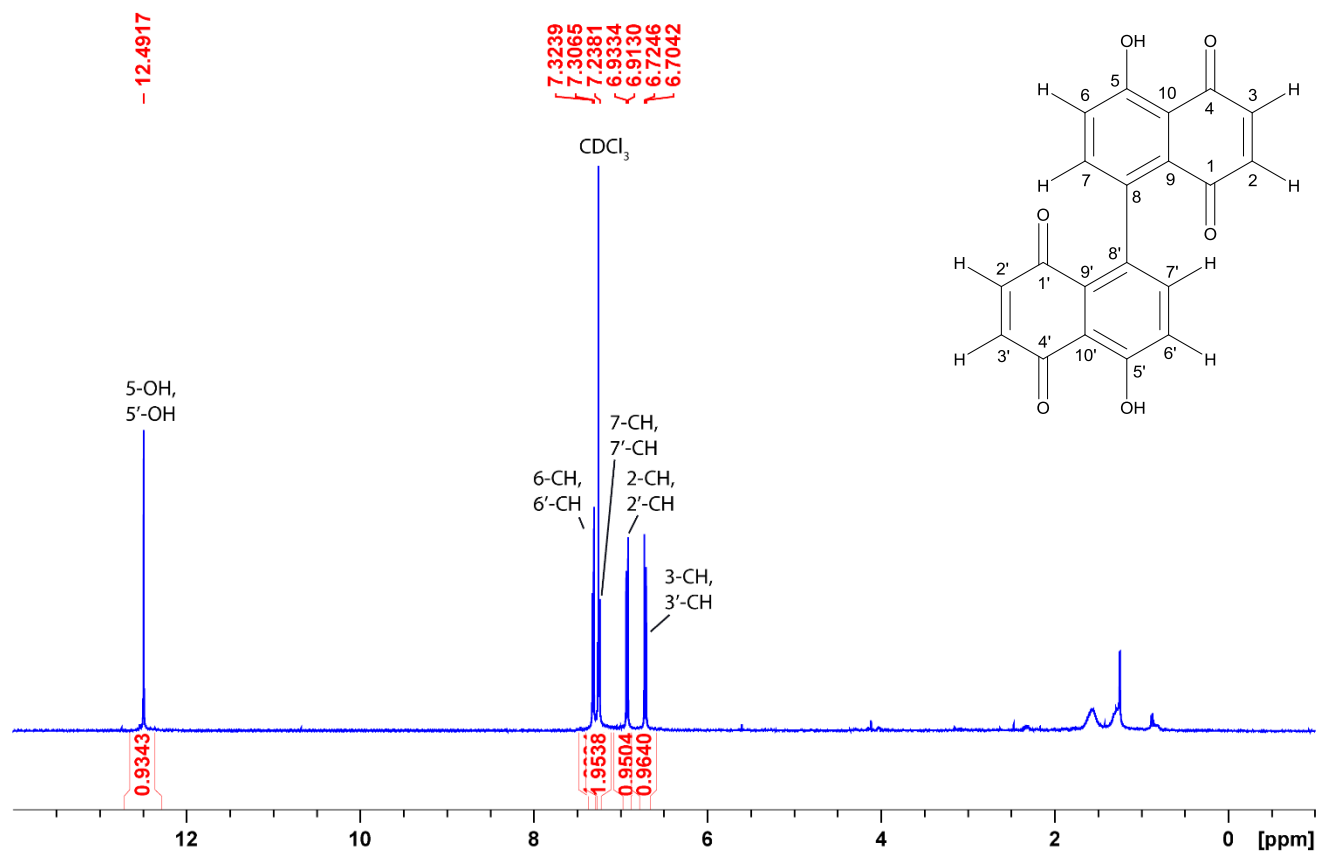


Figure A2. ¹H-NMR spectrum of 8,8'-bijuglone (1) in CDCl₃ (500MHz)

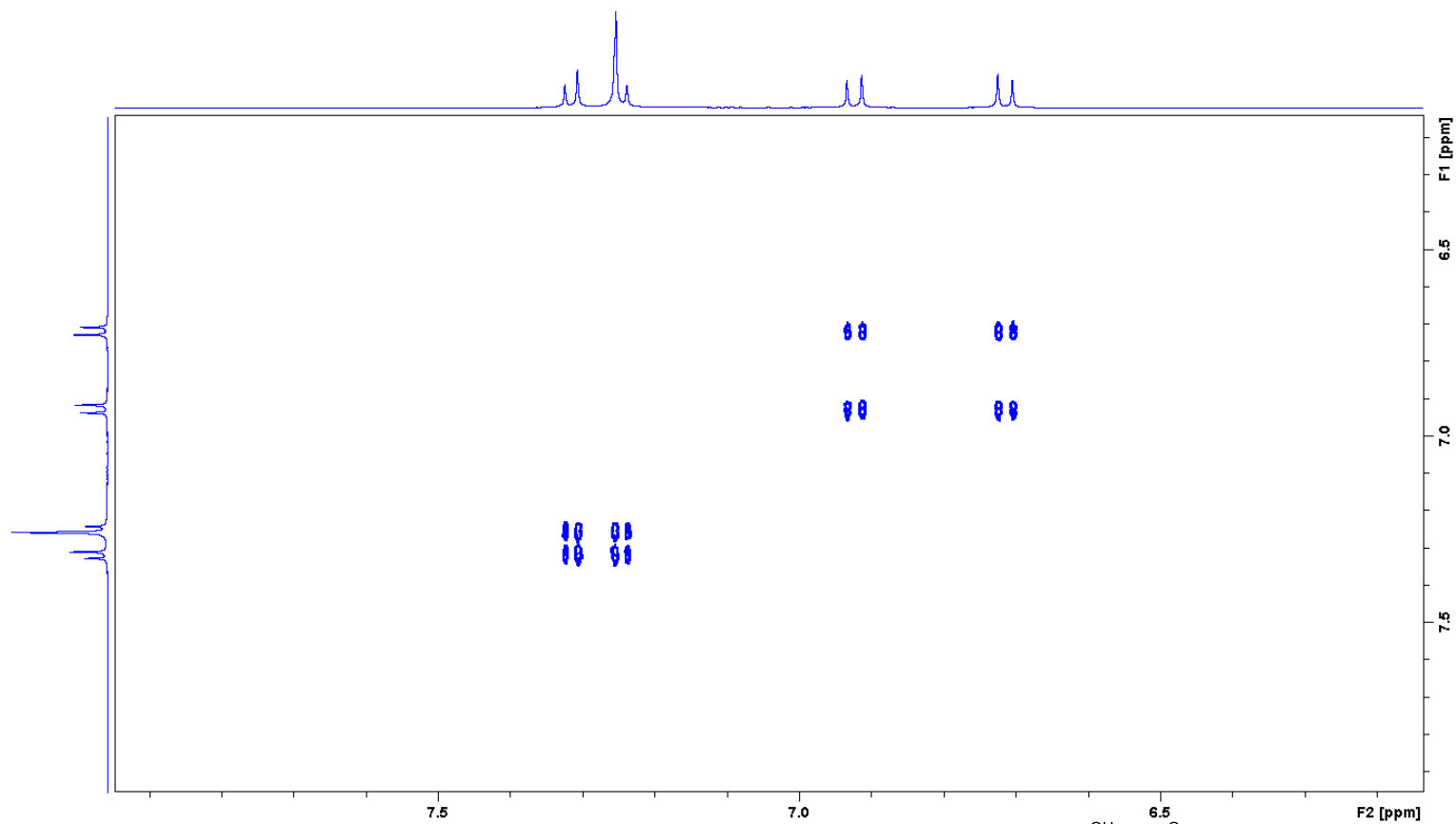
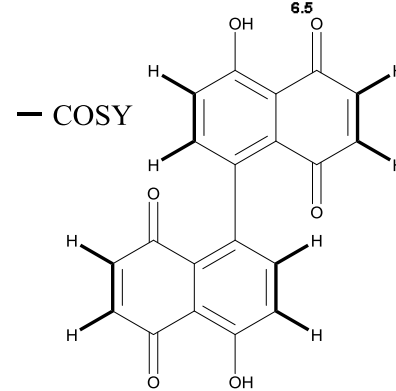


Figure A3. COSY spectrum of 8,8'-bijuglone (**1**) in CDCl₃ (500MHz).



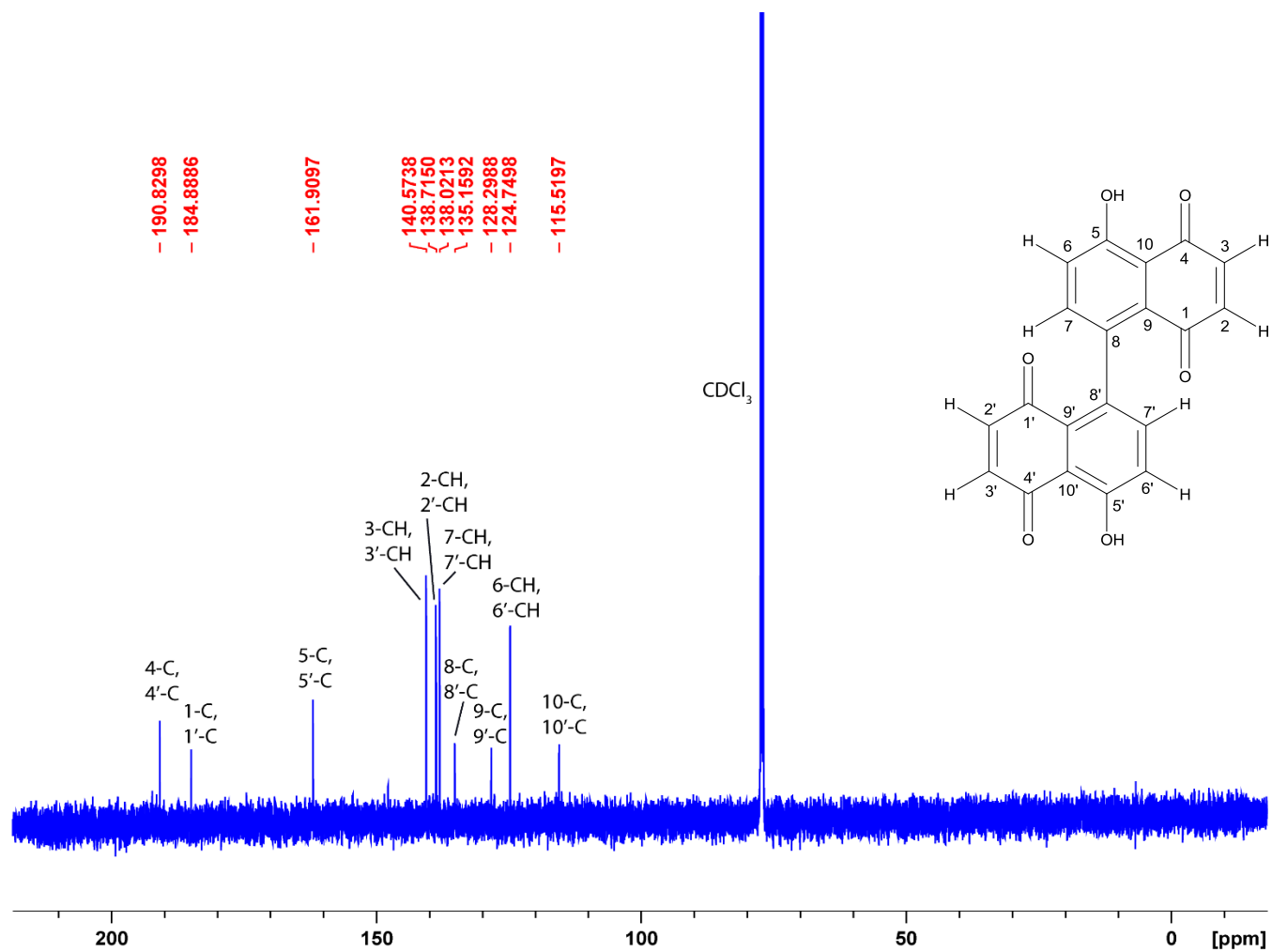


Figure A4. ¹³C-NMR spectrum of 8,8'-bijuglone (1) in CDCl₃ (500MHz).

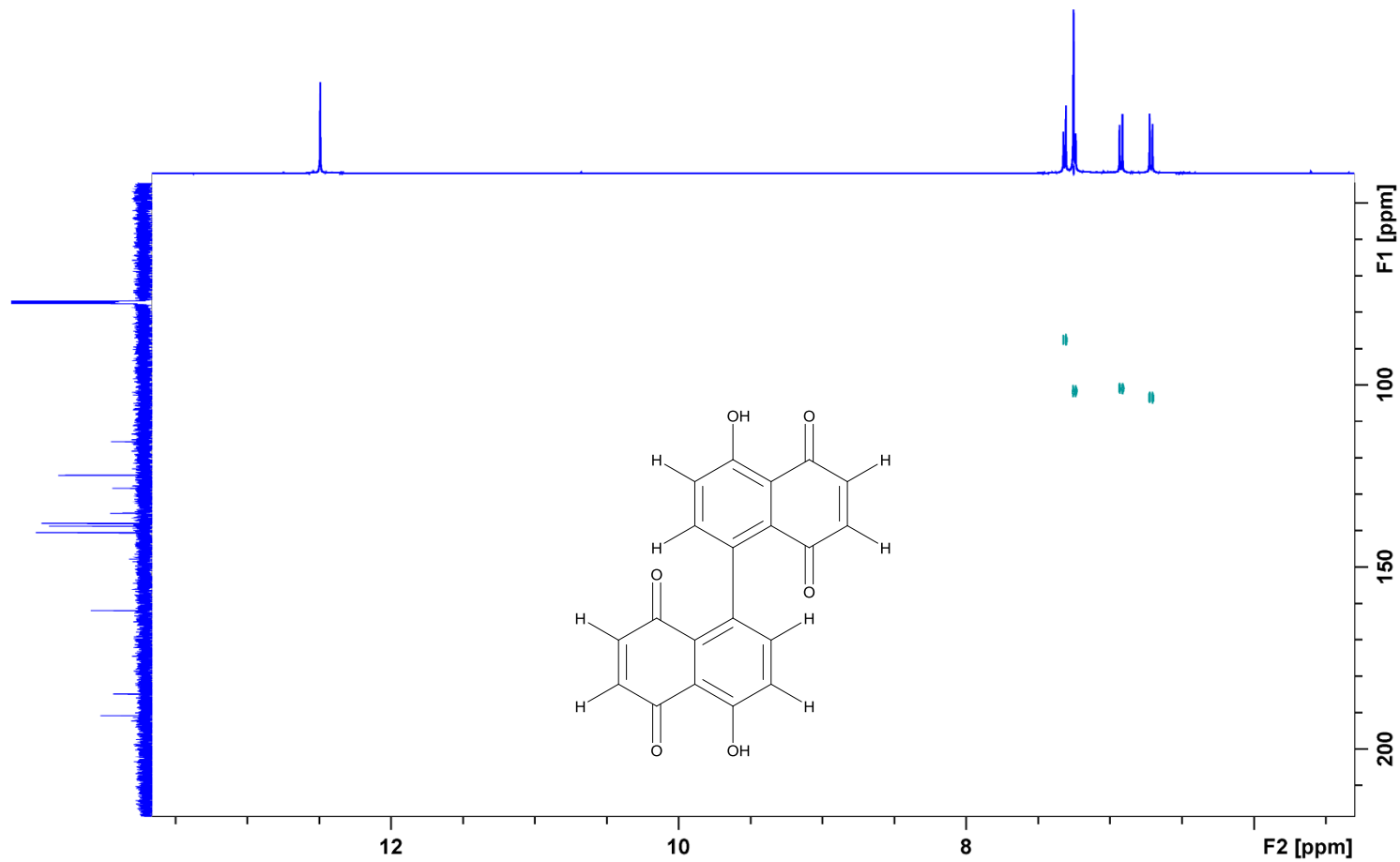


Figure A5. HSQC spectrum of 8,8'-bijuglone (1) in CDCl₃ (500MHz).

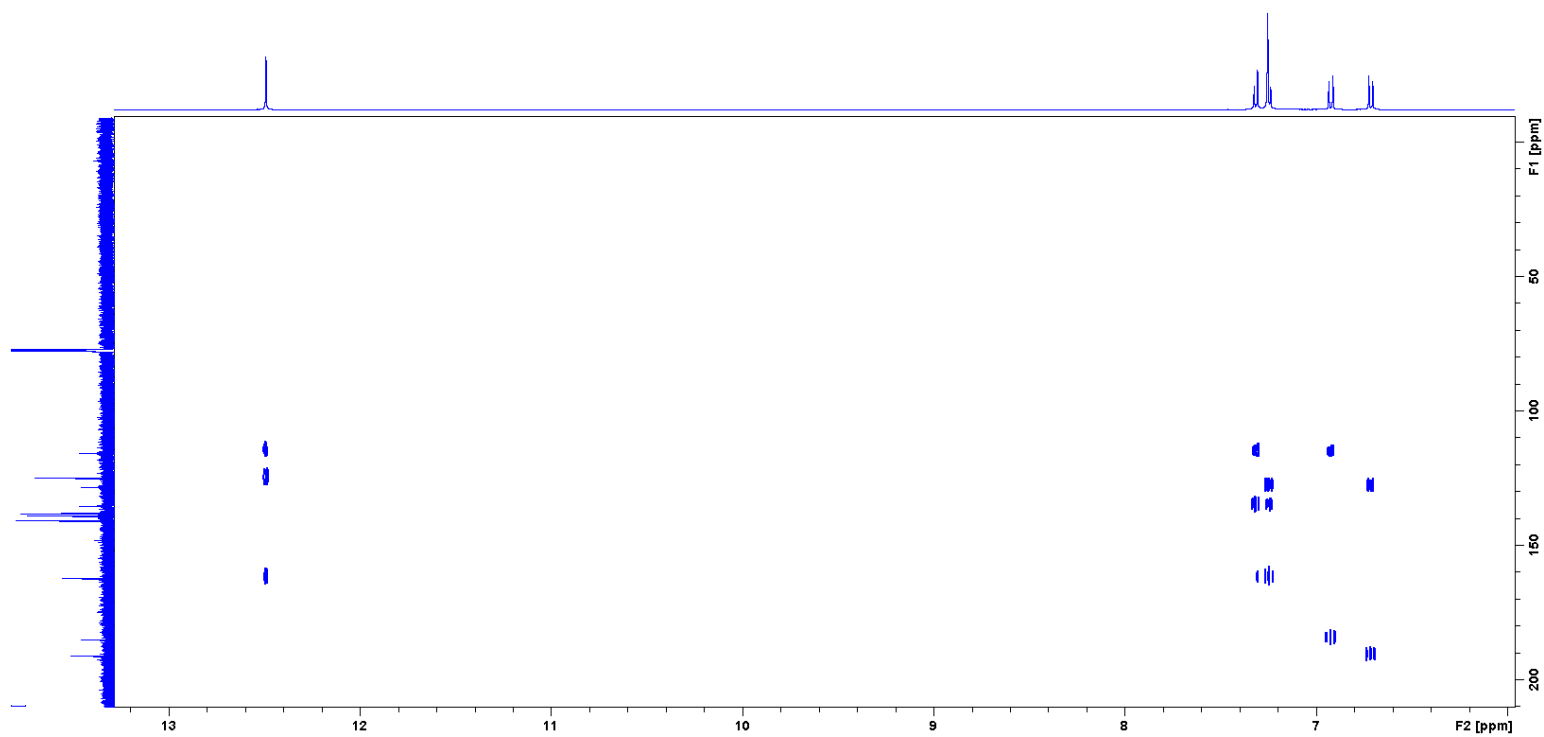
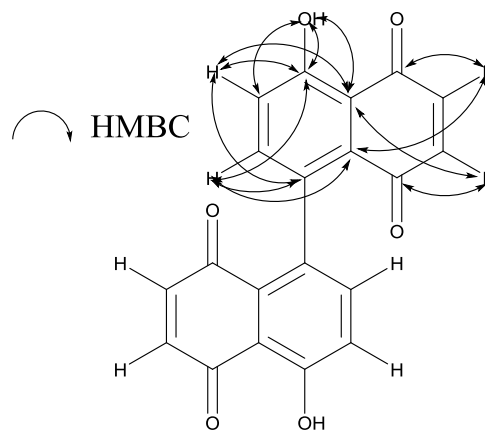


Figure A6. HMBC spectrum of 8,8'-bijuglone (**1**) in CDCl₃ (500MHz).



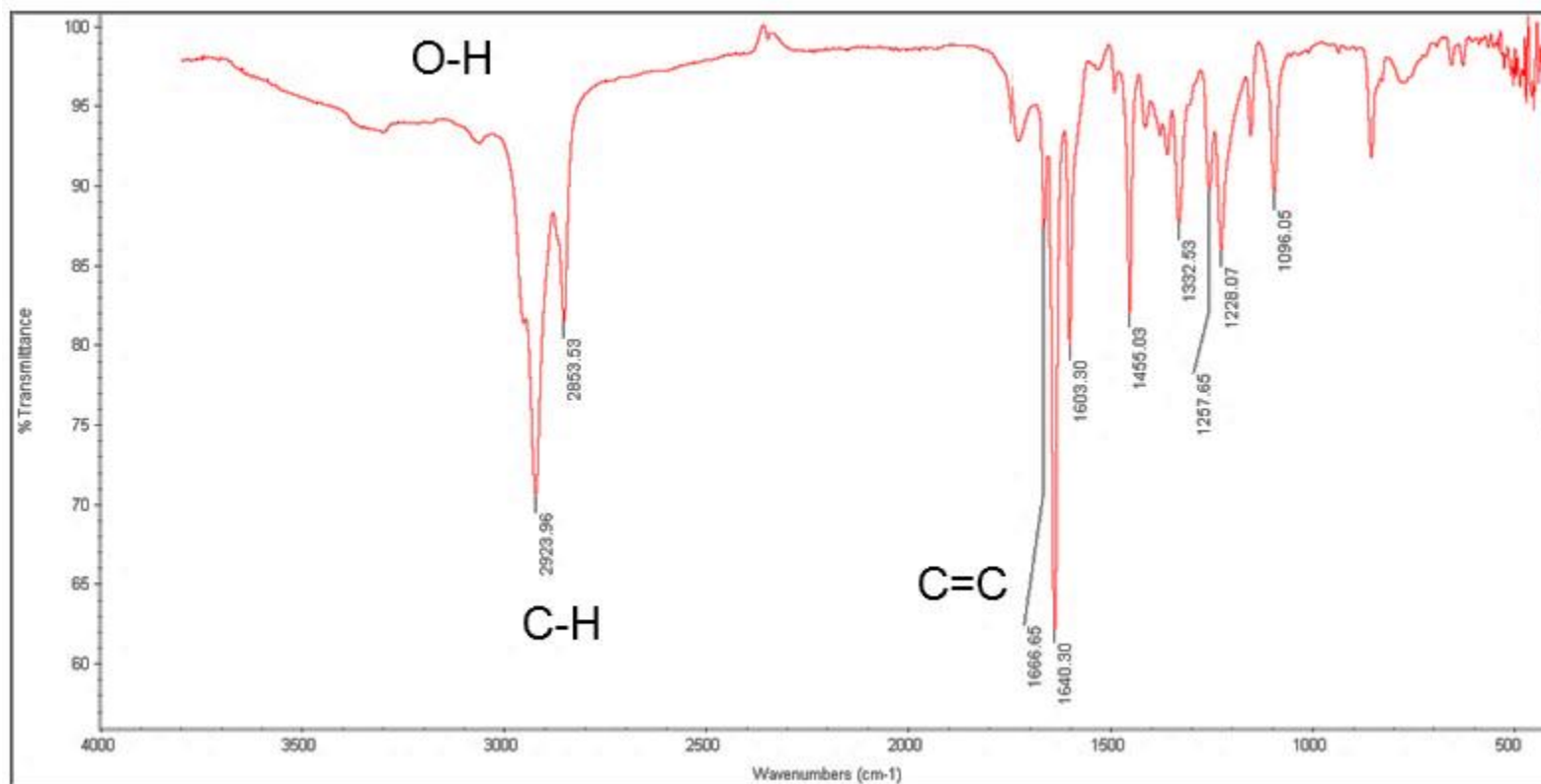


Figure A7. IR spectrum of 8,8'-bijuglone (1).

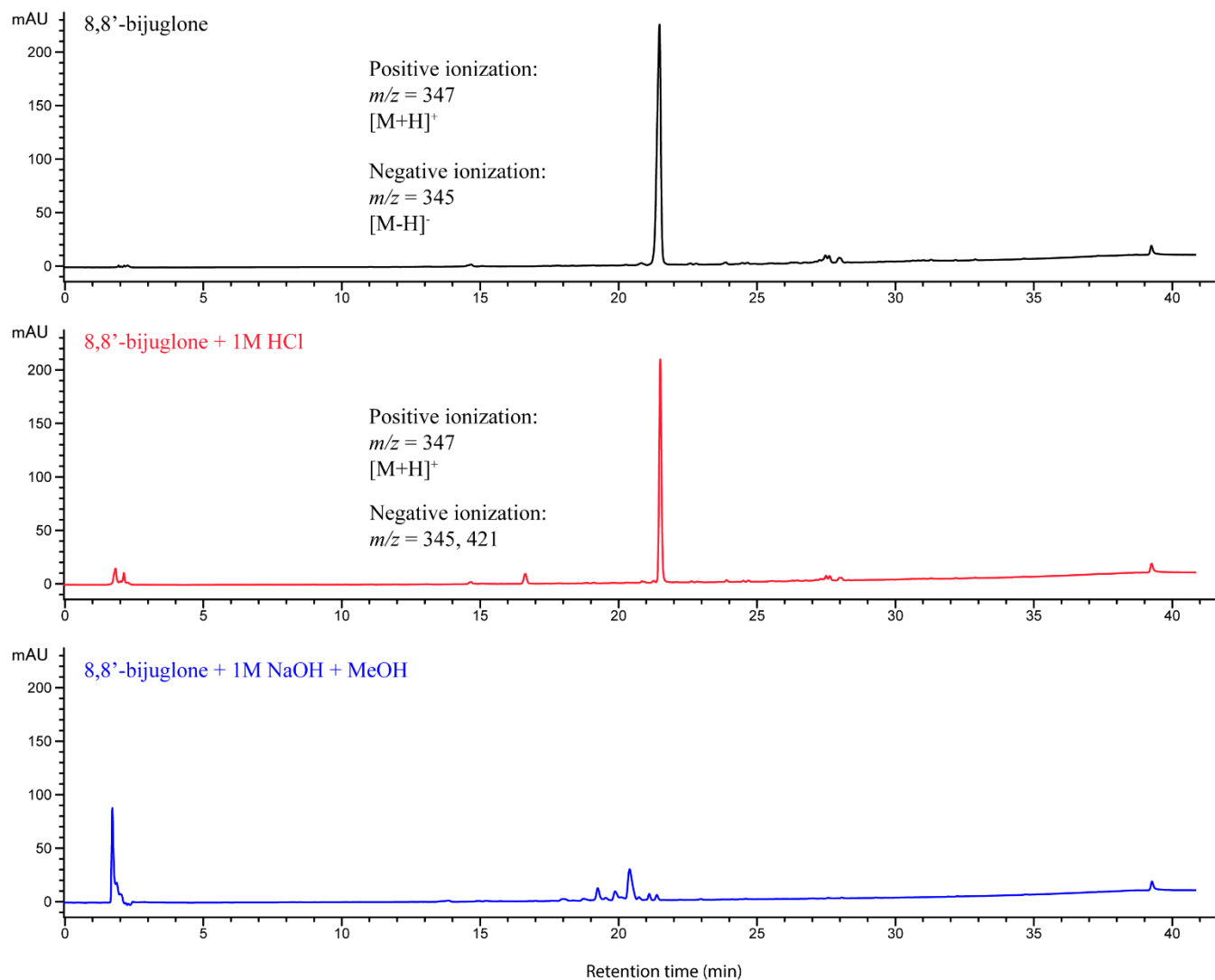


Figure A8. LC/MS traces of 8,8'-bijuglone in acidic and basic conditions. 8,8'-bijuglone in black, 8,8'-bijuglone + 1M HCl in red, and 8,8'-bijuglone + 1M NaOH + MeOH in blue. Chromatograms shown from 254 nm absorbance. Detectable positive and negative ionization m/z values are shown.

7.2 Material for Section 3

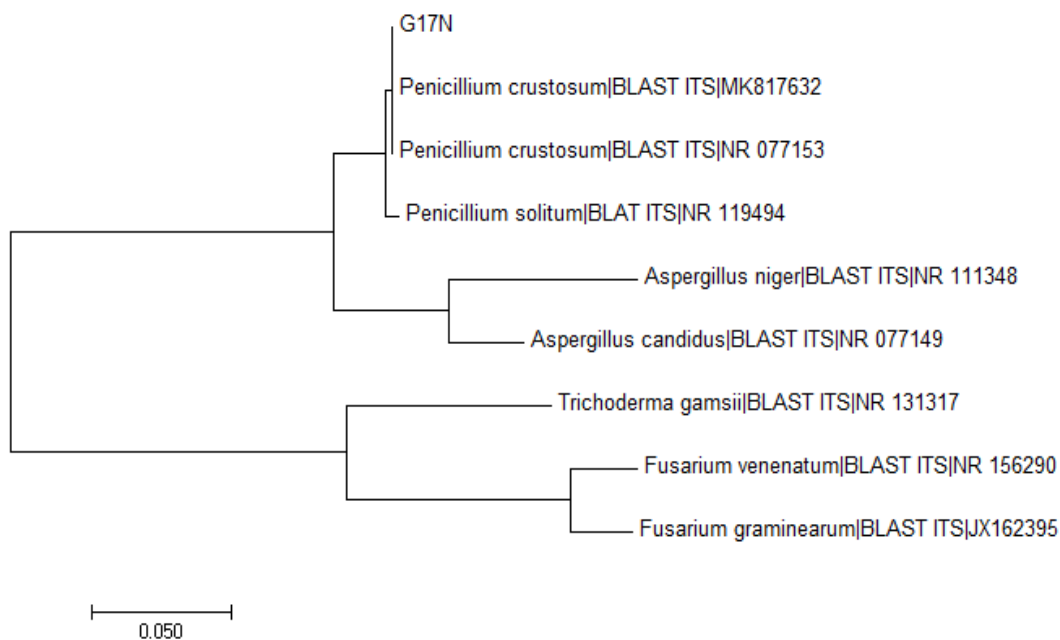


Figure A9. Phylogenetic analysis of *Penicillium* sp. (G17N) strain by maximum likelihood method of ITS region.

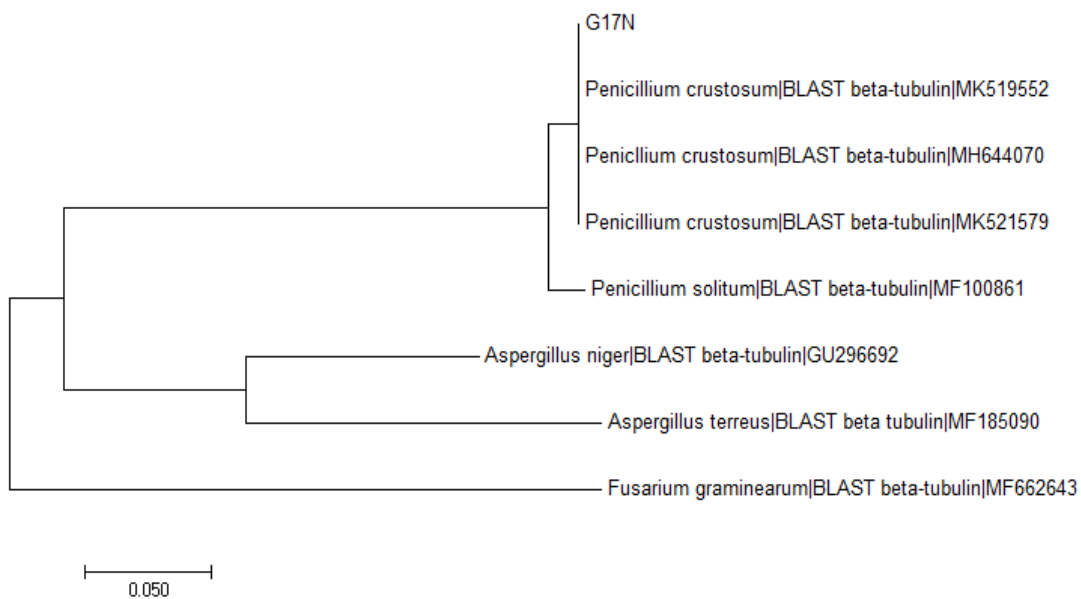


Figure A10. Phylogenetic analysis of *Penicillium* sp. (G17N) strain by maximum likelihood method of beta-tubulin region.

ACCTCCCACCCGTGTTTATTTTACCTTGTTGCTTCGGCGGGCCCGCCTTAA
 CTGGCCGCCGGGGGGCTTACGCCCCGGGCCC GCGCCCGCCGAAGACACC
 CTCGAACTCTGTCTGAAGATTGAAGTCTGAGTGAAAATATAAATTATTTA
 AACTTTCAACAACGGATCTCTTGGTTCCGGCATCGATGAAGAACGCAGC
 GAAATGCGATACGTAATGTGAATTGCAAATTCAGTGAATCATCGAGTCTT
 TGAACGCACATTGCGCCCCCTGGTATTCCGGGGGGCATGCCTGTCCGAGC
 GTCATTGCTGCCCTCAAGCCCGGCTTGTGTGTTGGGCCCCGTCCCCGATC
 TCCGGGGGACGGGCCCCGAAAGGCAGCGGCGGCACCGCGTCCGGTCCTCG
 AGCGTATGGGGCTTTGTCACCCGCTCTGTAGGCCCGGCCGGCGCTTGCCG
 ATCAACCCAAATTTTTATCCAGGT

Figure A11. Consensus sequence of *Penicillium* genus from the ITS region using primers ITS1 and ITS4.

TTTTTTTCGCGTTGGGTATCAATTGACAGGTTCTAACTGGATTACAGGCA
 AACCATCTCTGGCGAGCACGGTCTCGATGGCGATGGACAGTAAGTTTTAA
 CAGTGATAGGGGTTTCCGGTGGATTACACATCTGATATCTTCCTAGGTACA
 ATGGTACCTCCGACCTCCAGCTCGAGCGTATGAACGTCTACTTCAACCAT
 GTGAGTCCAACGACAGGAAACCGAATAATAGTGCATCATCTGATCGGATG
 TTTTCCTTGATAATCTAGGCCAGCGGTGACAAGTACGTTCCCCGTGCCGTT
 CTCGTGATTTGGAGCCTGGTACCATGGACGCTGTCCGCTCCGGTCCCTTC
 GGCAAGCTTTTCCGCCCCGACAACTTCGTCT

Figure A12. Consensus sequence of *P. crustosum* species from the β -tubulin region using primers Bt2a and Bt2b.

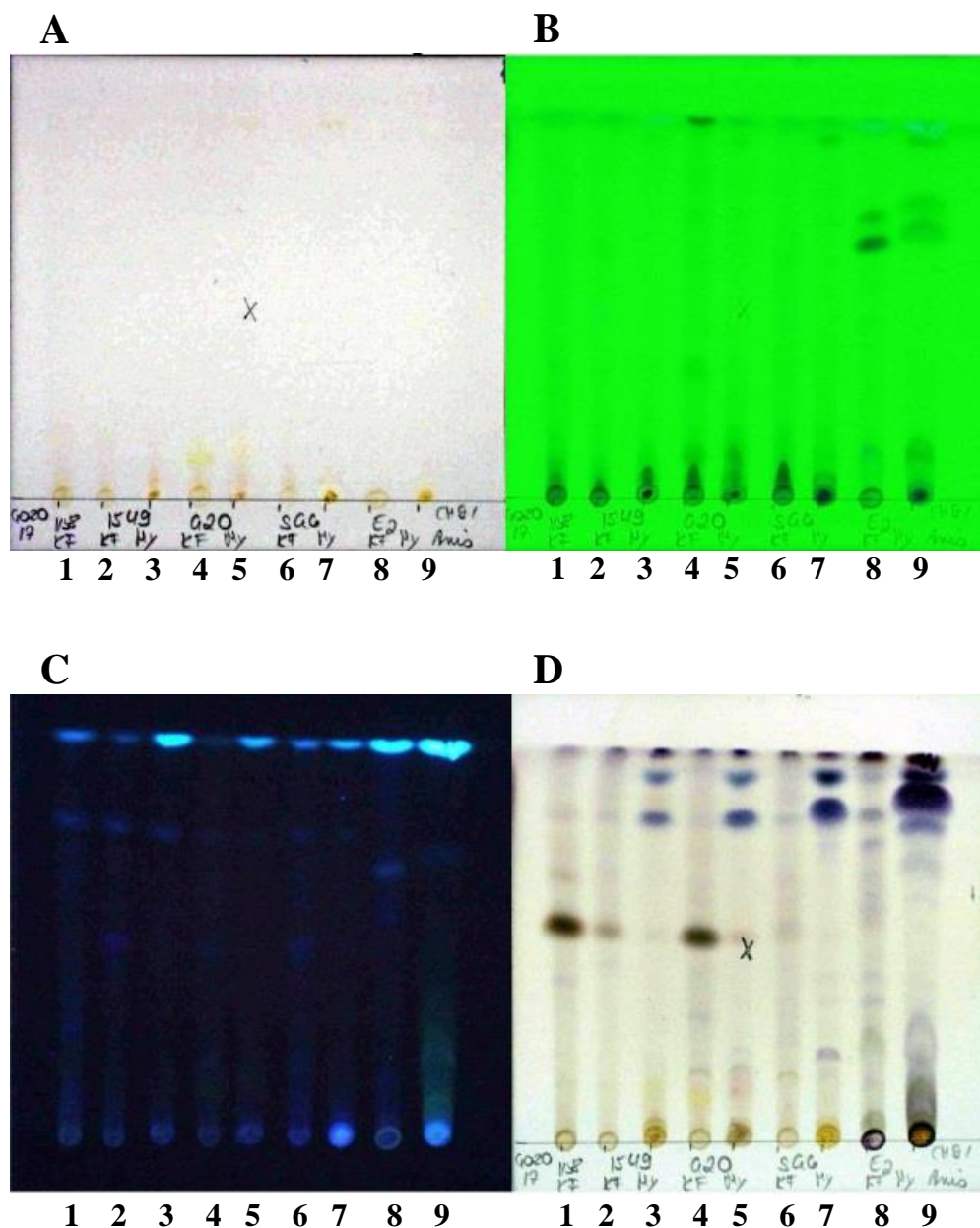


Figure A13. Thin layer chromatography of *P. crustosum* (G17N) organic extracts. A) Silica gel plate before UV light and stain exposure. B) Silica gel plate exposed to UV light at 254 nm. C) Silica gel plate exposed to UV light at 350 nm. D) Silica gel plate exposed to a strain. Lanes correspond to different media conditions and organic extracts from either the supernatant or cells of the fungal cultures. Lanes 4 and 5 are of interest since the fungus was grown in glycerin-based medium (G20).

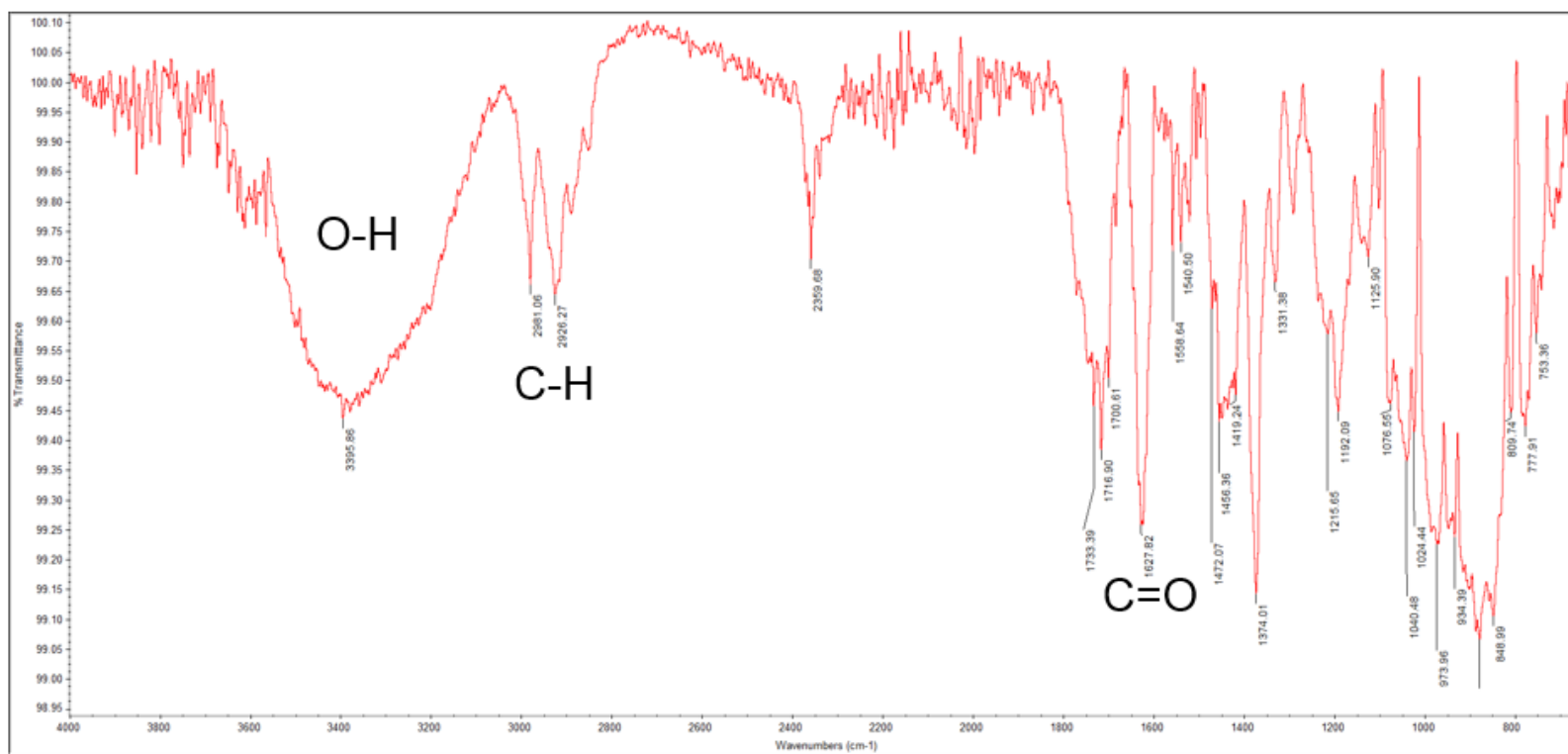
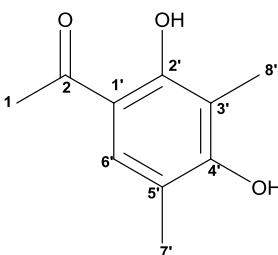


Figure A14. IR spectrum of clavotol (2).

Table A3. ^1H -NMR and ^{13}C -NMR data of clavatul (**2**) at 700MHz in CDCl_3

Compound



Position	δ_{C} , type	δ_{H} , mult (J in Hz)
1	26.52, CH_3	2.54, s, 3H
2	202.98, C	-
1'	110.38, C	-
2'	158.92, C	-
3'	113.61, C	-
4'	161.4, C	-
5'	114.65, C	-
6'	130.06, C	7.35, s 1H
7'	15.76, CH_3	2.19, d, 3H (0.73 Hz)
8'	7.64, CH_3	2.12, s, 3H
2'-OH	-	12.86, s, 1H
4'-OH	-	5.22, s, 1H

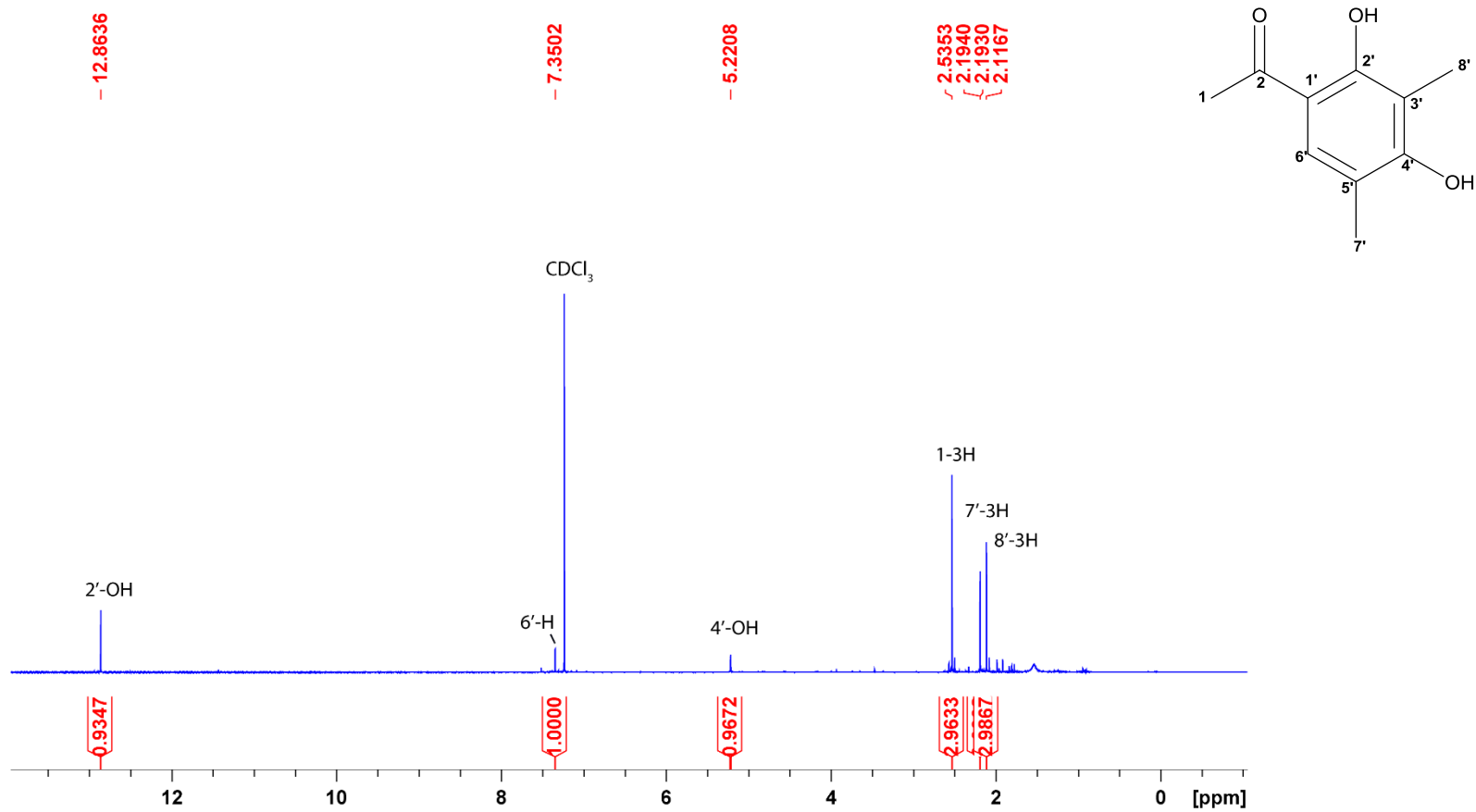


Figure A15. ¹H-NMR spectrum of clavotol (2) in CDCl₃ (700MHz).

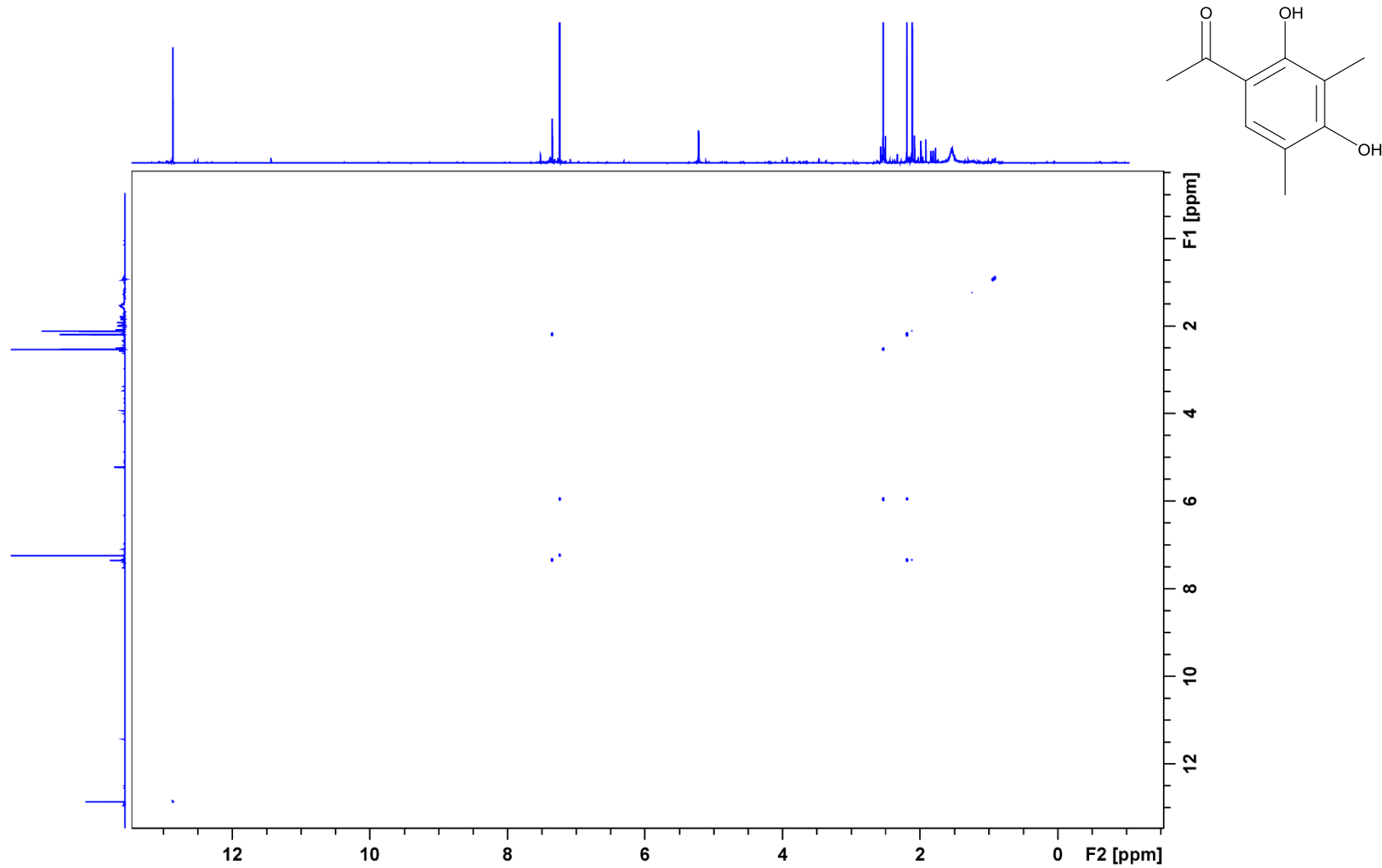


Figure A16. COSY spectrum of clavatol (2) in CDCl₃ (700MHz).

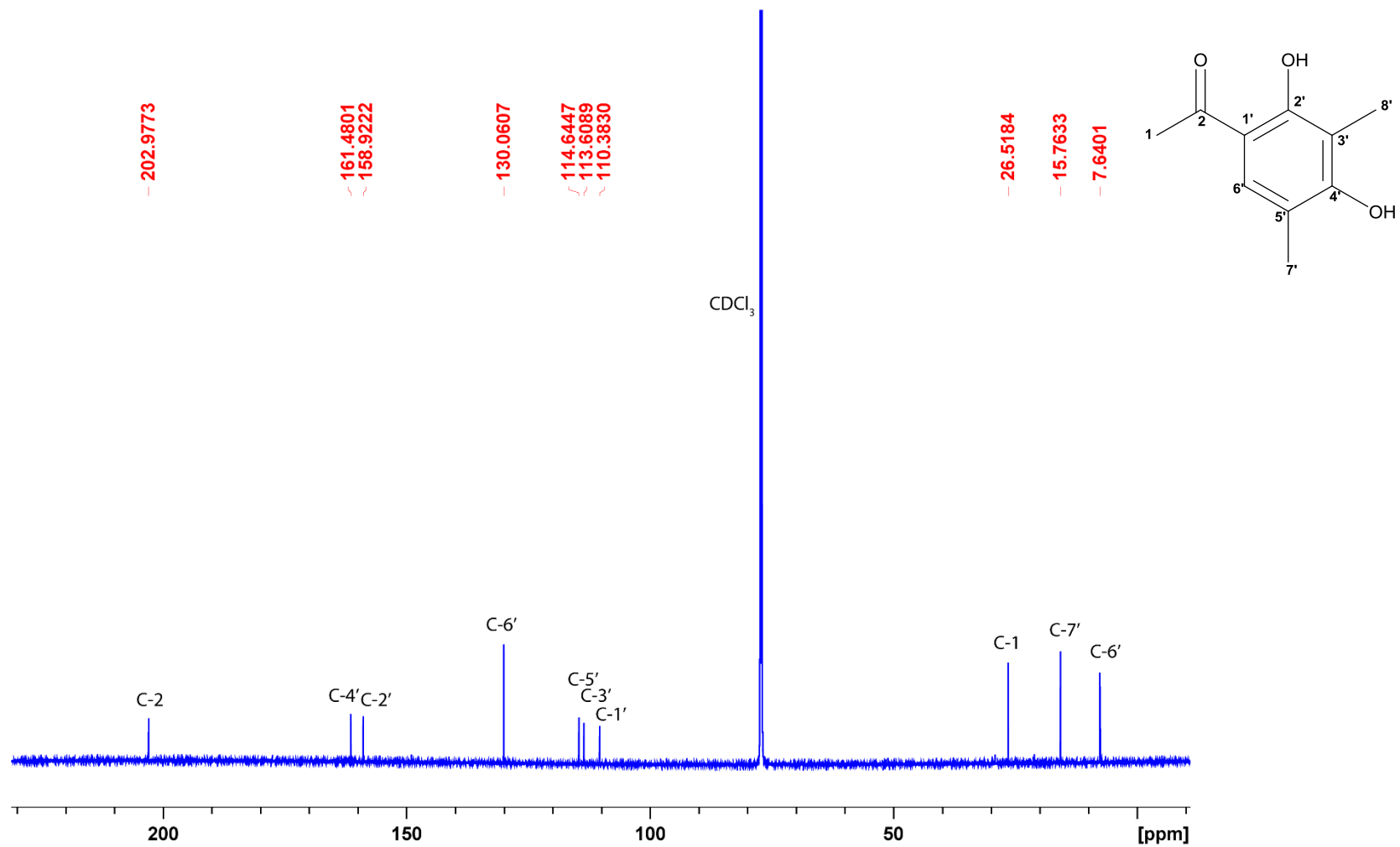


Figure A17. ¹³C-NMR spectrum of clavatul (2) in CDCl₃ (700MHz).

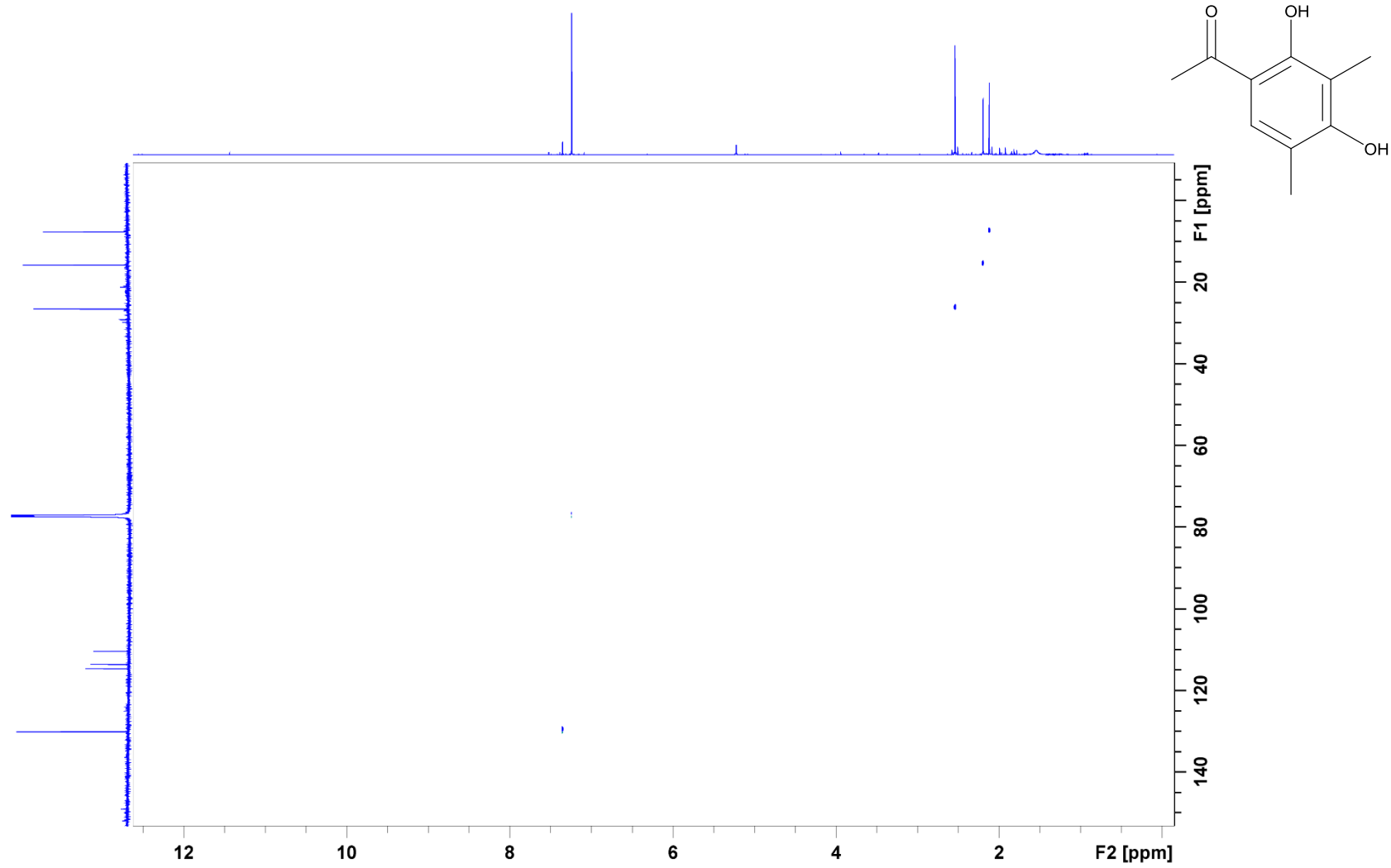


Figure A18. HSQC spectrum of clavatol (2) in CDCl_3 (700MHz).

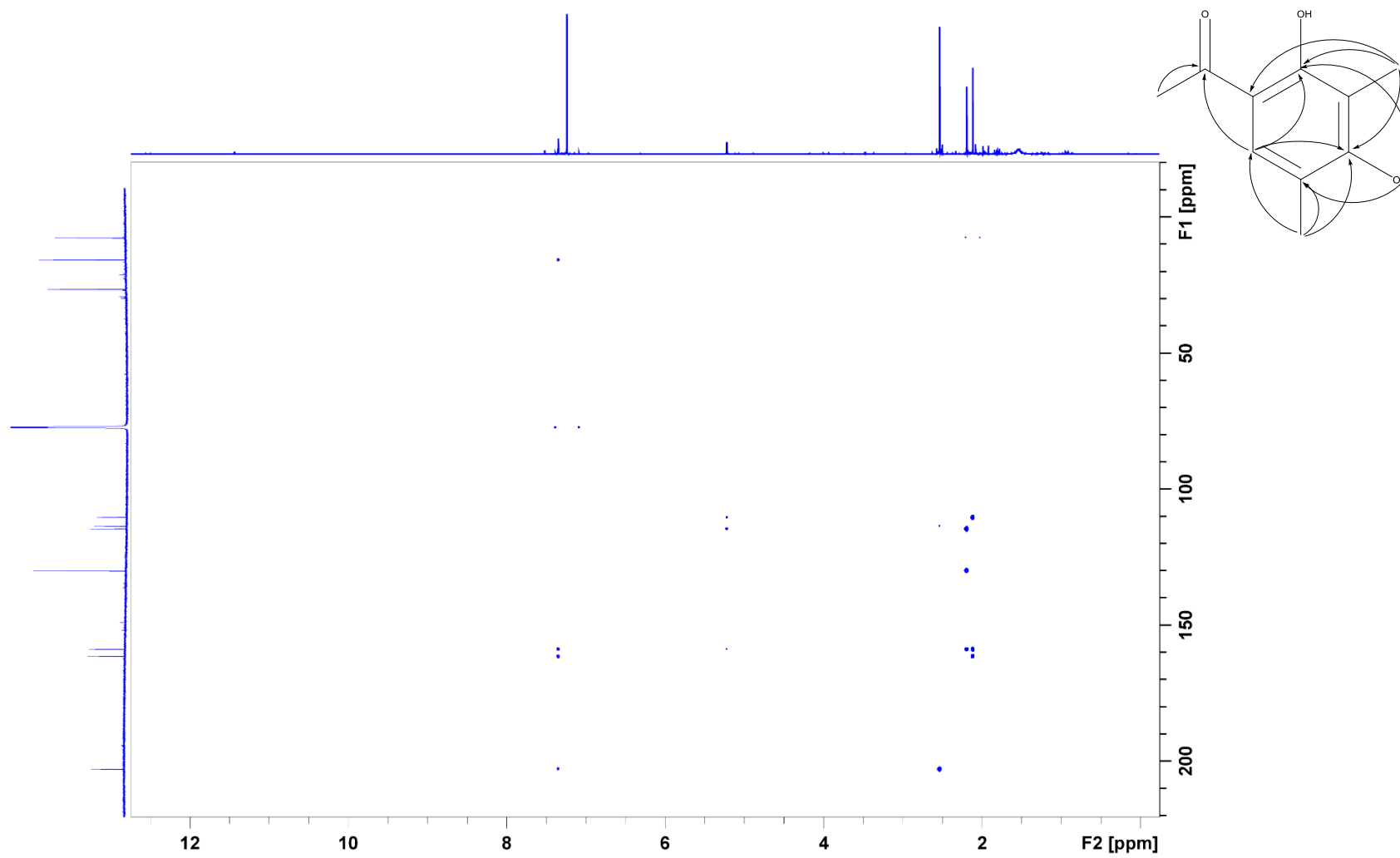


Figure A19. HMBC spectrum of clavatul (**2**) in CDCl₃ (700MHz).